Implementation and integration into new system concepts

Deliverable 4.4.2

OASE_WP4_D4.4.2_EAB_V2.0.doc

Version: 2.0

Last Update: 07/06/2013

Distribution Level:
PU (Public)

SEVENTH FRAMEWORK PROGRAMME

Information Society Technologies

Partner Name	Short name	Country
INTERDISCIPLINARY INSTITUTE FOR BROADBAND TECHNOLOGY	IBBT	B
KUNGLIGA TEKNISKA HOEGSKOLAN	KTH	S
ADVA AG OPTICAL NETWORKING	ADVA	D
ERICSSON AB	EA	S
ERICSSON TELECOMUNICAZIONI S.P.A	TEI	I
ACREO AB.	ACREO	S
MAGYAR TELEKOM TAVKOZLESI NYILVANOSAN MUKODO RESZVENYTARSASAG	MT	H
UNIVERSITY of ESSEX	UESSEX	UK

Abstract:
This Deliverable presents research and development on system concepts selected as candidates for next-generation optical access based on OASE requirements. The deliverable presents research performed within the scope of OASE concerning specific challenges of the different concepts. Such work includes validation and demonstration of particular concepts, development and evaluation of resource allocation and power saving techniques, control plane implementation and various concept proposals related to e.g resiliency, longer reach and higher bit-rates. Part of the deliverable also presents, for each selected system concept, an equipment implementation description which is to be used in the total-cost-of-ownership (TCO) calculations in WP5.

"The research leading to these results has received funding from the European Union's Seventh Framework Programme (FP7/2007-2013) under grant agreement n° 249025"

Document Identity

Title:	Implementation and integration into new system concepts
Subject:	WP4 “System concepts for Next Generation optical access networks”
Number:	D4.4
File name:	OASE_WP4_D4.4.2_EAB_V2.0.doc
Registration Date:	June, 12th 2011
Last Update:	07/06/2013

Revision History

No.	Version	Edition	Author(s)	Date
1	0	1	A. Bianchi (TEI)	09/01/2012
	Comments:	Creation of document		
2	0	2	A. Bianchi (TEI), J. Chen (KTH), A. Dixit (IBBT), A. Gavler (Acreo), K. Grobe (ADVA), B. Lannoo (IBBT), V. Nordell (Acreo), M. Parker (UESSEX), B. Skubic (EAB)	03/02/2012 - 17/09/2012
	Comments:	Technical contributions		
3	0	3	R. Martin (UESSEX) & D. Breuer (DTAG)	02/10/2012
	Comments:	Internal review		
4	0	4	J. Chen (KTH), A. Dixit (IBBT), M. Parker (UESSEX), V. Nordell (Acreo)	03/10/2012
	Comments:	Updates		
5	0	5	B. Skubic (EAB)	04/10/2012
	Comments:	Final editing		
6	2	0	B. Skubic (EAB)	07/06/2013
	Comments:	Updates based on final review		

Table of Contents

Executive Summary

This deliverable D4.4 provides an in-depth study of selected challenges of the OASE system concepts for next-generation optical access (NGOA). The deliverable presents research and development on these concepts performed within the scope of OASE.

The study builds on previous work within workpackage WP4. In terms of concept selection, it was found that a large number of system variants satisfy the lower end of the OASE requirements from D2.1. Thus, it is not possible to further select or reduce the number of candidate systems based on the available technical and operational requirements. The final discussion on selection of systems for NGOA will be part of the comprehensive techno-economic analysis in WP5.

For the remaining OASE system concepts there are various challenges, both general and concept specific, that need to be addressed. Considered topics range from validation of feasibility to aspects concerning resiliency, resource allocation, power saving techniques and further developments for higher capacity, reach and client counts.

Some of the main outcomes and conclusions of this deliverable are summarized below:

- For mobile/business backhaul it was shown that the initial requirements defined in D2.1 can be supported within all the presented concepts with limited or some additional effort, where “some additional effort” may at most consist of manual patching work for service provisioning.
- The ONU represents the dominating contribution to access network power, a comparision of ONU power saving modes for the different system concepts shows that average ONU power consumption can be reduced by about 90% when it is applied to NGOA system concepts with a burst mode transmission and reception like high bit rate TDMA-PONs and about 80% in hybrid TWDM-PONs. Moderate savings between 35 to 41% are found for WDM-PON, AON and PtP systems.
- A master-slave scheme that can enable significant energy-efficiency savings across a range of equipment and system types in the next-generation access network area was developed and evaluated.
- An efficient ODN fault-localization scheme was developed that can enable accurate identification of faults in a wave-length routed ODN providing operational advantages for this particular ODN with respect to ODN fault localization and repair costs.
- For the hybrid WDM/TDM-PON architecture, resource allocation is of critical importance. Schemes for efficient TDMA resource allocation in the long-reach limit are developed and evaluated in a test-bed. Schemes for dynamic wavelength allocation are developed and evaluated by means of simulations.
- For the hybrid WDM/TDM-PON architecture, power saving techniques for the ONU are particularly important due to large active power consumption. A scheme for sleep mode control based on service requirements was delevloped and evaluated in a simulation demonstrating some of the assumed energy saving opportunities within this architecture.
- For the NG-AON architecture a control plane implementation was implemented in order to demonstrate intelligent control mechanisms which enable reduction of network energy consumption, reduction in core load and reduction in transit costs.

- For the WDM-PON backhaul architecture to which much of the work associated with the WDM-PON architecture and NG-AON applies, the deliverable reports work related to future developments in mobile networks and support for CPRI transport.

Referred documents

[1] Project Contract - Annex 1 "Description of the Work" *(DoW)*

[2] OASE Deliverable D2.1: "Requirements for European next-generation optical access networks", September 2010.

[3] OASE Deliverable D3.1: "Overview and assessment of existing optical access network architectures", December 2010.

[4] OASE Deliverable D4.1: "Survey of next-generation optical access system concepts", October 2010, available online: www.ict-oase.eu/public/files/OASE_WP4_D4_1_29th_October_2010_v1_0.pdf

[5] EU FP7 Project OASE (Optical Access Seamless Evolution), available online: http://www.ict-oase.eu/

[6] EU FP7 Project C-3PO (Coolerless and Colourless Components for low-Power Optical networks), available online: http://www.greenc3po.eu/

[7] A. Dixit, B. Lannoo, S. Lambert, D. Colle, M. Pickavet, P. Demeester, "Evaluation of ONU Power Saving Modes in Next Generation Optical Access Networks," ECOC, Sep. 2012.

[8] Available at: http://download.micron.com/downloads/misc/SDRAM_Power_Calc_10.xls

[9] A. Dixit, B. Lannoo, D. Colle, M. Pickavet, P. Demeester, "Energy Efficient Dynamic Bandwidth Allocation for Ethernet Passive Optical Networks," submitted to IEEE ANTS 2012.

[10] Oleksii Chyrkov, "Investigation and testing of a low-cost long fiber optic link without external electric power", master thesis, 2012.

[11] Time and Date AS. (2012) Sunrise and Sunset Calculator. [Online]. http://www.timeanddate.com/worldclock/sunrise.html

[12] Hong Kong Observatory. (2003) Climatological Normals of Stockholm. [Online]. http://www.hko.gov.hk/wxinfo/climat/world/eng/europe/n_europe/stockholm_e.htm

[13] Hong Kong Observatory. (2003) Climatological Normals of Djibouti. [Online]. http://www.hko.gov.hk/wxinfo/climat/world/eng/africa/sudan/djibouti_e.htm

[14] Mohammed M. Rad, Kerim Fouli, Habib A. Fathallah, Laslie A. Rusch and Martin Maier, "Passive Optical Network Monitoring: Challenges and Requirements" in IEEE Communications Magazine, February 2011.

[15] Agerekibre Getaneh, "OTDR based WDM-PON Monitoring", master thesis, 2012.

[16] M.C. Parker, S.D. Walker, 'Roadmapping ICT: An Absolute Energy Efficiency Metric ', Journal of Optical Communications and Networks, vol.3(8), pA49-A58, 2011

[17] Kubo, J.-i. Kani, H. Ujikawa, T. Sakamoto, Y. Fujimoto, N. Yoshimoto, and H. Hadama, "Study and Demonstration of Sleep and Adaptive Link Rate Control Mechanisms for Energy Efficient 10G-EPON," Optical Communications and Networking, IEEE/OSA Journal of, vol. 2, no. 9, pp. 716 –729, september 2010.

[18] R. Kubo et al., "Adaptive Power Saving Mechanism for 10 Gigabit Class PON Systems," IEICE E93-B, 280-287 (2010).

[19] M. Fiammengo et. al.,"Experimental Evaluation of Cyclic Sleep with Adaptable Sleep Period Length for PON", ECOC 2011, We.8.C.3.

[20] ITU-T Recommendation G.1010: "End-user Multimedia QoS Categories", URL: http://www.itu-t.org.

[21] ITU-T Recommendation Y.1541: "Network Performance Objectives for IP-based Services", URL: http://www.itu-t.org.

[22] A G. Bolch et al., "Queueing Networks and Markov Chains", Wiley, May 2006, pp. 148-151.

[23] Hideaki Takagi, "Analyisis of Polling Systems", The MIT Press, 1986, pp. 105-117.

[24] RFC3954, Cisco Systems NetFlows Flow Version 5, http://www.sflow.org/sflow_version_5.txt

[25] OpenFlow Switch Specication 1.1, http://www.openflow.org/documents/openflow-spec-v1.1.0.pdf

[26] 120 Gbps Intelligent Policy Enforcement for Broadband Networks, http://www.proceranetworks.com/pdf/products/pre/PRE_PL10000_Q3_2012_7_7_WEB.pdf

[27] Internet Transit Prices - Historical and Projected, http://drpeering.net/white-papers/Internet-Transit-Pricing-Historical-And-Projected.php

[28] TeleGeography, Global Internet Geography, http://www.telegeography.com/research-services/global-internet-geography/

[29] TeleGeography, Price Benchmarks, http://www.telegeography.com/telecom-resources/telegeography-infographics/price-benchmarks/index.html]

Table of figures

Table of tables

Abbreviations

AF	Asymmetricity Factor
AMGAV	Adaptive Multi-Gate polling with void filling
AON	Active Optical Network
APD	Avalanche Photodiode
ATM	Asynchronous Transfer Mode
BER	Bit Error Rate
BERT	BER Tester
BF	Burst Factor
CAN	Central Access Node
CAPEX	Capital Expenditure
CDN	Content Delivery Network
CO	Central Office
CPRI	Common Public Radio Interface
CRAN	Cload RAN
DBA	Dynamic Bandwidth Assignment
DC	Dispersion Compensation
DL	Down Link
DF	Distribution Fiber
DO	Digital Optics
DS	Downstream
DSP	Digital Signal Processing
DST	Destination
DTLP	Design-to-low-power
DWDM	Dense WDM
ECC	Error Correcting Code
EDFA	Erbium Doped Fiber Amplifier
EFT	Earliest Finish Time
EWAM	External Wavelength Adaptation Module
FAW	First Available Wavelength
FEC	Forward Error Correcting
FF	Feeder Fiber
FOM	Figure of Merit
FTTH	Fiber-to-the-home
GbE	Gigabit Ethernet
G-PON	Gigabit-capable PON
HB-TDMA	High bit rate-TDMA
HTTP	Hypertext Transfer Protocol
HVAC	Heating, Ventilation, and Air Conditioning
IP	Internet Protocol
IPACT	Interleaved Polling with Adaptive Cycle Time
IPACT-SMA	IPACT with Sleep Mode Awareness
LFT	Latest Finish Time
LLID	Logical Link ID
LMF	Last Mile Fiber
LoS	Loss of Signal
LT	Line Termination

LTE	Long Term Evolution
LXC	Linux Containers
MAC	Media Access Control
MoCA	Multimedia over Coax Alliance
MPCP	Multi-Point Control Protocol
MTBF	Mean Time Before Failure
MU	Main Unit
MWS	Minimized Wavelength Switching
NetFPGA	Networked Field Programmable Gate Arrays
NGA	Next Generation Access
NG-AON	Next Generation AON
NGOA	Next Generation Optical Access
NIC	Network Interface Card
NMS	Network Management System
ODN	Optical Distribution Network
OEO	Optical Electrical Optical
OFDM	Orthogonal Frequency Division Multiplexing
OFDMA	Orthogonal Frequency Division Multiple Access
OLT	Optical Line Terminal
OMCI	ONT/ONU Management and Control Interface
ONU	Optical Network Unit
OPEX	Operational Expenditures
OSPF	Open Shortest Path First
OTDR	Optical Time Domain Reflectometer
P2MP	Point-to-multipoint
PCB	Power Controller Board
PCE	Path Computation Element
PHY	Physical Layer
PIC	Photonic Integrated Circuit
PIN	PIN photo diode
PLOAM	Physical Layer Operations And Maintenance
PON	Passive Optical Network
PSU	Power Supply Unit
PtP	Point-to-point
PUE	Power Usage Effectiveness
PV	Photo-Voltaic
QoS	Quality-of-Service
RAN	Radio Access Network
RBS	Radio Base Station
RE	Reach Extender
RN	Remote Node
ROADM	Reconfigurable Optical Add Drop Multiplexer
ROP	Received Optical Power
RRU	Remote Radio Unit
RSOA	Reflective SOA
RSVP-TE	Resource Reservation Protocol Traffic Engineering
RTMP	Real Time Messaging Protocol
RTT	Round Trip Time
SFP	Small Form factor Pluggable
SLA	Service Level Agreement

SLIC	Subscriber Line Interface Circuit
SMF	Single Mode Fiber
SNMP	Simple Network Management Protocol
SOA	Semiconductor Optical Amplifier
SoC	System on Chip
SPW	Sleep and Periodic Wake-up
SRC	Source
TCO	Total Cost of Ownership
TDM	Time Division Multiplexing
TDMA	Time Division Multiple Access
TEC	Thermo-Electric Cooler
TRX	Transceiver
TIA	Tranimpedance Amplifier
TS	Transmission Slot
TCP	Transmission Control Protocol
TWDM-PON	Time and Wavelength Division Multiplexing PON
UDWDM	Ultra Dense WDM
UL	Uplink
US	Upstream
VLAN	Virtual LAN
WBF	Wavelength Blocking Filter
WDM-PON	Wavelength Division Multiplexing PON
WR	Wavelength Routed
WR-WDM-PON	Wavelength-Routed WDM-PON
WS	Wavelength Selected
WS-WDM-PON	Wavelength-Selected WDM-PON
WSS	Wavelength Selective Switch

1. Introduction

This deliverable D4.4 provides an in-depth study of selected challenges that the OASE system concepts for next-generation optical access (NGOA) must address. The study builds on previous work within workpackage WP4. An earlier deliverable D4.1 [4] in workpackage WP4 (System concepts for next-generation optical access networks) provided a comprehensive background overview of the system and sub-system technologies for NGOA. Subsequent to the deliverable D4.1, there has been a deeper investigation of the candidate architectures satisfying the criteria identified in deliverable D2.1 [2]. This study of candidate architectures was presented in deliverable D3.1 [3] which proposed a set of four generic architecture concepts, each of which offers a realistic solution satisfying the deliverable D2.1 NGOA technical requirements. Two companion deliverables D4.2.2 and D4.3.2 within workpackage WP4 provided an in-depth assessment of technical and operation aspects of the candidate OASE system concepts. Deliverable D4.2.2 provided a quantitative assessment of the costs, power consumption, reach, data-rates, and client count numbers for a set of possible NGOA systems and their variants. It also discusses fulfillment of requirements on resilience, security, upgradeability, and mobile backhaul capability, which are of a more qualitative nature. Deliverable 4.3.2 provided an assessment of operational aspects of the different system concepts including floor space, power consumption and parameters associated with service provisioning, maintenance and fault management.

In this final deliverable D4.4 of workpackage WP4 we address specific challenges for selected concepts and present further research and development on these concepts performed within the scope of OASE. Section 2 describes the selection of concepts and challenges that are addressed in this deliverable. Considered topics range from validation of feasibility to aspects concerning resiliency, resource allocation, power saving techniques and further developments for higher capacity, reach and client counts. Different system concepts will address these specific challenges in different ways, and pose different problems. For example, development of resource allocation algorithms may be particularly important for TDMA based systems, whereas challenges for AON mostly involve the control and management plane. Section 3 in this deliverable addresses challenges that are common among the concepts and that are most appropriately treated in a common framework, such as fulfillment of backhaul requirements and power saving techniques. Section 4 describes individual work related to specific challenges for different system concepts performed within the scope of OASE Task 4.4. In addition to presenting research and development on selected concepts, this deliverable (Section 5) also describes work related to taking the system concept descriptions provided in D4.2.2 and producing an equipment implementation description which is then adequate for the total-cost-of-ownership (TCO) calculations performed within WP5.

2. Selection of system concepts

One of the ambitions of WP4 was to provide a short-list of NGOA candidate systems for further examination in WP5 based on considerations of technical and operational aspects. However, several of the relevant requirements identified in the deliverable D2.1 (e.g. reach, customers per feeder fibre) are specified through permissible ranges, allowing for flexibility in the system design in order to ensure that the overarching OASE objective of minimum total-cost of ownership (TCO) is met. In deliverable D4.2.2 it was found that a large number of system variants satisfy at least the lower end of these ranges. Thus, it was not possible to further select or reduce the number of candidate systems based on the technical and operational requirements from D2.1. As seen in D4.2.2, systems satisfying the high end

requirements in general are also more costly. Hence to further select the most promising candidates requires an understanding of which design parameters are most cost-driving. Only by means of such an analysis can the requirements be sharpened and a selection of a smaller number of systems or system configuations be made. With the complex relation between different system design paramenters and total cost making it difficult to isolate requirements that are more important from a cost perspective, the final discussion on selection of systems for NGOA will be part of the comprehensive techno-economic analysis in WP5.

For the remaining OASE system concepts there are various challenges that need to be addressed. For novel system concepts proposed within OASE, validation of feasibility is of primary importance. For TDMA based systems efficient resource allocation is critical where QoS requirements must be met without sacrificing performance. For NG-AON the key challenges lie in the implementation of the control plane and how to optimally control and allocate resources. For WDM-PON systems the main challenges lie in the physical layer which is primarily addressed in WP7. Aside from the system specific challenges, common challenges include support for backhaul requirements and energy saving potential of power saving techniques.

3. Selected topics

This section covers an assortment of topics that are best discussed in a common section, as they are similar for all the different system concepts. One of the key requirements for NGOA is the support for mobile/business backhaul. In section 3.1 we discuss how this mobile/business backhaul requirement can be supported by the different concepts and the amount of additional effort required in achieving this. In section 3.2 we discuss general aspects of power saving techniques that are expected to be increasingly important for any NGOA system concept. Detailed discussions, modeling, and simulations for a particular concept are handled within the respective chapter for each system concept.

3.1 MOBILE/BUSINESS BACKHAUL

The OASE requirements specify mobile/business backhaul requirements of 10Gb/s. D4.2 describes how the 10Gb/s can be provided in NGOA in general. This section, however, provides a description of backhaul within the different system concepts for NGOA in more detail. In D4.2 it was concluded that, due to bandwidth and latency requirements, backhaul needs to be provided by dedicated PtP links or wavelengths. In any NGOA architecture, backhaul could, with effort, be provided by means of dedicated 10Gb/s PtP links. However, this requires that the necessary fiber infrastructure be made available, as well as dedicated 10G backhaul interfaces and associated fiber patching, at the access node. Alternatively, different system concepts support (or could be made to support) the backhaul requirements. This will be discussed below for each of the four main architectures identified in D3.1 [3].

3.1.1 WDM-PON

The NGOA WDM-PON concept provides dedicated 1Gb/s wavelengths to each client. There are two ways 10Gb/s service could be provided over a WDM-PON ODN (considering both power and wavelength splitter variants).

10Gb/s service can be provided through 10Gb/s wavelengths in an overlay band in the WDM-PON ODN. The solution requires dedicated 10Gb/s transceiver cards at the OLT and additional patching at the CO site to connect the 10Gb/s interfaces to the WDM-PON ODN. Necessary signal amplification and dispersion compensation could be introduced to increase the reach of the 10Gb/s service such that it complies with the full reach of the WDM-PON

ODN. The main implications of this solution is a slightly increased cost for the provisioning of a backhaul service, which requires manual patching.

Alternatively, 10Gb/s service can be provided through the use of multi-rate transceivers at the OLT in order to provide 10Gb/s service at specified wavelengths. This solution has minimal implications at the CO site. The main implication is the associated cost and complexity of multi-rate transceivers at the OLT that adds to system cost.

In both cases, the additional path penalty for 10Gb/s within the long-reach WDM-PON ODN can partially be compensated by FEC.

3.1.2 Hybrid WDM/TDM-PON

Hybrid WDM/TDM-PON provides inherent support for provisioning 10Gb/s capacity to single clients. Single wavelengths can be dedicated to single clients. The 10Gb/s service is supported over the full passive system reach. However, as 10Gb/s wavelengths are commonly shared between multiple clients using TDM to provide access in the region of 300-600Mb/s, provisioning entire wavelengths with 10Gb/s service to single clients will reduce the client count.

3.1.3 NG-AON

For NG-AON, backhaul is provided by dedicated 10G PtP links. The home run case assumes dedicated fibers are provided to each client. 10G backhaul support is therefore provided by introducing 10G interfaces at the OLT site combined with necessary fiber patching. For AON with remote nodes, backhaul support can be realized through different approaches. One approach is fiber patching at the remote node to provide a dedicated fiber connection to the CO. An alternative is to install a number of 10G interfaces at the remote nodes. These solutions require either additional 10G interfaces at the remote nodes (increased CAPEX) or additional complexity for provisioning new clients, since repatching in the remote node is required (increased OPEX). A third alternative which is possible in the case of WDM-based uplink is to provide a dedicated wavelength for backhauling. In this case a wavelength would patch directly from the AWG in the remote node to the PtP link leading to the end node. However, there could be reach limitations in the backhaul system preventing the feasibility of this approach.

3.1.4 WDM-PON backhaul

For systems based on WDM-PON backhaul, similar considerations to the NG-AON apply. Backhaul is provided either by means of the 10G WDM-PON backhaul system connecting the client directly to the CO. This assumed there is an available PtP fiber connection between the remote node and the client. Provisioning new clients would then require patching at the remote node to connect the client to the backhaul system. However, there could be reach limitations in the backhaul system preventing the feasibility of this approach. The alternative is to connect the client to the customer facing side of the remote node, depending on technology. In the case of Ethernet PtP, 10G interfaces should be provided at the remote nodes to provide dedicated 10G PtP links as for NG-AON. For PON ODNs dedicated 10G wavelengths can be carried in the overlay part of the spectrum.

3.2 ENERGY EFFICIENCY

Reduction of energy consumption of networks has become increasingly important, driven by rising energy costs and an increasing awareness of global climate change. Energy efficiency in next-generation optical access networks is a critical issue, both now and also looking to future. Currently, access networks are estimated to consume approximately 90% of total (i.e.

core+metro+access) power, due to its predominantly copper-based infrastructure. Of course, this is rapidly reducing as photonics-based technologies are introduced ever more deeply into the access network. However, looking to the future, data-rates are also expected to increase at a similar exponential rate to Moore's Law (i.e. Nielsen's Law), so that bandwidth capacities are also expected to increase by similar orders of magnitude over the next 10-15 years. With power consumption generally increasing in proportion (or more optimally, to the power of 2/3 with bandwidth capacity) it is clear that energy-efficiency in the optical telecommunications continues to be an important issue. Fortunately, there are many technological approaches which can be employed to reduce the overall carbon footprint of photonic networks.

Section 3.2.1 presents on overview of different aspects related to reducing the power consumption of NGOA. In the original assessment of equipment power consumption presented in D4.2.2, the effects of potential power saving modes were excluded. However, as the optical network unit (ONU) power consumption represents a relatively large portion of the total network power, low power modes at the ONUs are particularly important. In section 3.2.2 the impact of ONU power saving modes within the different technologies is evaluated. Section 3.2.3 describes stochastic power saving approaches applicable to different segments in the network and which can be used to gain further savings. Finally, in Section 3.2.4 we discuss alternative energy solutions that investigate ways of providing access to low cost and clean energy instead of reducing network power consumption. In particular, we consider a solution for solar powered remote nodes.

3.2.1 Reducing network energy consumption

In order to identify suitable areas and mechanisms for power saving, the main contributors to power consumption must be identified. If we assume that power consumption for common functions like Layer-2 aggregation, management or inefficiency of Power Supply Units (PSUs) is in the same range for all NGOA contenders, then a somewhat transceiver-centric, implementation-specific analysis if the main power-consumption contributors results. For example for a WDM-PON the main consumers are:

- Key components OLT
  - Laser array (semi-/uncooled)
  - Laser driver array
  - PIN (APD) array
  - TIA, LA array
  - Optional pre-amplifier
  - Shared locker (incl. DSP, if applicable)
  - (L2) Port aggregator
  - Commons (shelf PSU, management I/F, etc.)
- Key components ONU
  - Laser, no wavelocker, no TEC
  - Laser driver
  - PIN or APD
  - TIA, LA
  - Small FPGA or DSP for ECC, tuning (if applicable)
  - Commons (system PSU, management I/F, client SoC, etc.)

Note this list assumes identical power consumption for common function like client interfaces, displays, PSU. Strictly, this is not true for the OLTs. Different approaches (AON, WDM-PON, Hybrid PON) may require different amounts of shelves (and, finally, racks) and may hence lead to slightly different power consumption in the OLT. Strictly, identical

common-parts power consumption does not apply to ONUs, neither. For example, an ONU of a WR-WDM-PON does not need to provide burst-mode TDMA upstream functionality, whereas, an ONU of a 10-Gb/s Hybrid WDM/TDMA-PON may have 10GbE client interfaces in order to provide ultra-high burst bit rates. In this case, the client-side power consumption will clearly differ from a 1-Gb/s WR-WDM-PON ONU, for example. These effects are further blurred by different power-saving modes employed in the client side or common parts of an ONU. In general (and without further detailed study), it can be concluded that client-side power consumption will be lower the less functionality and bandwidth (e.g., less MAC functionality like TDMA, less per-wavelength bit rate) needs to be handled. From this, slight advantages for the client side (the System-on-Chip, or SoC) for WR-WDM-PON ONUs can be derived. New G-PON SoCs already can consume as little as <1 W, hence larger differences occur with respect to the PON interface (the (colored) transceiver) therefore power-save modes for this interface are considered.

Power saving over the normal working conditions can be achieved by partial deactivation of subsystems or components or, possibly, by bandwidth throttling. The first case is descussed more in detain in Section 3.2.2. In the latter case, it is expected that less power needs to be consumed in the electronic domain if smaller bit rates are processed. This, however, requires multi-bit-rate / multi-clock design of all related components and may be contradicted by resulting effort and cost.

With regard to power consumption and the related saving through power-saving modes, the most useful power-consumption metric must also be identified. This is particularly true when (as is the case within the scope of OASE) high sustainable bandwidths are required. Two overall metrics can be used, power-per-client [average W/client], and power-per-Gb/s [W/Gb/s]. In addition, there is a clear conflict between lowest end-to-end (or per-client) power consumption, and power consumption in the central offices. Clearly, power consumption, and in particular its per-rack density, is an important parameter for near-future central offices (which, from today's perspective, in many cases will not be prepared to allow the increased total power consumption for massive site-reduction scenarios[1]). Also, from the network operators' view it is the OLT- and hence central-office-related power consumption that counts (because this is the portion of end-to-end power consumption which has to be paid by the operator, possibly complemented by the portion which results from active remote nodes). On the other hand, on a global scale, it is clearly the end-to-end power consumption which urgently requires reduction and limitation in order to reduce and finally limit global IT-related carbon emissions.

For NGOA low-power design will be required from the beginning. In analogy to design-to-cost, this may be referred to as design-to-low-power (DTLP). The related design process must consider all relevant components choices, subsystem implementations, and also modes of operation. As an example for the latter, even in a WDMA WDM-PON (i.e., dedicated wavelengths for dedicated clients), burst-mode operation may be chosen. In single-channel WDMA, this will have little effect on bandwidth efficiency, but it will shut down transmitters in periods of small utilization. Efficiency of single-channel burst-mode operation for WDMA systems is for further study outside the scope of OASE.

[1] This results from both, site design limitations and short-term capabilities of local utilities. Conventional point-of-presence design may limit per-rack power consumption including HVAC to ~2.5 kW. On the other hand, highly integrated NGOA systems can exceed 5 kW per rack, though being much more energy-efficient. In addition, utilities plan in much longer cycles, e.g., 10…25 years. Typically, they will not be in a position be increase power supply to a certain site, on short notice, say, from 1 MW to 3 MW.

For all NGOA contenders, the client-side interfaces of the ONU also have to be considered when it comes to efficient power-saving modes. This is particularly true since the client-side interfaces will, over time, develop towards very fast (broadband) interfaces as well. Here, an interesting difference between WDM/WDMA-PON (both, WS and WR types) and shared approaches (e.g., WDM/TDMA-PON) can be derived. For WDM-PON, per-wavelength bit rates of 1.25 Gb/s are expected to be sufficient for the Year-2020 time scale, and possible some years beyond. At such points in time the client-side interfaces may run GbE or even Fast Ethernet, depending on the application. In a hybrid WDM/TDMA-PON, higher per-wavelength bit rates will most likely be implemented. Depending on US/DS symmetry requirements, 5/10 Gb/s or 10/10 Gb/s are the most likely Upstream/Downstream bit rate combinations. This would imply that 10GbE client-side interfaces could be implemented. Only then ONUs could take advantage of ultra-high burst-mode bandwidths. (The alternative would be to implement suitably large buffers in the ONU which in turn add to ONU power consumption.) Since client interfaces also have power consumption which increases with bandwidth, they need to be considered for efficient power-saving modes. As said, this holds for all NGOA contenders. This argument also holds for 40-Gb/s-per-wavelength TDMA or OFDMA approaches. In order to compensate for the lack of sustainable bandwidth, ultra-high burst bit rates enabled by ultra-high-speed client interfaces should be foreseen. This, in turn, will increase power consumption.

Irrespective of power-save mode efficiencies, the power-consumption differences for SoCs which support 1 Gb/s, 10 Gb/s or even 40 Gb/s can be derived from the respective Ethernet interfaces. SoCs for 1 Gb/s exist which consume <1 W. Latest 10GbE interfaces (not SoCs, which do not exist yet) can consume similarly low power (~1 W). Implemented in latest (40 nm, 28 nm) CMOS, a 10GbE SoC consuming ~1.5 W is therefore considered feasible. For 40GbE, however, the latest interfaces (CFP modules) consume ~8 W. Therefore, it must be concluded that 40G SoCs potentially increase ONU power consumption to beyond EU Broadband Code of Conduct allowances.

Finally, the question of a one-fits-all general-purpose ONU vs. a certain limited number of specialized ONUs has a strong influence on power-saving efficiency. A single one-fits-all design may have advantages in inventory, planning, installation and possibly per-unit cost. On the other hand, too much functionality, causing too much power consumption and possibly also corrupting efficient power-saving modes, may have to be implemented. This may lead to a cost trade-off, and it may lead to disadvantages with regard to lowest-possible power consumption and highest power-saving-mode efficiency.

3.2.2 Power saving modes

In this section, we evaluate the the impact of ONU power saving modes within the different NGOA architectures. ITU-T G.sup 45 proposes a number of power saving modes, namely power shedding, doze, deep sleep and fast (cyclic) sleep. These approaches differ based on the parts of the ONU that are switched off. The power shedding approach shuts down the unused ONU interfaces. In “doze” state, non-essential functions are powered off with an additional powering off of the ONU transmitter while the receiver remains on. In sleep state, non essential functios and both the ONU transmitter and receiver are turned off. The functional blocks are shown in Figure 1. Deep and fast sleep approaches differ in the period of sleep and, obviously, the deep sleep approach has comparatively longer periods of sleep. Note that, there can be many classes of power shedding approach based on the interfaces that can be shut down. In addition, a power saving scheme can use a combination of shedding, doze and sleep approach. We digress here to mention the difference between the term ‘state’ and ‘mode’ as

used in this section: i.e. a mode is a combination of states, according to the traffic load. For example, doze mode is referred to as the cyclic transitions between power shedding and doze state, and sleep mode as the cyclic transitions between power shedding and doze/sleep state.

To evaluate the power consumption of the various architectures, we developed the ONU power consumption model, as shown in Figure 1. The model takes data from a large survey of component datasheets and was initially proposed in [7]. The ONU may support gigabit Ethernet (GbE), digital optics (DO), analog optics and multimedia over coax alliance (MoCA) capabilities. The miscellaneous and power conversion losses are assumed at 5 % and 20%, respectively. The memory requirement in different concepts may vary, and we have assumed a power consumption of 30 mW per MB of memory [8]. The system on chip (SoC) and Dual subscriber line interface circuit (SLIC) power consumptions are assumed for a simple point to point link with no additional functionalities. For a specific system, we add the power consumption for special functionalities like TDMA, dispersion compensation (DC), optical amplification (OA), and digital signal processing (DSP), as required. For example, we add TDMA power consumption for hybrid TDMA/WDM (TWDM) PON and GPON, and TDMA, DC and OA functionality for HB-TDMA-PON. HB-TDMA PON is a simple power splitter based with 40 G downstream and 10 G upstream and is included as it has enormous potential to benefit from low power modes. DSP is required for system concepts like orthogonal frequency division multiplexing (OFDM) PON or UDWDM PON which are not considered in the evaluation. Table 1 gives the detailed power consumption of various components for active, power shedding, doze and sleep states.

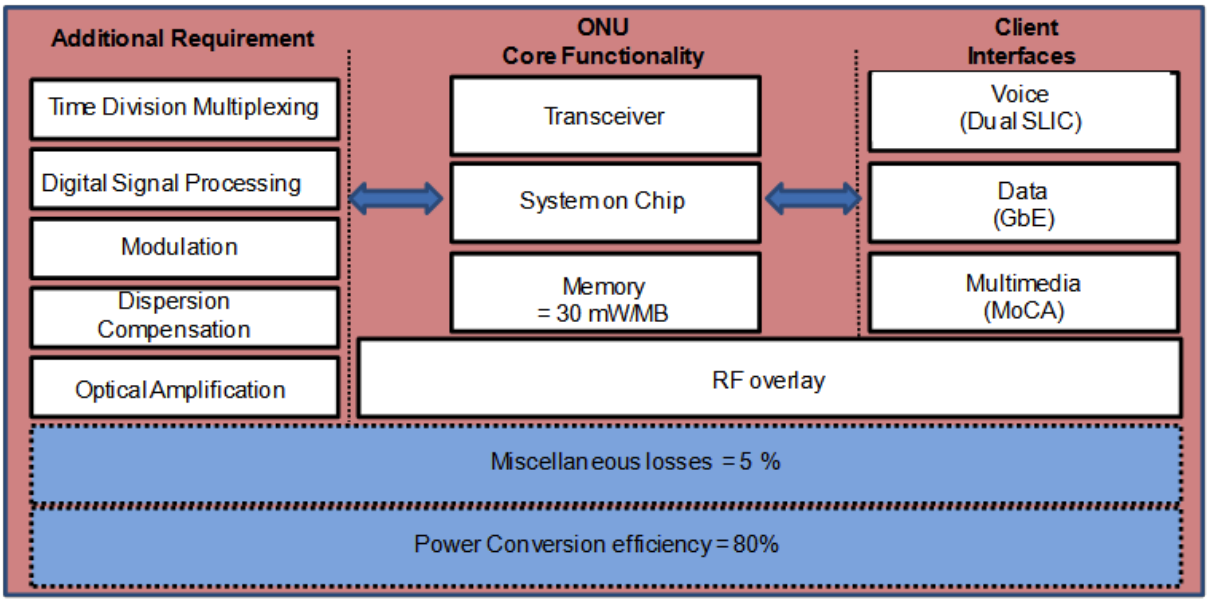

Figure 1: ONU power consumption model

Table 1: Power consumption values in mW

Components	Active	Power Shedding	Doze	Sleep
SoC	1200	700	535	300
Dual SLIC	250	150	150	150
GbE	700	0	0	0
TDMA	500	500	500	250
Optical Amplification	2000	2000	2000	0
Dispersion Compensators	2000	2000	2000	1000
Digital Signal Processing	4000	4000	4000	2000
Modulators	500	500	500	250
1 G Fixed TRX (for GPON/AON/PtP)	700	700	350	0
1 G Tunable TRX with APD (for WDM PON)	1700	1700	900	0
1 G Reflective SOA based TRX with APD (for WDM-RSOA)	1300	1300	900	0
10/5 G Tunable TRX with APD (for TWDM PON)	2500	2500	1670	0
40/10 G TRX (for High Bitrate-TDMA PON)	4000	4000	3200	0

Evaluation and simulation results

Several mechanisms to facilitate sleep mode (like physical layer operations and maintenance (PLOAM), ONT/ONU management and control interface (OMCI) and implicit signaling) are proposed. Furthermore, interleaved polling with adaptive cycle time (IPACT) is considered as the dynamic bandwidth allocation (DBA) algorithm for scheduling upstream transmission in TDMA PON (particularly Ethernet PON). However, IPACT does not support sleep mode and thus we have modified IPACT and propose a new DBA algorithm, which we refer to as the IPACT with Sleep Mode Awareness (IPACT-SMA) [9], to evaluate sleep mode gains in the various NGOA technologies. In IPACT, downstream traffic for an ONU is transmitted on a first come first serve basis, and thus the ONU receiver has to be on at all times. First of all, we eliminate the necessity of an ONU to be awake all the time and instead utilize a system where the OLT informs an ONU about the awake period. The downstream traffic is transmitted during this awake period. This necessitates buffering for both the downstream and upstream traffic. Note that buffering in this manner introduces delay and jitter in traffic which has to be within the quality of service (QoS) limits. The QoS limits are also to be considered for backhauling. Further, we maximize the alignment of the transmission of upstream traffic and reception of downstream traffic for an ONU, maximizing the time during which an ONU can sleep. The optical line terminal (OLT) determines the sleep period according to the upstream and downstream bandwidth backlog of an ONU and grants a transmission slot (TS) according to:

$$TS = Min\{\frac{T_{cycle}}{N_u}, Max\ (\frac{B_u}{R_u}, \frac{B_D}{R_D})\} \qquad (1)$$

where *Min*/*Max* represents the minimum and maximum value of the function, T_{cycle} is the cycle time in which ONUs are polled, N_u is the number of users, B_u and B_D are the backlogged upstream and downstream bytes for an ONU, R_u and R_D are the upstream and downstream data rate, respectively. Note that the ONU may be allocated a longer transmission slot than it requested, in which the newly arrived packets between the time of a previous request and present grant are transmitted. If however, the ONU has no additional packet arrivals, it goes to doze mode. The ONU sleeps for a period of T_{cycle}- TS. The proposed algorithm is adopted to study the sleep mode in all NGOA architectures. For example, for WDM PON, PtP, and AON, N_u is chosen as 1.

In OPNET, we have simulated various NGOA architectures, with a cycle time of 5 ms, an overhead time for clock recovery (T_o) of 125 µs, an upstream and downstream average user rate of 500 Mbps and a peak user rate of 1Gbps. The latter value is chosen as it is one of the key requirements of NGOA architectures. The NGOA architectures that are chosen for evaluation are GPON, HB-TDMA PON, WDM-PON with tunable lasers at OLT (WDM-TL), WDM-PON with RSOA (WDM-RSOA), PtP, AON, and passive and semi-passive TWDM-PONs. Different NGOA architectures have different advantages and are proposed for different reach and fan out scenarios. As we are evaluating only the ONU power consumption, the number of users does not impact our study. However, what matters is the upstream and downstream line rate of the architectures as it is one of the main factors influencing sleep and doze periods.

Figure 2 gives the power consumption in sleep (S), doze (D) and active (A) states and the considered downstream and upstream line rate of the architectures. The burst factor (BF) is the ratio between the upstream line rate and the average user rate, and the asymmetricity factor (AF) is the ratio between the downstream and upstream line rate. Figure 3 gives the variation of the sleep period with BF and AF. An ONU can sleep for more time with a higher BF. Also AF affects the sleep period as, with a high downstream line rate, the reception time of downstream traffic is smaller resulting in a better alignment of upstream and downstream transmission slots. Figure 4 gives the power consumption of the different NGOA architectures when applying doze and sleep modes.

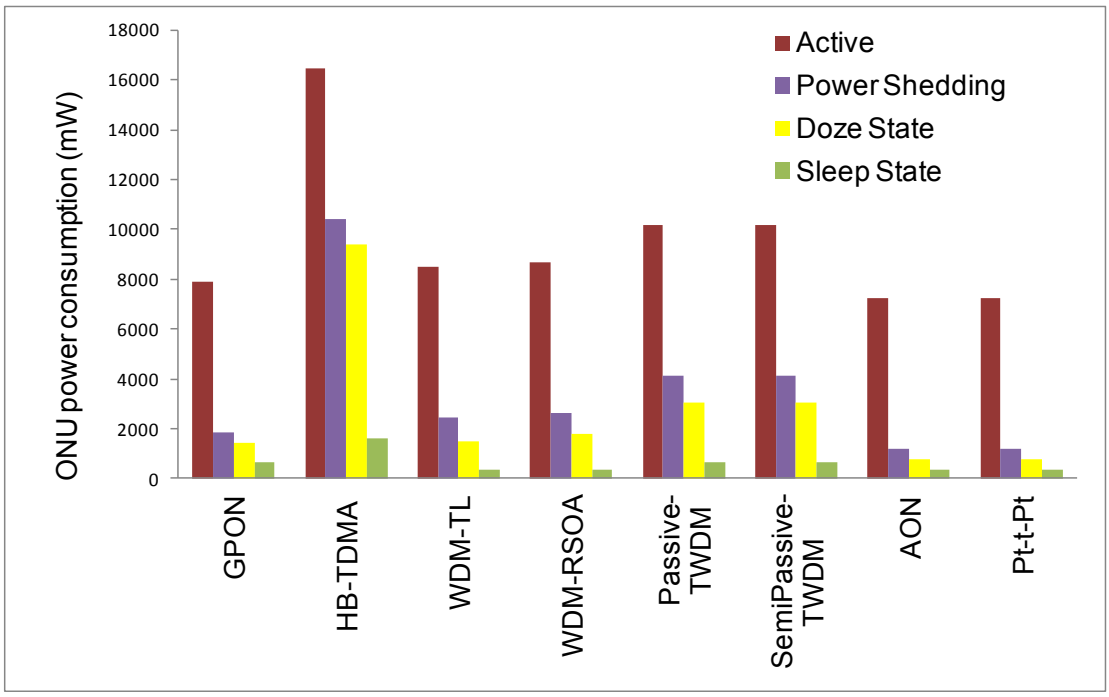

Figure 2: The power consumption of various NGOA architectures in various low power states.

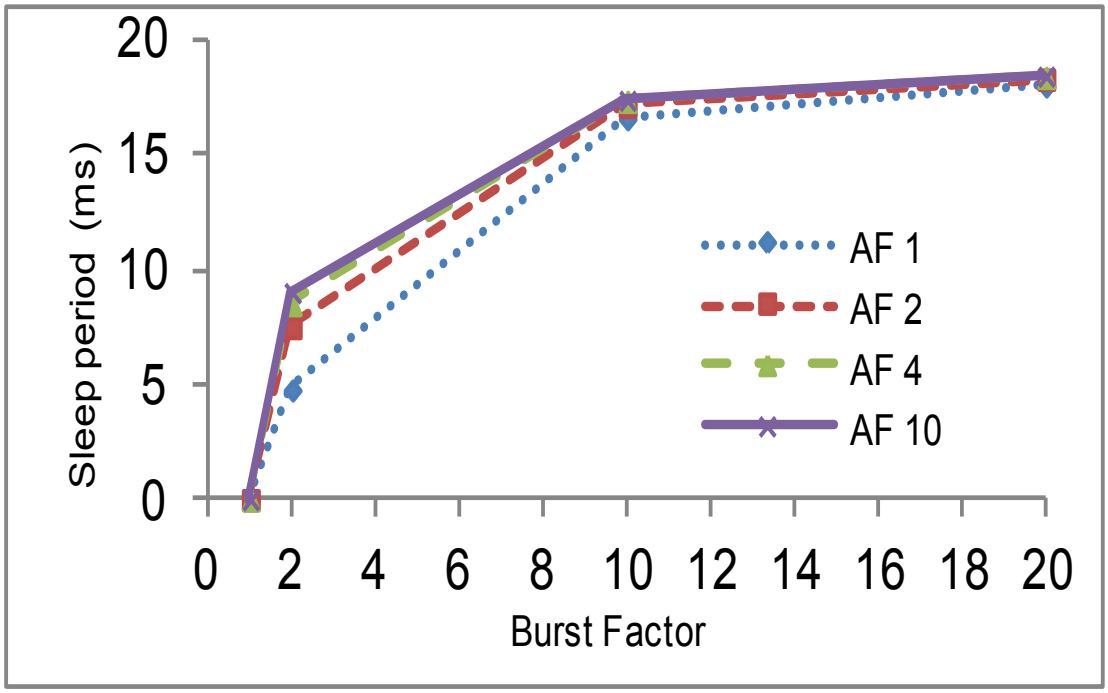

Figure 3: Sleep period as a function of the burst factor (BF) and asymmetricity factor (AF)

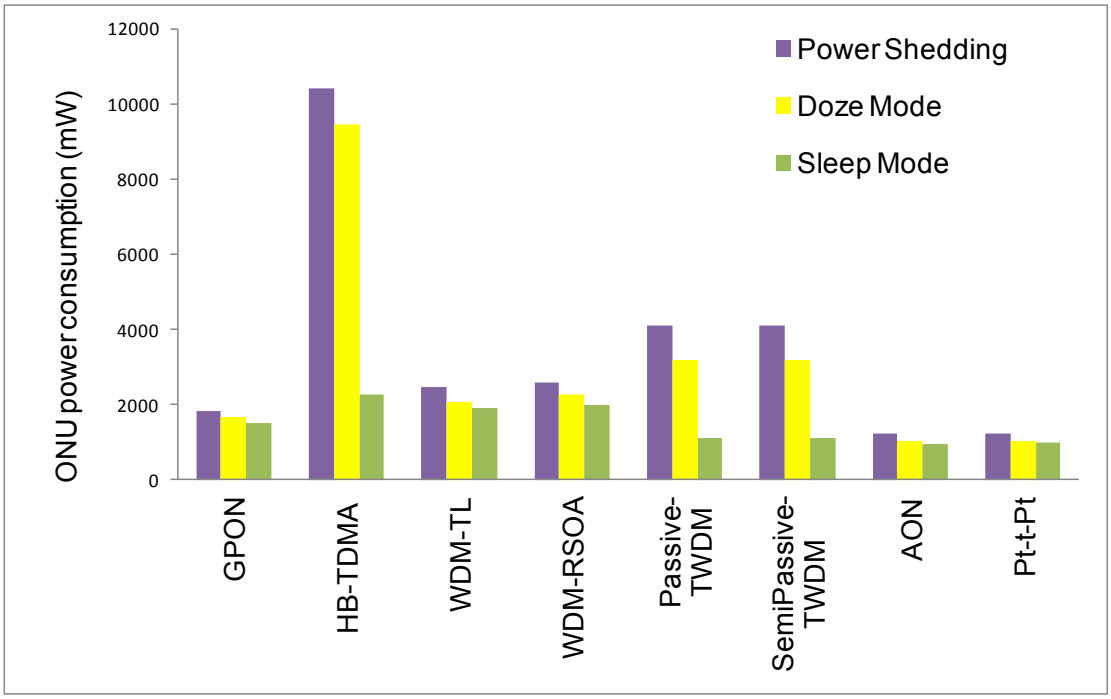

Figure 4: The power consumption of various NGOA architectures in various low power modes.

3.2.3 Master-Slave System Configurations

With regard to access networking, innovation at the customer premises to reduce energy consumption is an on-going endeavour assisted by work such as that outlined in 3.2.1 above, with results reflecting the general reductions in carbon footprint in line with that of consumer electronics in general. In this regard, the greatest energy efficiency savings in the access network environment are to be accrued further up the chain, towards the core, principally in the central office (CO) and central access node (CAN) locations. Here, the largest sources of power dissipation are again found in the rack equipment, and similar to the case of core IP routers, the energy consumption is in proportion to the amount of processing that takes place. As such, a key contribution to reducing the power dissipation in the CAN/CO is to minimize the fixed overheads associated with data processing, achieved in part by the use of hybrid equipment approaches. Here we discuss the use of master-slave equipment configurations (as shown in Figure 5 and Figure 6) to minimize the power consumption of network equipment by surfing the statistics of the data traffic.

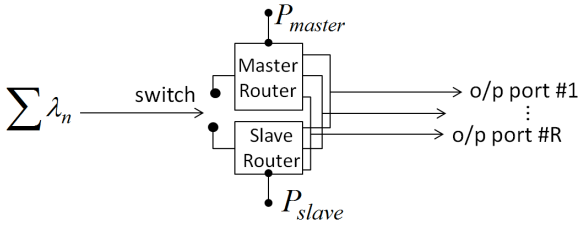

Figure 5: Use of a master-slave parallel configuration for stochastic energy-efficient management of IP routers.

In particular, rather than attempting to design a single item of equipment to exhibit a power consumption profile that tracks the intensity of traffic demand (i.e. so that the equipment

exhibits a high differential energy-efficiency), we employ a dualized configuration of the equipment. In this case, the master equipment can deal with the periods of time when there is a high traffic demand, and which is also associated with a high powering requirement; whilst the slave equipment has been optimally designed to cope with smaller traffic loads, up to a threshold level, and also to consume a significantly lower amount of power. This master-slave configuration is most appropriate for those items of telecoms equipment that exhibit a relatively inelastic energy consumption profile with respect to traffic demand, e.g. IP routers are well known to continue consuming up to 90% of maximum power even in their idle states. Of course, the design of next-generation IP routers that exhibit a more elastic power consumption profile (i.e. the fixed energy dissipation overhead component is reduced) is an important research topic but here we discuss an alternative approach that potentially offers a more convenient and generic alternative solution to this problem.

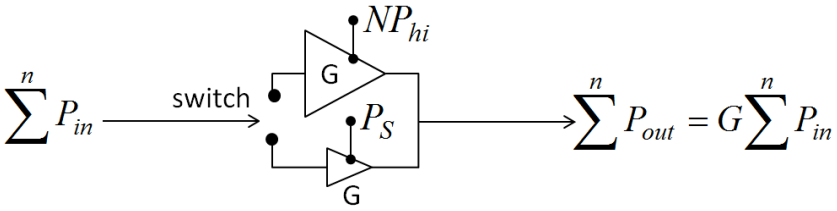

Figure 6: Dual-rail (master-slave) switching amplifiers for optimal energy efficiency operation.

In addition to the advantages of statistical multiplexing to increase the efficiency of utilization of networking resources, network stochastic dynamics also allow interesting approaches towards increasing the inherent energy efficiency of photonic networking. In particular, the theoretical studies in the area of stochastic energy efficiency techniques we present here can offer greater than 90% improvement in the energy efficiency of operation in an access network. We take advantage of the central limit tendency of an ensemble of independent stochastic variables, where the variables can either be a set of wavelengths, or an ensemble of data packets arriving in a single (or multiple) fibre(s) at a routing node. In the case of a router or statistical multiplexer, Figure 7 schematically shows how an ensemble of packets on a set of wavelengths arrives at node, which has a parallel set of master and slave routers. If the traffic intensity is high then the master router is powered up (switched on) to service the packets and is associated with a (high) power consumption P_{master}. However once the traffic intensity reduces below a given threshold, then the master router is powered down, and the smaller slave router switched on to operate at a lower power consumption, P_{slave}. Depending on the traffic intensity (load factor, α) and the relative powerings of the master-slave routers, significant power savings are possible. Such a stochastic approach offers a wide range of application. For example, it is also applicable to optical amplification, (e.g. EDFAs, SOAs, and co-propagating Raman amplifiers) which also tend to exhibit a fixed power consumption characteristic independent of traffic load. In the case of optical amplification, the ensemble of independent variables is the set of wavelength channels in an optical fibre, e.g. encompassing all of the S, C and L bands, and potentially comprising more than 200 λ channels. It should be noted that, in Gaussian statistics, confidence levels in the accuracy of the statistic tends to vary as $1/\sqrt{N}$, such that for N=100 independent channels, we can assume a 90% degree of confidence that out statistical approach will yield the predicted improvements in energy efficiency.

We now perform an analysis based on a master-slave configuration of optical amplifiers as shown in Figure 6, but note that the method is also straightforwardly applied to routers and

similar switching/aggregating equipment. Here, we assume a set of N independent wavelength channels, each of a uniform optical power P_{hi} when carrying data, and a nominal power P_{lo} when data is not present on that channel. For a variety of reasons (e.g. operating lasers only just below threshold, as well as the possibility of noise, amplified spontaneous emission (ASE) or spectral regrowth etc.) P_{lo} does not necessarily have to equal zero. Clearly, when all N channels are carrying data, the total instantaneous power in the optical fibre is $N \times P_{hi}$; whilst when all the channels are not populated with data, the total power is $N \times P_{lo}$. Through the implications of the central limit tendency (alternatively, the law of large numbers) we can assume that for large N, the distribution of possible powers in an optical fibre will tend towards a Gaussian, with a peak (i.e. most likely, or modal position) power of $N \times (P_{hi} + P_{lo})/2$ located when $N/2$ channels are each carrying an instantaneous power of P_{hi}. Even in the case where the λ-channels feature on-off keying (OOK) signals, such that the power spectral density of an individual channel consists of two delta functions at P_{hi} and P_{lo} respectively (see Figure 7) multiple convolutions of such a pair of delta functions will still yield a Gaussian distribution (i.e. proportional to the well-known Pascal triangle coefficients associated with the binomial expansion, as N tends towards infinity.) In the more general case, where there is a probability that a wavelength channel is being used to carry data (e.g. particularly for a burst-switching mode of operation, or for a varyingly loaded circuit-switched network), then the resulting distribution of power follows the Poisson distribution, where the loading factor l, is given by $l = \alpha N/2$, where α is the probability of a wavelength channel carrying data. In which case, the resulting probability that out of a set of N channels, n are carrying a signal is given by:

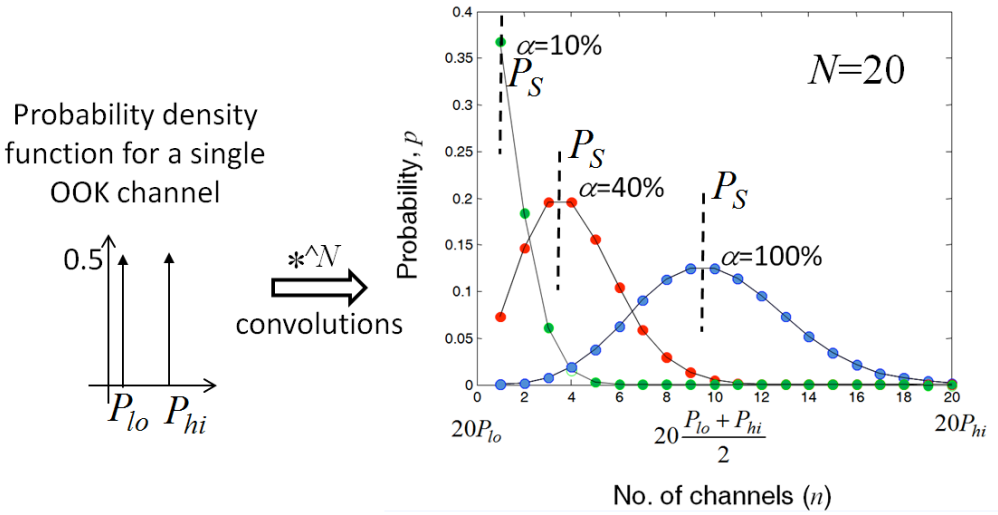

Figure 7: Power (probability) density curves for a single channel, and for multiple wavelength channels in an optical fibre, featuring different loading factors α, with varying optimum switching powers P_s.

$$p(n,l) = \frac{l^n e^{-l}}{n!} \tag{1}$$

Figure 7 plots the results for a small N=20 channel example, and with the load factor varying as $\alpha = 100\%, 40\%$ and 10%. As the loading factor α tends towards 100% then, as can be seen in Figure 7, the resulting distribution becomes ever closer to the conventionally symmetric Gaussian curve with a mean of $N/2$. However, as the loading factor α reduces, and

the number of wavelength channels in use at any one time becomes more sparse, the resulting distribution becomes asymmetric (skewed) with the maximum (modal) point (indicated with the vertical, dashed line and the symbol P_S) also occurring at a lower aggregated power.

Similar to the operational power consumption characteristics of IP routers (which exhibit a high fixed power dissipation even at low loads) optical amplifiers tend to operate at a fixed pump power and constant gain, independent of the power of the input signal(s) up to a threshold input power, after which saturation effects start to occur, e.g. clipping. On the one hand, an amplifier is at its most energy efficient as it operates close to its saturation point; but signal distortion (i.e. clipping and spectral regrowth etc.) occurs when an amplifier is driven into saturation. As such, without considerations of the power dissipation (power loss) of an amplifier for a constant gain G, its optimum operating point is when it accepts an input power of P_{in} such that the output power $P_{out}=GP_{in}$, where P_{out} corresponds to its maximum threshold power before saturation starts to occur. Maximum efficiency occurs when the power required to operate the amplifier equals the maximum output power (assuming 100% internal efficiency of amplifier operation), i.e. $P_{amp} = P_{out}\big|_{\max}$. In order to maximize energy efficiency at a minimal complexity, we can also adopt a master-slave configuration by employing a dual amplifier rail design as indicated in Figure 6. Here, for an aggregated input power $\sum_n P_{in}$ below a threshold (switching) power P_S, the lower amplifier (requiring operational power $P_{slave} \equiv P_{amp} = P_S$ at maximum gain G) is used. As such, the total power consumed by the lower amplifier is $P_S\left(\equiv P_{slave}\right)$, as long as the aggregated input power $\sum_n P_{in} \le P_S$. However, once the aggregated input power exceeds the threshold power P_S then the dual rail amplifier switch routes the optical signals to the upper, more powerful (master) amplifier, which provides the same gain G, but has an operating power consumption of $P_{master} \equiv P_{amp} = NP_{hi}$. The total power dissipated by the master-slave configuration of devices is given by the probabilistically-weighted sum of the individual power consumptions of the two items of equipment:

$$P_{total} = P_{slave}\int_0^{P_S} p(n)dn + P_{master}\int_{P_S}^{N} p(n)dn \tag{2a}$$

which in the specific optical amplifier case is also given by:

$$P_{total} = P_S\int_0^{P_S} p(n)dn + NP_{hi}\int_{P_S}^{NP_{hi}} p(n)dn \tag{2b}$$

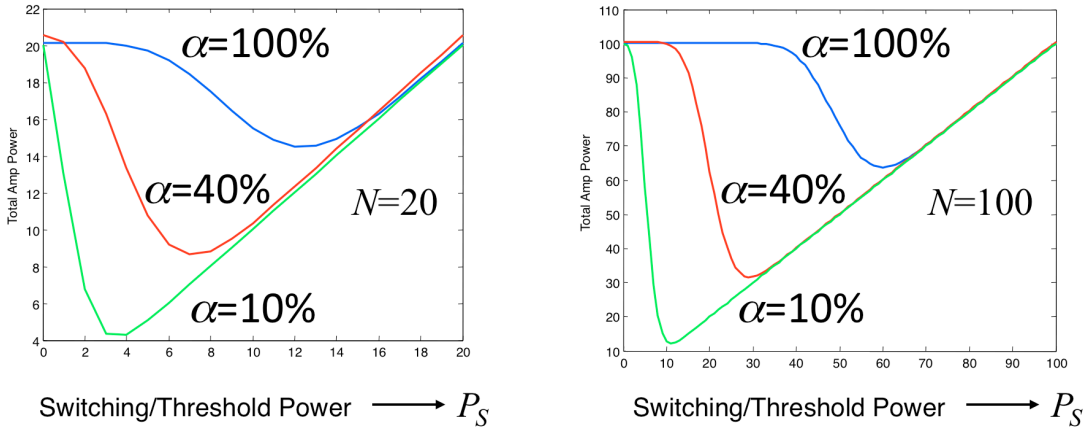

Figure 8: Total operating powers of the amplifiers, for (a) *N*=20, and (b) *N*=100 wavelength channels

Figure 8 plots the total power as given by equation (2b) for the case of a master-slave optical amplifier configuration, for various traffic loads, as the switching threshold P_S is varied. The two figures of Figure 8 show the cases for N=20 and N=100 wavelengths in the optical fibre, and indicate that even for modest numbers of wavelengths (i.e. N=20) there is an appreciable variation in total amplifier power, with a clear optimum value for P_S in each case for the varying traffic loads α. The case for N=100 shows the same tendency, but also accentuates the fact that as N increases towards infinity, there is a sharp "diagonal" tendency for the total power to increase linearly with the threshold or switching power P_S. Also clear is that the optimum threshold switching power P_S reduces as the traffic load α reduces. As the threshold power P_S reduces towards zero, then most of the total power P_{total} is due to the large power requirement of the master amplifier, and hence the total power requirement is large, and in fact becomes the master amplifier power P_{master} when P_S=0. As the switching threshold increases above zero, then the slave device's lower operating power P_{slave} becomes more evident, and the total power P_{total} starts reducing until a minimum is reached as can be seen in the graphs. The total power then starts increasing again with increasing P_S as the master device's larger power starts to dominate again.

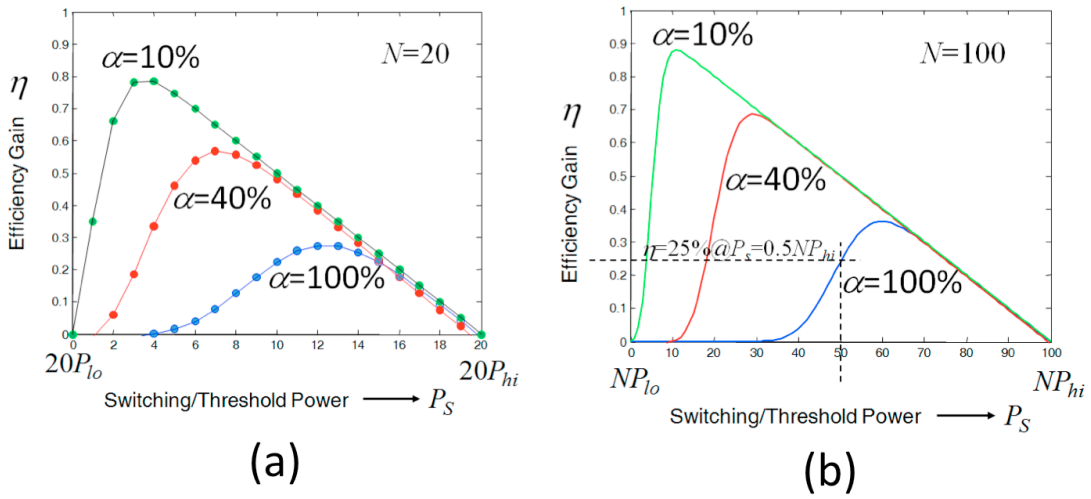

Figure 9: (a) Plot of marginal improvements in energy efficiency gain (η) for varying switching/threshold power P_S, for varying load factors α, and N=20 channels. (b) Same plot of marginal improvements in energy efficiency gain (η) for varying switching/threshold power P_S, for varying load factors α, and N=100 channels.

The overall energy saving possible in such a scheme is given by the appropriate weighted summation (integration) of the operating powers of the two optical amplifiers divided by the power of the master device (amplifier) – i.e. the energy saving comparison is made with the case of the master device being the sole device being used:

$$\eta = 1 - \frac{P_S \int_0^{P_S} p(n)dn + NP_{hi} \int_{P_S}^{NP_{hi}} p(n)dn}{NP_{hi} \int_0^{NP_{hi}} p(n)dn} \tag{3a}$$

$$\eta = 1 - \frac{P_S \int_0^{P_S} p(n)dn + NP_{hi} \int_{P_S}^{NP_{hi}} p(n)dn}{NP_{hi}} \tag{3b}$$

As might be expected, for the two extreme cases of P_S=0 and P_S=NP_{hi} when the master amplifier is used for 100% of the time, then the marginal improvement (gain) in energy efficiency reduces to zero. But between these two extreme cases, the energy efficiency improvement shows a useful gain, particularly for the case of low traffic loads, $\alpha \to 0$. In performing a "sanity check" on the results (which show surprisingly large energy efficiency gains, and a somewhat unintuitive position of the maximum energy efficiency improvement) the most transparently intuitive case is for the maximum loading factor $\alpha = 100\%$, where we see that half the time the lower amplifier is used for a threshold switching power of $P_S = NP_{hi}/2$, such that the overall energy efficiency improvement would be $\eta = 25\%$, as indicated in Figure 9(b). We note that these results have also been derived by assuming the best possible case, where $P_{lo} = 0$.

However, as already indicated above, with regard to Figure 9(a) although intuitively we might believe that the optimum position for the switching threshold in the case of the traffic loading factor $\alpha = 100\%$ is at $P_S = 0.5NP_{hi} = 10P_{hi}$, in fact as can be seen, even greater energy efficiency gains can be accrued by placing the switching threshold at $P_S = 13P_{hi}$, with an associated energy efficiency gain of close to 27.4%. Indeed, in Figure 9(b) we can see that for the case where N=100 channels, at maximum loading $\alpha = 100\%$, the maximum energy efficiency gain can be increased to $\eta = 37.1\%$ with an optimum switching threshold power at $P_S = 0.6NP_{hi}$. Of even greater interest is that Figure 9(a) & (b) also indicate that as the loading factor α reduces, ever greater marginal increases in energy efficiency can also be achieved, e.g. for a loading factor $\alpha = 40\%$ we find that $\eta = 69.4\%$ at $P_S = 0.3NP_{hi}$; and for a loading factor $\alpha = 10\%$ we also see that $\eta = 88.8\%$ at $P_S = 0.1NP_{hi}$. Clearly, there appears to be a trend that as $\alpha \to 0$ then the optimum switching power needs to reduce to approximately $P_S \approx \alpha NP_{hi}$, with the marginal increase in energy efficiency savings as compared to the unswitched situation tending towards $\eta \to 1 - \alpha$.

Additional Advantages of Master-Slave Approach

An operational aspect to the master-slave design approach described here is related to switching between the master and slave devices when the threshold decision level is crossed. For a single device which is able to successfully operate in sleep- and idle-modes (i.e. it is fully elastic in its ability to track the instantaneous traffic demand presented) a key aspect to its success is the ability to turn back on (as well as off, in the first place) in a very short time –

i.e. at best within the time duration of a single packet. Technically, this is a very challenging requirement, and is one of the major objectives (obstacles) of research programmes in this area. However, the master-slave configuration allows a relaxation in the speed of the powering-down and –on time requirements. Rather, it is only the actual (simple) switch at the input to the master-slave configuration that has to be able to exhibit the very fast switching times. This is because close to the threshold, both master and slave devices can be in a switched-on state, in anticipation of a potential crossing of the threshold. On the one hand, if the traffic demand is below (but close to) the threshold, the master device can be switched on in anticipation of the threshold being crossed. Hence there is a time ΔT when both master and slave devices are concurrently active. The time ΔT is likely to be significantly longer than the individual bit-rate time-period, but closer in magnitude to the average packet length time. In the same way, when the traffic is above threshold and the master device is in operation, should the traffic intensity start reducing and approach the threshold, then the slave device can likewise be powered-up in anticipation of the threshold being crossed. As such, a "hysteresis" threshold decisioning approach can also be adopted to avoid high-frequency switching between the master and slave devices should the traffic load have a tendency to oscillate about the threshold level. In this case, the threshold decision level can be varied to create a hysteresis effect so as to minimize unnecessary high-frequency switching between the two devices.

The optimum value of ΔT requires a joint-optimisation approach. For example, such a concurrent time of operation ΔT comes at the cost of a slight reduction in the overall energy-efficiency of operation of the overall master-slave configuration, since both devices will be consuming energy at the same time for the short period ΔT. However, since ΔT isn't necessarily associated with a high-speed value, no particularly undue demands are placed upon the technical specifications of the equipment.

It is also worth pointing out that since there is a degree of capacity redundancy in the master-slave configuration, this offers the possibility of greater resilience (and hence reliability) during operation. In addition, the more relaxed technical specifications, and the possibility of having slower switching-on and –off times (also with overlapping operating times) means that master-slave devices can be operated in a somewhat less "aggressive" or "hard" fashion. In this way, the devices may be expected to exhibit greater longevity before failure, i.e. higher mean-time before failure (MTBF) times.

The relative balance between the higher CAPEX associated with the dual deployment of a master-slave configuration (albeit, each individual device with a lower specification of switching-on and –off speeds), and the lower associated OPEX costs (due to a lower overall energy consumption, and a higher reliability) is also an issue, which we consider in the next section in the context of upgrade scenarios.

Upgrade Path Optimisation for Routing and Switching Equipment

In this section, we apply the above analysis to the specific case of optimisation of IP router power consumption, and also consider how to apply the technique to optimised capacity-upgrade scenarios. In this aspect, we exploit the empirical assumption that router power consumption P tends to increase sub-linearly with capacity C, i.e. $P \propto C^{2/3}$. Although IP routers are currently more associated with core networking, when looking over a longer-term horizon to NGOA architectures, it is clear that core technologies tend to migrate down to the metro/access networks. In addition, when considering longer-term NGOA architectures, one important technology trend is for the introduction of ever-higher system functionalities and network-intelligence nearer towards end-users. For example, there is an expectation for advanced networking functionalities at active remote nodes (ARNs), e.g. which also act as the

location for a radio access node for mobile broadband access, as well as the servers for a CDN with commonly-accessed data sets stored in closer proximity to end-users. Aggregation and routing functionalities will also be performed at such active RN sites, thus requiring the presence of router switches at these locations. In addition, with access data rates and bandwidth also expected to continue their exponential increase, the size (capacities) of such ARN routers, aggregators and functional switches will also similarly increase, with their associated ever-higher energy consumptions. In which case, the master-slave approach outlined here, whose quantitative analysis is provided through the example of IP routers, is indeed of significance for energy-efficiency optimization as applied to the NGOA context.

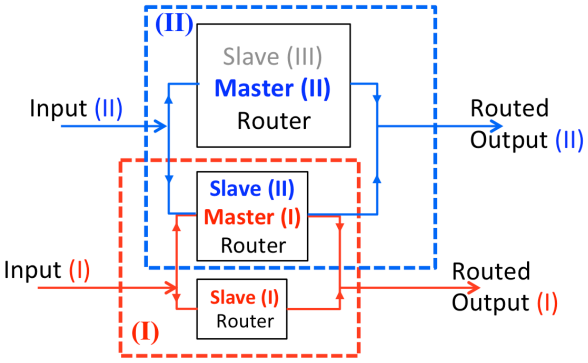

Figure 10: Schematic of two successive generations (I) & (II) of cascaded IP router master-slave configurations.

Table 2: Maximum energy-efficiency gains (η_{max}) at optimised normalized switching threshold (l_T=L_T/N) for different average traffic intensities α.

α	η_{max} (%)	Normalised Threshold Load (l_T) for Switching
0.1	68.1	0.18
0.2	54.1	0.30
0.3	45.7	0.40
0.4	34.3	0.51
0.5	26.3	0.61
0.65	16.9	0.74
0.8	8.3	0.86
0.9	2.8	0.94

As already discussed, switching-on and powering-down times can also be relaxed when a master-slave configuration is used, since only the (simple) switch at the input requires a very fast switching time. In addition, redundancy in the master-slave configuration offers greater resilience (and reliability) during operation; assisted by relaxed router equipment technical specifications, i.e. slower switch-on and -off times (with overlapping operating times), so that the master-slave devices can be operated less "aggressively". For lower traffic intensities, e.g. a normalised traffic load of α=10%, substantial energy-efficiency savings of η>68% are theoretically possible. However, for future system upgrades, the migration trajectory offers

possibilities for energy-efficiency (OpEx) as well as cost (CapEx) optimization. E.g. when upgrading throughput node capacity, the larger master router of a first generation (I) configuration can be re-used to become the slave router for a master-slave configuration in the second generation (II). This is shown in Figure 10, where the master (I) router in the red generation (I) set-up, becomes the slave (II) router in the next-generation (II) architecture.

The future-proofed design of routers which change role from master to slave in a subsequent upgrade presents an interesting optimization problem. There is a trade-off between anticipated energy-efficiency savings as a function of expected average traffic intensity α, versus the CapEx costs of either adopting relatively few system upgrades by building-in generous future-proofing and hence greater over-provisioning; as opposed to assuming a higher frequency of system upgrades over time, but operating each system at closer to its maximum capacity, however with reduced opportunity for energy-efficiency savings.

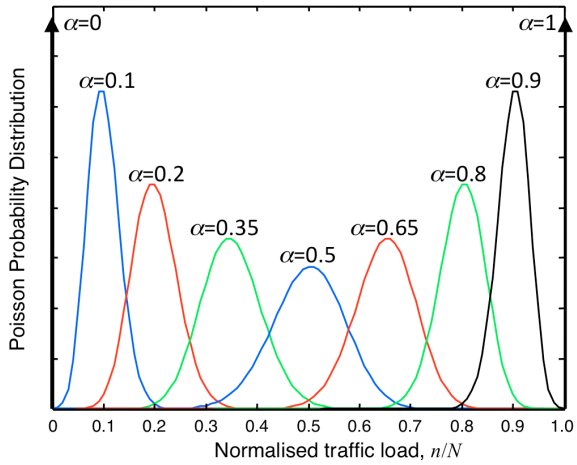

Figure 11: Poisson probability distributions (for normalised load *n*/*N*) for different average traffic intensities α.

We again assume that packets arrive at an edge-routing node with a Poisson probability distribution, such that for a maximum capacity N packets/s (i.e. corresponding to the master router capacity, $C_{master} = \bar{b}N$, where $\bar{b}$ is the average packet length in bits), the instantaneous traffic load is n, with an average (modal) traffic intensity $L = \alpha N$, where α is the normalized average traffic intensity. The resulting probability that at any instant n packets/s are incoming is given by:

$$p(n,L) = \frac{L^n e^{-L}}{n!} \tag{4}$$

We employ equation (4) to be symmetrical about α=0.5, as shown in Figure 11, so that, as is intuitively expected, for a full capacity (α=1), as well as the zero load case (α=0), the distribution becomes a delta function. The total power dissipated by the master-slave router configuration is given by the probabilistically-weighted sum of individual power consumptions of the two devices:

$$P_{total} = P_{slave}\int_0^{L_T} p(n)dn + P_{master}\int_{L_T}^{N} p(n)dn \tag{5}$$

Equation (5) indicates that once the traffic intensity reaches a threshold value L_T, then traffic is switched between the routers; the required value of L_T (which corresponds to the maximum

capacity of the slave router $C_{slave} = \bar{b}L_T$) is an optimization problem, depending on the average (expected) traffic intensity α, and the relative values of P_{master} and P_{slave} (proportional to $C_{master}^{2/3}$ and $C_{slave}^{2/3}$, respectively.) The overall energy saving possible is given by the appropriate weighted summation (integration) of the operating powers of the two routers divided by the power of the master device:

$$\eta = 1 - \frac{P_{slave}\int_0^{L_T} p(n)dn + P_{master}\int_{L_T}^{N} p(n)dn}{P_{master}\int_0^{N} p(n)dn} \qquad (6)$$

Figure 12 plots equation (6) as the normalised threshold value $l_T = L_T/N$ is varied. As might be expected, for the two extreme cases of $l_T = 0$ and $l_T = 1$ when the master router is used for 100% of the time, then the marginal improvement (gain) in energy efficiency reduces to zero. But between these two extreme cases, the energy efficiency shows a maximum, particularly for the cases of low traffic loads, $\alpha \to 0$. Inset in Figure 12 is a plot of the locus of the energy-efficiency maxima for varying α; its convexity arising from the sub-linear $P \propto C^{2/3}$ relationship. Figure 12 tabulates the values of the optimised maximum energy-efficiency gains η with their optimum normalised threshold levels l_T for different average loads α.

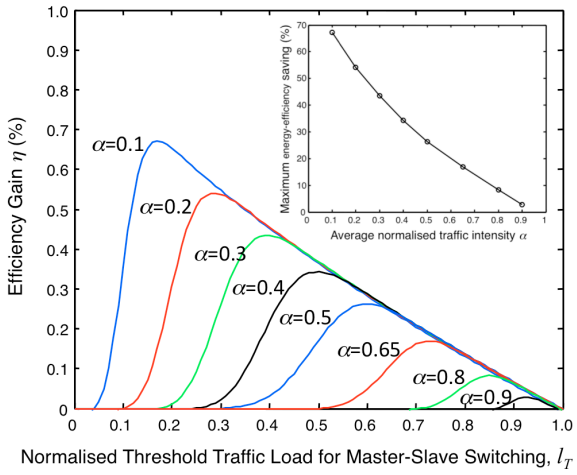

Figure 12: Efficiency gain curves for different α values as a function of varying normalised threshold traffic load l_T.

As the average traffic intensity α increases towards maximum capacity, the possible energy-efficiency savings from the master-slave approach reduce; intuitively this can be understood by noting that the switching threshold l_T increases with α, meaning that the slave router capacity (and therefore its power consumption) approaches that of the master device. The normalised threshold load l_T can now also be understood to be the ratio of the master and slave router capacities: $l_T = \frac{C_{slave}}{C_{master}}$.

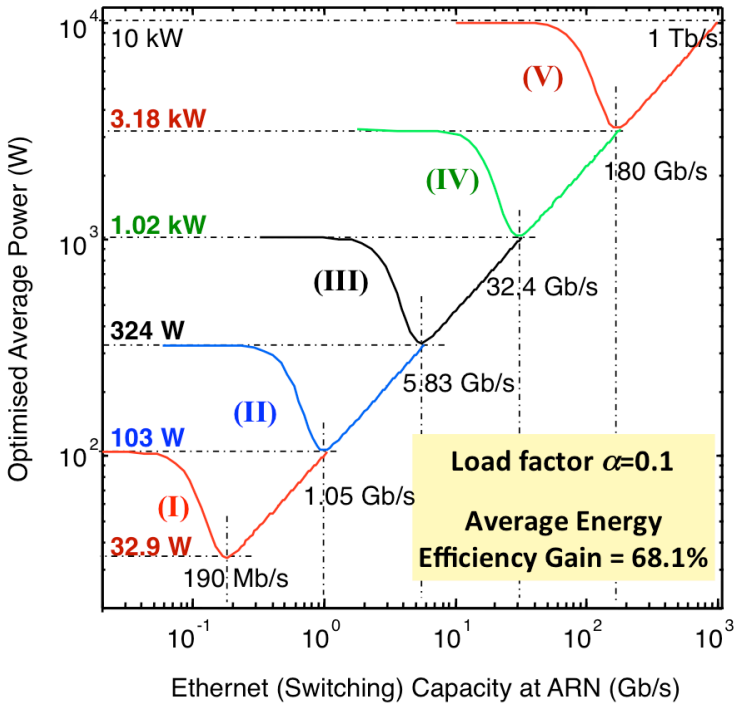

Figure 13: Upgrade trajectory from 1Gb/s→1Tb/s master-slave edge-router over 5 generations for α=0.1, with efficiency gain η=68.1%.

We can therefore use the optimized normalized threshold load l_T (which depends on the value assumed for α) as a design tool to calculate optimum values for master routers in a future upgrade scenario. Re-employing a master router as the new slave in a next-generation system means we adopt the following design rule:

$$C_{master}^{(II)} = \frac{C_{master}^{(I)}}{l_T(\alpha)} \tag{7}$$

Here, the superscripts (II) and (I), respectively, indicate the next (second) generation, and previous (first) generation. By adopting a next-generation master router with capacity indicated by (7), we maintain the same relative master-slave scaling, and hence the same optimum energy-efficiency gain. In the following analysis, we calculate two possible upgrade trajectory scenarios, based on α=0.1 and α=0.3. The energy-efficiency gain η rapidly reduces for high α, so we don't consider scenarios with higher α values. Figure 13 shows the upgrade path for α=0.1 as we increase overall edge-router node capacity from 1.05 Gb/s through to 1 Tb/s. Our baseline assumes a 1-Gb/s router consumes of the order of 100 W power. Each generation is shown as a different colour, where each curve is the appropriate plot of equation (5), representing the expected average power consumption as l_T is varied for the particular master-slave configuration. The minimum in each curve (e.g. for generation (I) this is at 32.9 W @ 190 Mb/s) represents the optimum operating point for l_T; and hence in this case the average (expected) power consumption for a configuration with maximum master capacity at the high end of the curve (1.05 Gb/s) and slave capacity at that minimum point (190 Mb/s), i.e. $l_T = 0.18$. The high end of each curve coincides with the minimum (i.e. optimum operating point) of the next-generation curve. Hence the master capacity of the previous generation becomes the slave capacity of the subsequent upgrade. In such a way we follow the $P \propto C^{2/3}$ relationship (i.e. the main diagonal of the graph) but continue to enjoy an average 68.1% energy-efficiency gain. Five upgrade generations are required to attain a 1-Tb/s ARN edge-router capacity, e.g. as may be required in the 2030 timeframe. If we assume a higher

average traffic intensity of α=0.3, then we follow a different upgrade trajectory, consisting of nine generations to upgrade from 655 Mb/s to 1 Tb/s, but with a lower average energy-efficiency gain of only 45.7%. This is shown in Figure 14.

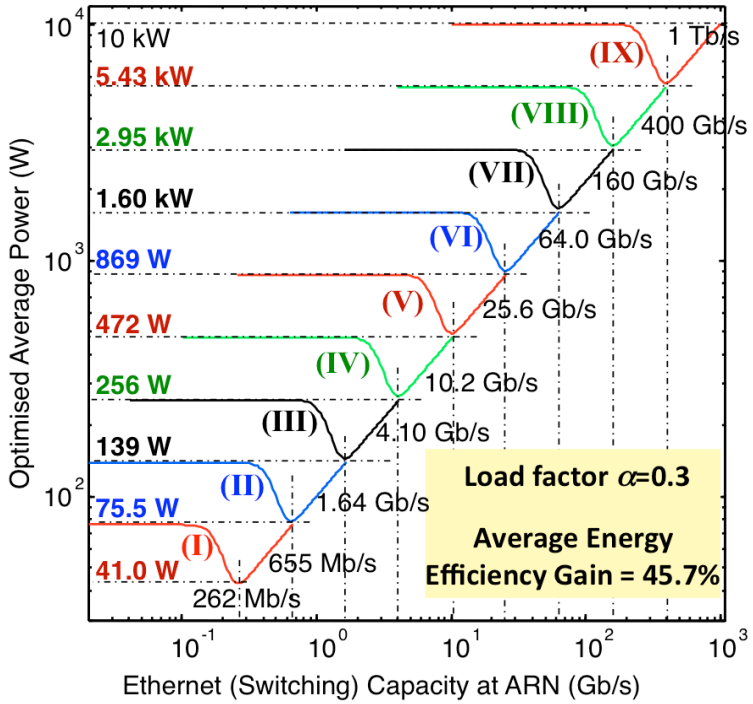

Figure 14: Upgrade trajectory from 1Gb/s→1Tb/s over 9 generations for α=0.3, with efficiency gain η=45.7%.

Clearly the two upgrade trajectories presented here offer very different migration profiles. While Figure 13 offers fewer upgrade stages and a higher energy-efficiency gain, the system is highly over-provisioned; whereas Figure 14 indicates an approach that runs closer to maximum capacity for each generation, but requires more frequent upgrades and offers a somewhat lower energy-efficiency gain.

Conclusions

We have shown how a master-slave configuration for networking equipment can be adopted to make significant statistical improvements in energy-efficiency. In particular, as traffic load varies, the savings in power consumption can be made to be proportional to the instantaneous traffic intensity. The master-slave approach is particularly suited for those systems and sub-systems that tend to exhibit a constant power dissipation characteristic independent of load, such as current IP routers, and optical amplifiers. Indeed, the results presented here indicate that the master-slave configuration can offer a similar energy consumption saving as would be found in the ideal of a single operating device that features fully elastic (differential) power dissipation that is proportional to the presented traffic load. Although managing a dualised system setup requires additional equipment (i.e. both switching and combining subsystems at the input and output of the master-slave configuration, as well as the smaller-scale "slave" version of the main, full-capacity master equipment), the additional CapEx that is associated may also be offset by the inherent redundancy that is associated with such a master-slave design, with its concomitant higher reliability. In addition, we have presented how such a master-slave approach can also offer an optimised upgrade path, with a minimised CapEx (and OpEx profile). We have discussed a novel design rule offering maximally energy-

efficient and future-proofed Gb/s→Tb/s upgrade paths for ARN edge-routers and similar switching or aggregating equipment. One path assumes 10% average Poisson traffic intensity with 68.1% energy-efficiency gains over only 5 upgrade generations; while when we assume a 30% average traffic load, only 45.7% energy-efficiency gains are possible, and 9 generations are required.

3.2.4 Solar powered reach extender

Node consolidation is particularly driven by network operator concerns for reducing operational cost of the network, and it offers significant challenges to the NGOA solutions. In order to cover larger service areas and a higher number of the customers, both longer reach and higher splitting ratio at the remote node (RN) are required, causing larger propagation delay, and higher optical power loss. Node consolidation by means of extended reach and increased splitting ratio requires use of active elements in the optical distribution network (ODN) to compensate for power loss, in particular for passive and semi-passive NGOA architectures, e.g. WDM PON and hybrid WDM/TDM PON [3].

Several types of active Reach Extenders (RE) for long reach PON have been considered, such as semiconductor optical amplifiers (SOA), Erbium doped fiber amplifiers (EDFA) and optical electrical optical converters (OEO). The SOA and EDFA solutions offer optical amplification of the optical signal. The OEO solution provides extensive reach extension through signal regeneration. Compared with the SOA and EDFA, the OEO solution is sensitive to the line rate, and consequently cannot flexibly support line-rate upgrades, e.g. to allow multiple line rates to coexist which has been ratified as the requirement in both IEEE 802.3av and ITU-T-proposed architectures (in NGA1, Next-Generation Access 1). The idea of introducing active elements is in a sense contradictory to the concept of PON. It is important to understand, however, that what is important for the evolution of access networks is not the presence or absence of active equipment but rather the properties of different active elements and how they contribute to costs. If placing simple active elements with high reliability in the outside plant can significantly increase the PON service area and enable node consolidation, then the ultimate goal of cost-efficient networks may still be achieved.

The work described in this section aims to demonstrate a working long-distance fiber link with an inline EDFA-based RE which is fully or partially powered from an alternative energy source (i.e. solar power) and can be controlled remotely. The motivation for creating such a setup is that these techniques can be adapted to use in some countries which have a large potential for solar power generation and hence reduce electronic energy consumption and conventional power infrastructure.

Setup for solar powering system

After going through several variants, a setup of the powering system has been proposed that may be used in different weather and insolation conditions [10]. The layout of the proposed powering system is as shown in Figure 15.

As we can see, the solar power system is used to provide backup power for two EDFAs (one for each direction), which are the most crucial element of the link. The EDFAs get power from the solar battery if it is available, and otherwise switch over to the general power network. The power controller board (PCB) is also connected to a standard power outlet through a step-down controller, getting power from the general power infrastructure when there is no sun available and the battery is discharged. It should be noted that our proposed solution could vary in performance if employed in different weather environments. In Sweden, the remote control gateway proves to be too hard to power from a solar battery and is thus connected to external power all the time.

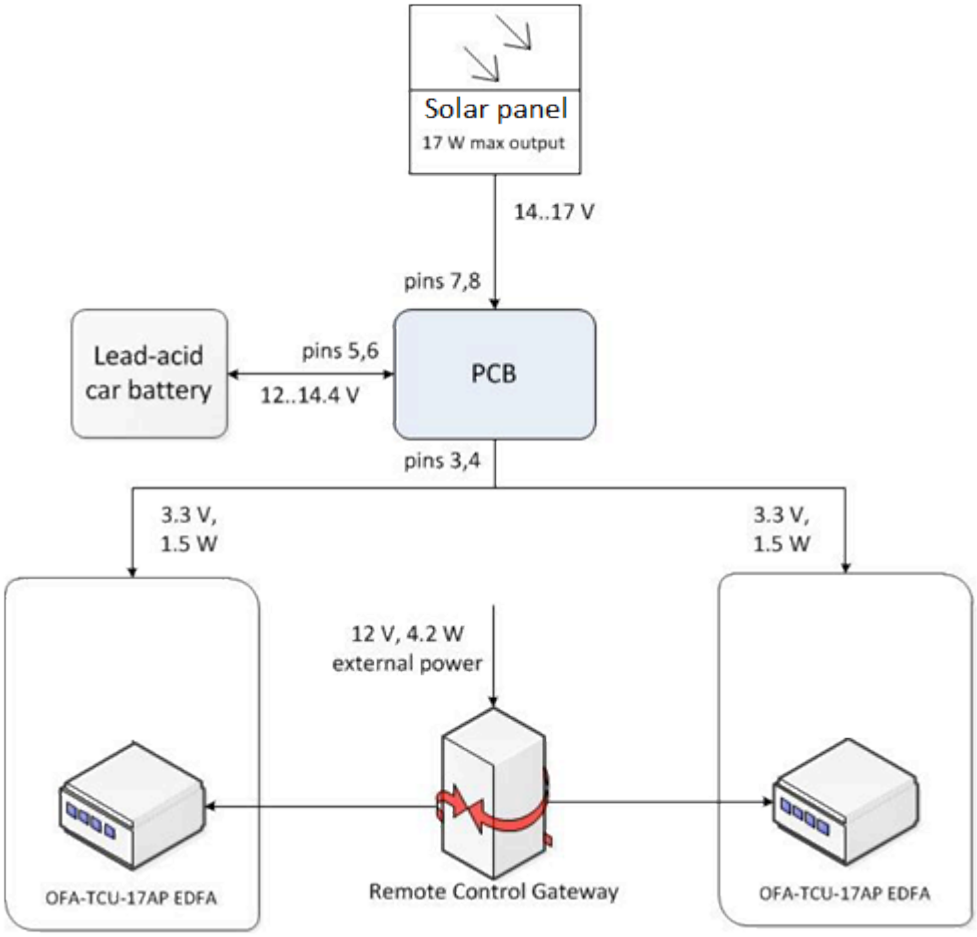

Figure 15: Powering system design (PCB: power controller board) [10]

Experimental scenarios and results

Sweden and Somalia, as two countries of quite opposite climates, have been considered as pessimistic and optimistic scenario for performance evaluation, respectively. As only a limited number of experiments with the solar panel in Sweden has been possible (and it was unfeasible to conduct a similar experiment in Somalia) we had to find statistical data to justify whether using the system would be possible in both of these scenarios. The information used in this assessment included sunrise and sunset times for each day of the year, as well as average insolation (a measure of solar energy) data. The basis for our calculations was the data available at [11] for the year of 2011. According to that data, the duration of day in Stockholm may vary from 6 to 18 hours throughout the year. However, according to [12], the mean daily sunshine duration is much less and can be as little as 1 hour per day in December, with the maximum of 9.7 hours in June. It is difficult that such a small amount of daylight fully charge batteries with a reasonable panel size in a stable way throughout the year. We propose that in Swedish conditions the power-saving system is used from May to July, falling back to a centralized power supply during the rest of the year.

The climate conditions in some other countries, e.g. Somalia, are totally different. Firstly, as this country lies close to the equator, the duration of the day remain almost constant and gives us a possibility to make the system design simpler as the amount of daylight does not changed a lot throughout the year. Secondly, there is much more sun available, with Somalia having around 250 sunny days per year by some estimates. While precise information on insolation

in Somalia has not been available, the neighboring country of Djibouti has from 7.9 to 10.2 sunlight hours per day [13]. This makes it feasible to use our proposed solar power system in Somalian conditions all year round.

In Somalia, however, there is often no power infrastructure at all, with the solar batteries remaining the only way to maintain stable power for the link. This means that the setup is the same, but its use case is different: the EDFAs as well as the remote control system could be powered with abundant solar energy.

We have witnessed that the system can last on battery power aided with a solar panel for at least one week. It is tolerable and the uptime could be in theory as long as one month. To make the system reliable, we recommend that the equivalent of six solar panels (such as those used for two EDFAs) should be installed for reach extender. That would ensure that the battery charges quickly with high current while not requiring any special cabling or fusing. After doing the experiments with powering, we also outline the extra costs that would be required for a solar power system. Approximate cost is 900$ for 6 solar panels (including battery) and 270$ for charge controller which are found based on the market survey in Sweden.

4. Concept-specific challenges

Thusfar, we have focussed on discussing techniques which are common to all the candidate architectures. However, more-specific work has been concentrated on the four main NGOA candidate architectures, as previously discussed in depth in the Deliverable D3.1 [3]. These four architecture candidates were selected based on the list of technical performance requirements as initially drawn up in the Deliverable D2.1 [2]. This section addresses activities related to concept specific challenges.

4.1 WDM-PON

There are a number of evolutionary challenges that must be faced by WDM-PON. Some rely in the development of WDM technologies and components, and these are addressed specifically in WP7 and will not be discussed here. The work in this area performed in WP4 and detailed in the section below provides a description of various aspect concerning resource allocation, resilience, fault management, power saving techniques and futher developments for WDM-PON.

4.1.1 Implementation of resource allocation

With regard to resource allocation, WR-WDM-PON and WS-WDM-PON shall be considered separately.

WS-WDM-PON may lead to cost or performance penalties, however, in general it is possible to assign any wavelength to any ONU. Combined with appropriate Layer-2 functionality (and also, possibly, with partial re-configurability of the ODN), this can offer greater flexibility with regard to per-client bandwidth allocation when compared with the WR-WDM-PON approach. Here, it must be checked if the capability to assign any wavelength to any ONU can lead to cost savings.

For WR-WDM-PON, bandwidth allocation is performed on Layer-2, in the OLT. This reduces the shared components to the Layer-2 switch/aggregator, the feeder fiber, and the RN. On the other hand, it provides relatively simple (and hence cost-efficient) per-client transport pipes and allows for scaling, in the transport part, to larger future bandwidth requirements. In this respect, WR-WDM-PON follows the same approach which originally made Ethernet a

success over the more sophisticated approach (and more bandwith-efficient approach at least for grooming and multiplexing of different services) of ATM.

4.1.2 Implementation of resilience techniques

Due to the protocol agnosticism of WDM-PON, resilience can be implemented in both the wavelength/wavelength-adaptation layer and the PON client layer. In case of an Ethernet client layer, existing standardized protocols such as G.8031 (Ethernet linear protection), G.8032 (Ethernet ring protection switching) and 802.3ad (Ethernet link aggregation) can be leveraged.

In the combined WDM-PON wavelength/wavelength-adaptation layer, several PON-specific resilience mechanisms can be employed. G.984.1 lists protection and dual-parenting options for both the entire PON segment and feeder fiber section.

WS-WDM-PONs can support all resilience concepts described in G.984.1. An example, including two protection cases (entire PON segment, feeder fiber section only), is shown in Figure 16. Here, LT denotes line termination.

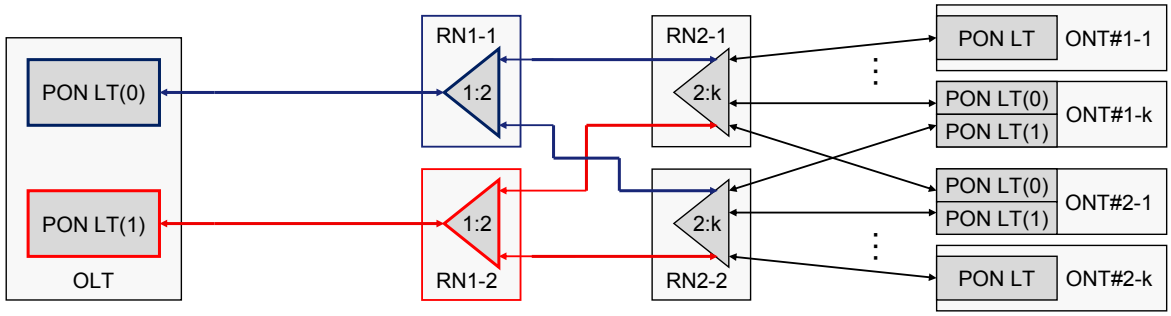

Figure 16: Protection for wavelength-selected WDM-PON

The scheme shown in Figure 16 can also be used for dual-parenting configurations. In order to do so, the single OLT must be split into two OLTs with, a signaling channel for coordinating switch-over events.

An additional solution for feeder-fiber protection is to use 2:1 power splitters and 1:N AWGs. This configuration is a derivative of the scheme shown in G.984.1, Figure 4a, where the AWG replaces the x:N power splitter for WR-WDM-PON. The additional 2:1 power splitter used for resilience also adds insertion loss, which may impact system reach.

AWG-based remote nodes support an additional protection mode for WR-WDM-PON by adding a second feeder-fiber port to the AWG. This port has the same insertion loss as the first feeder port, without increasing total insertion loss (the latter follows from symmetry considerations). 2:N AWGs can be used for feeder protection or dual parenting.

The base configuration for feeder fiber resilience is shown in Figure 17. Two PON LTs are connected to two feeder fibers in the OLT. Dual parenting can be similarly configured. In the RN, the two feeder fibers connect to the two AWG ports that carry the optical multiplex sections. Preferably, these two ports are adjacent ports in a generic M:N AWG. This is also an important aspect of WDM-PON standardization.

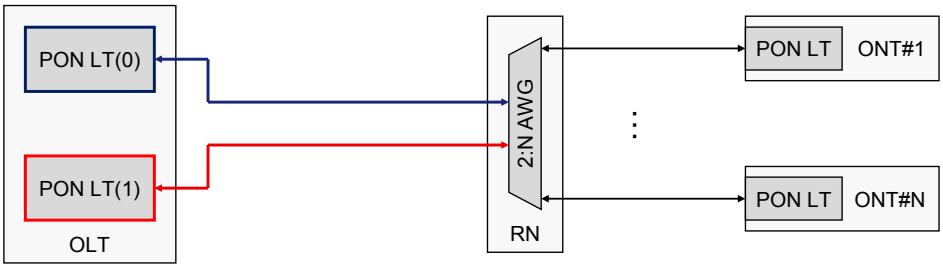

Figure 17: 2:N-AWG-based protection of feeder fiber

When switching from one feeder-fiber port of the 2:N AWG to the second (and given that these are adjacent ports of an M:N device), while keeping the OLT wavelengths the same, a wavelength shift by one channel occurs at all AWG fanout (distribution-fiber) ports in the downstream direction. By default, then, the downstream signals would be routed to the wrong ONUs. In the upstream direction, the second feeder fiber port would remain dark if the ONUs retained their original working wavelengths. The second feeder fiber can be lighted correctly and the downstream wavelength shift can be compensated by re-tuning both OLT and ONUs by one channel. In the seeded WDM-PON, seed light, which includes broadband light sources or multi-frequency "comb" sources, is switched onto the respective feeder fiber in the OLT, and ONU re-tuning happens automatically.

The re-tuning requirement by one channel implies that a 41st channel be supported in a 40-port AWG, or that an 81st channel be supported in an 80-port device and likewise for other port counts. This is inherent in the AWG grids discussed for NGOA.

Figure 18 shows two specific implementation examples for 2:N-AWG-based protection for two relevant cases of WR-WDM-PON. Figure 18 A) shows the configuration for a fully seeded PON with reflective transceivers, and Figure 18 B) shows the respective configuration for a PON with tunable lasers.

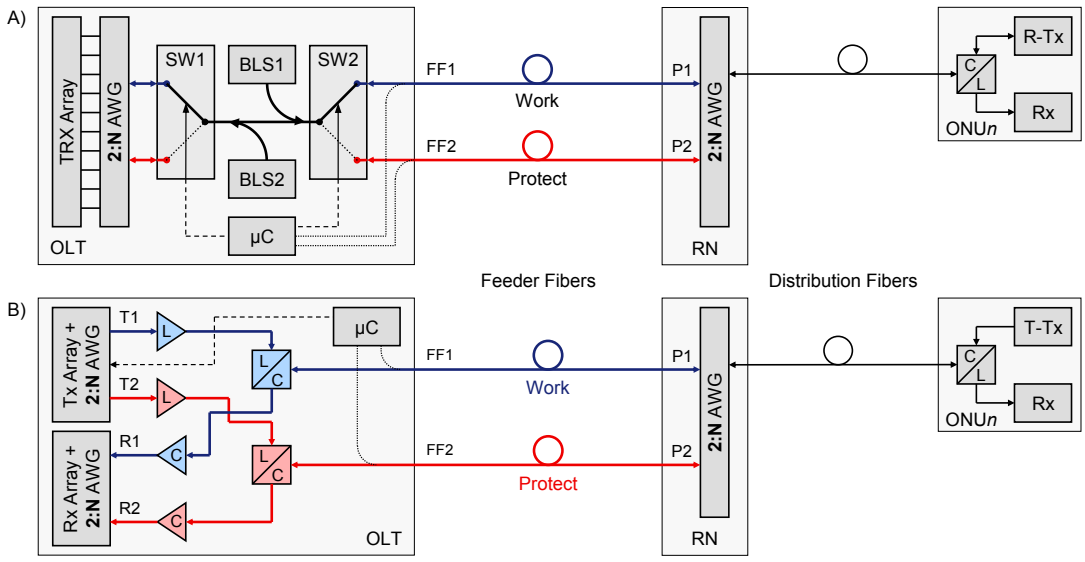

Figure 18: Implementation examples of 2:N-AWG-based protection

Protection configurations include the option to duplicate the OLT transceiver array. Figure 19 (a) shows the configuration for a non-duplicated transceiver array; Figure 19 (b) shows the respective configuration with duplicated transceiver arrays.

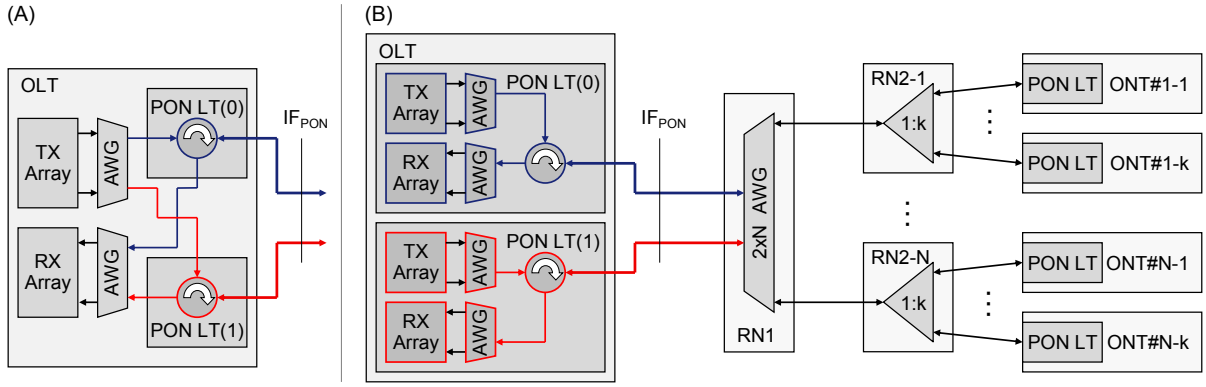

Figure 19: 2:N-AWG protection with a) non-duplicated transceiver array and b) duplicated transceiver array

Figure 19 shows an ODN where wavelengths are first de-/multiplexed in a 2:N AWG. Then groups of densely spaced wavelengths are further split/combined by power splitters. This is a hybrid wavelength-routed/wavelength-selected ODN. It can be used for UDWDM-PON or hybrid WDM/TDMA-PON.

Resilience for WDM PON can optionally be configured in rings that connect several RNs to a single OLT, or in open rings that dually parent several RNs to two OLTs. An example of ring protection is shown in Figure 20. It is based on adding/dropping (groups of) wavelengths in the respective RNs by means of group add/drop filters (G*n* in Figure 20). RNs are resiliently connected to the OLT(s), protecting the feeder fibers. Several RNs can be passively traversed. For rings with a large number of remote nodes, either a subset of the remote nodes must be active nodes with lumped amplifiers, e.g., EDFAs, or a very high loss budget must be available. These active remote nodes may include the function of reconfigurable optical add/drop multiplexers (ROADMs) to support flexible dynamic wavelength assignment. In addition, legacy G-PON/XG-PON could co-exist in this configuration through either transparently transmitted or wavelengths converted to the DWDM grid at the active remote nodes.

In the OLT, "all-groups" add/drop filters must de-/multiplex all wavelength groups used in the ring. Switchover is performed in the OLT by means of a switch matrix (one switch per group). It is triggered by upstream Loss of Signal (LoS).

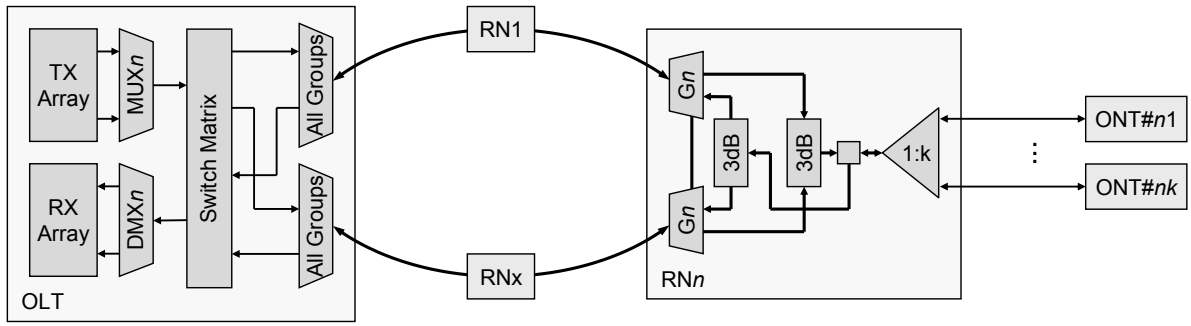

Figure 20: WDM-PON ring protection example

The ring protection shown in Figure 20 is also suited for resiliently connecting several power splitters. Per power splitter, groups of densely-spaced wavelengths can be used in wavelength-selected "sub-PONs." Alternatively, hybrid WDM/TDMA approaches can be

used. This facilitates the addition of resilience to existing infrastructure.

The protection shown in Figure 20 can be extended to chains of remote nodes that are connected to two OLTs (dual parenting) in an "open ring" structure. Between the OLTs, signaling or centralized management must be established.

Fault detection and localization technique for the WDM based PON

We have implemented the fault detection and localization technique for WDM PON in the lab and experiementally proved that the impact of the monitoring signal on data transmission is trival.

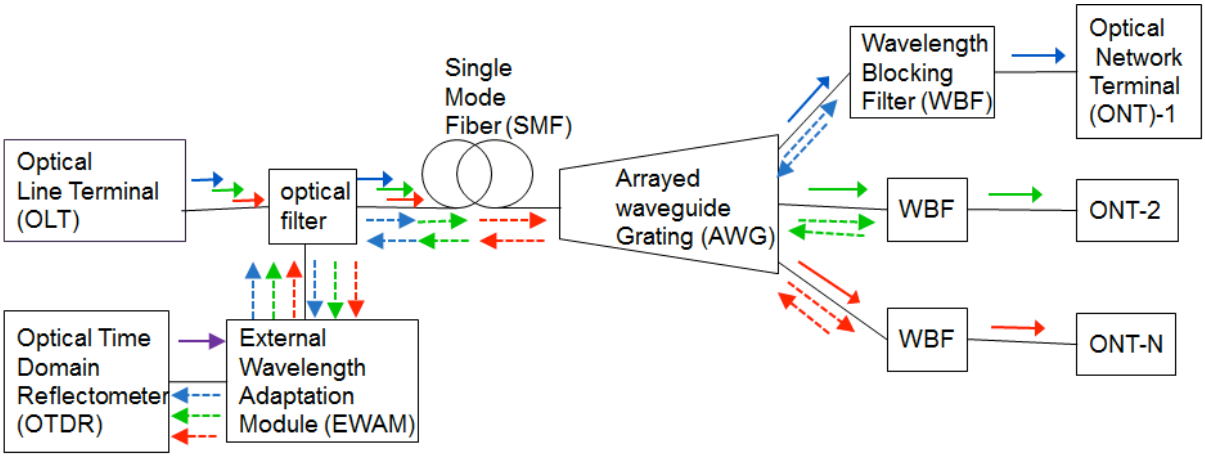

Figure 21: Fault supervision block in WDM PON.

All the devices for our considered fault monitoring scheme and their connections are shown in Figure 21. We use optical time domain reflectometer (OTDR) and external wavelength adaptation module (EWAM) to provide monitoring signals for fault detection and localization. The purpose of using EWAM is to add a wavelength tunability feature to the OTDR in order to enable supervision of any fault that occurres at any distribution fibers. It is also possible to use an internally tunable OTDR as an alternative. The optical filter mixes the signals from the OLT and the EWAM into the feeder cable. In our experiemental setup, we use 20 km long SMF with 4.62 dB loss for feeder fiber. For simplicity, only one input and one output port of the 1xN AWG are used and the wavelength set for the data transmission is 1534.35 nm. After the 1 km distribution fiber from the AWG to the wavelength blocking filter (WBF), which can block monitoring signal coming to the end user, the ONT is assigned with its own wavelength for data transmission.

To check whether there is a fault or not, the monitoring section (i.e. OTDR+EWAM+WBFs) performs supervision on the whole WDM PON system. For this purpose, a high power pulse is sent by the OTDR, converted to different wavelength (associated to a certain end user) after passing the EWAM, and finally reflected by WBF. The detector at the OTDR measures the backscattered signal together with the time delay between the moments that pulse is sent and reflected back. Since the speed of light when traveling along the fiber is known, the recorded time delay is converted to distance between the OLT and the place where the failure occured.

Figure 22 shows one example of OTDR trace, which can record any optical event caused by poor splice, bad connectors and other reasons. Furthermore, the exact distance to occurrence of these optical events in the network can also be displayed.

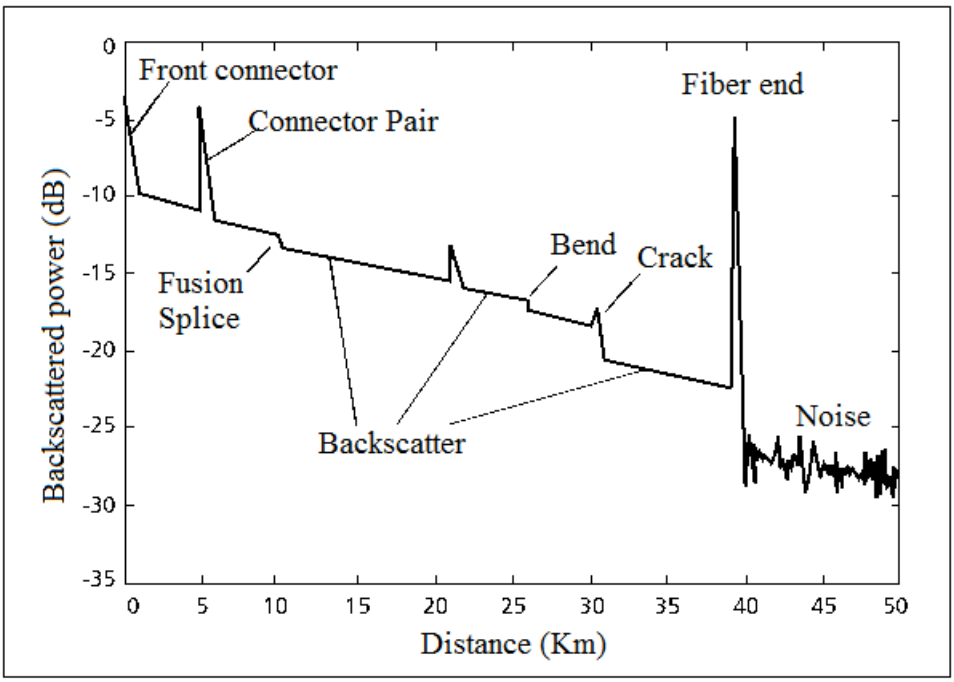

Figure 22: Example of OTDR display [14]

The measurements have been done in two steps [15]: 1) without OTDR signals and 2) with OTDR signal. For performance evaluation, received optical power (ROP) vs. bit error rate (BER) is measured for both upstream and downstream.

Experiment setup for the case without OTDR signal

Figure 23 shows the experiment setup for the case without OTDR signal. The BER tester (BERT) is used to measure the signal quality. The measurement has been carried out for both upstream and downstream.

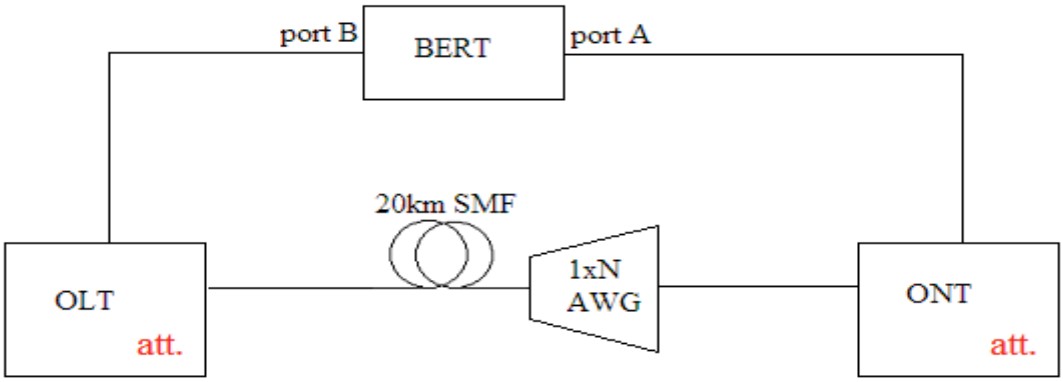

Figure 23: Experiment setup for the case without OTDR signal [15]

Experiment setup for the case with OTDR signal

By adding the monitoring section (as shown in Figure 21), all the measurements taken from the previous setup are repeated. The experiment setup is shown in Figure 24.

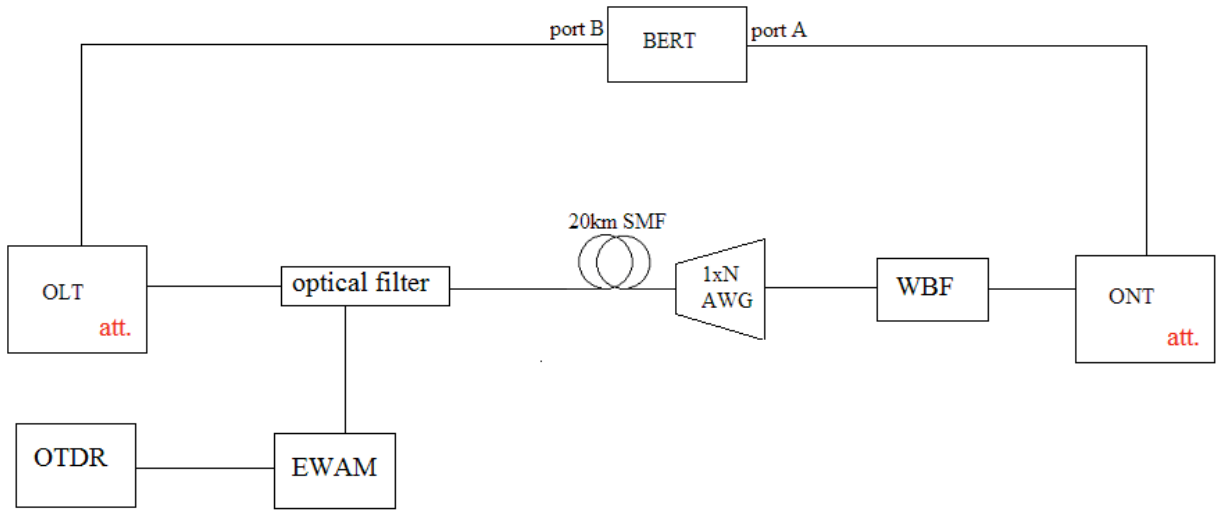

Figure 24: Experiment setup for the case with OTDR signal [15]

Experimental Results

The measurements are taken using two setups described previously. In both setups, an average result is taken from two consecutive measurements. The reason to teak measurements twice is the measured results have variations all the time and taking the average helps to get the stable values. Figure 25 and Figure 26 show our experimental results for downstream and upstream, respectively.

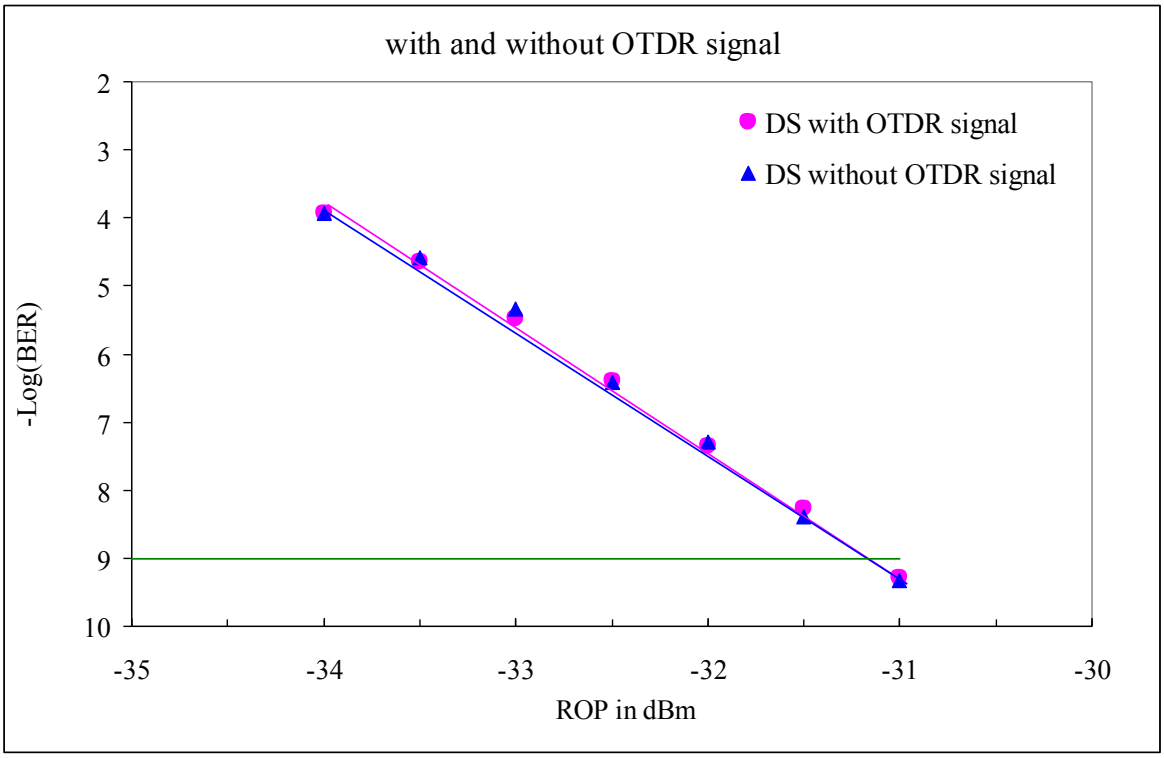

Figure 25: the measured BER as a function of ROP for downstream (DS)

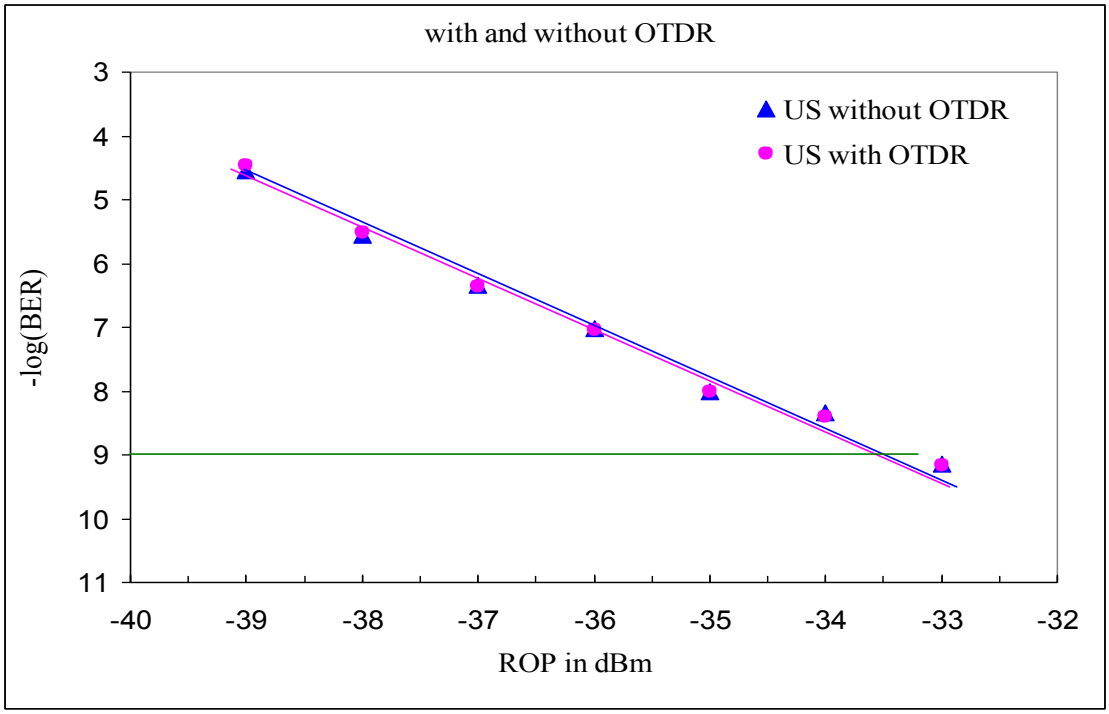

Figure 26: the measured BER as a function of ROP for upstream (US)

From the figures above, it is clear that the monitoring signal does not have any effect on transmitting the data signal. The point marked with green line shown the results when BER=10^{-9} which is a typical requirement on signal quality for optical transmission.

4.1.3 Power saving techniques

A general discussion on power saving modes within the context of NGOA is provided in Section 3.2 This section adresses power saving modes specifically for WDM-PON. In a WDM-PON, the potential efficiency of power-saving modes depends on some relevant system parameters. Power-saving modes are often referred to as (cyclic) sleep or doze modes. Then, relevant parameters which influence the power-saving efficiency (i.e., the decrease in power consumption over normal "full-load" working conditions) include:

1. Max. length of sleep cycles (i.e., allowed response delay)
2. Wavelength control (tuning) mechanism
    a. Automatic (e.g., seeded reflective)
    b. Autonomous (e.g., tuning via remote node)
    c. Supported by OLT via feedback signaling channel
3. Mode of operation (burst mode for WDMA?)
4. Bit rate (*including client-side I/F*)
5. Customized ONUs vs. general-purpose ONU (this also includes the differentiation between residential access, business access, and backhaul)

The maximum allowable sleep-cycle length, i.e. the allowable response delay of a transceiver, has an obvious impact on cyclic-sleep power-saving efficiency. The longer the sleep cycles are with respect to active periods, the higher the power-saving efficiency. With long sleep cycles in the ms-range, power saving in excess of 50% can be achieved. Maximum allowable response delay (i.e., sleep time) depends on the (primary) service type which is to be supported. In voice- or video-centric ("consumer") applications, response delay (for example, for incoming calls) of several 10s of ms may easily be tolerable, whereas in certain data-

centric (business) applications, shorter response times and hence sleep cycles will be required. Maximum sleep-cycle length may have to become part of Service-Level Agreements (SLAs). It is expected that sleep cycle length for residential applications can be extended into the range of at least 10 ms, whereas for business applications it may have to be limited to 1 ms or less.

The wavelength-control mechanism also has a clear impact on power-saving modes. If, for example, ONU transceivers autonomously tune with the help of feedback signals derived from RN reflections, the *related OLT transceivers can independently go into sleep mode*. This is not true for remotely seeded WDM-PON variants and variants which require the downstream signal for ONU tuning (this applies to tunable laser-based WDM-PON where the ONUs tune with the help of OLT feedback signals or where the ONUs make use of heterodyne tuning onto downstream wavelengths). In these variants, ONU transmitters require the downstream signal, and hence applicability of sleep modes to the downstream (OLT) transmitters is more complex, if it is possible at all. If ONUs can tune autonomously, higher flexibility and, as a result, somewhat higher power-saving efficiency are expected. This is for further study out side the scope of OASE.

An OLT multi-channel implementation also impacts potential power saving. On one hand, it is theoretically possible to shut down wavelengths independently from each other. This is regarded an advantage of WDM-PON over TDMA PONs where the common MAC layer has to be kept alive. On the other hand, it may be difficult to apply sleep cycles to individual channels in highly integrated multi-channel transceiver PICs. *Implementation of single-channel shut-down (cyclic sleep) capability for multi-channel PICs hence should be made one of the primary design goals of these PICs*. This is also for further study outside the scope of OASE.

As already mentioned, the general operation mode has strong impact on potential power saving. This applies to cyclic-sleep vs. burst-mode transmission and also to cyclic-sleep vs. bandwidth-throttling (which again can be achieved using burst-mode transmission). In case of bandwidth throttling, it is expected that the main power savings are generated in the electronic domain, for example, in Layer-2 port aggregators or aggregation switches. In any case, power saving well in advance of 50% when compared to fully loaded operation can be expected for any WDM-PON. For example, we note that when considering the aggregation switches, as well as any optical amplifier equipment for long-reach deployments, the master-slave approach discussed in section 3.2.2 can also be conveniently applied to the WDM-PON architecture to achieve useful energy efficiency savings.

4.1.4 Further development: longer reach, higher capacity and larger client count

WDM-PONs have the inherent potential for scaling to increased future demands. This is considered to be a relevant differentiator when compared to all approaches which make use of shared components. This includes ODN sharing by means of excessive power splitting.

Therefore, the three scaling areas are considered separately.

Longer Reach
Specially for WR-WDM-PON, with its inherently low ODN insertion loss, scaling to longer reach is straightforward. First, transceivers with higher ODN power budget can be implemented. This includes the scaling from simplest/cheapest PIN diodes via APDs to optically preamplified receivers and finally coherent receivers. This scaling holds for most WDM-PON variants. Likewise, a certain degree of scaling is possible for transmitters. For example, differentiated transmitters can be implemented where a lowest-cost variant has smaller launch power. This variant can be complemented by either a high-launch-power

transmitter variant, or by booster amplifiers. Booster amplifiers in turn can scale from lumped OLT-based boosters to OLT-forward-pumped fiber amplifiers (either Raman amplifiers or amplifiers based on remotely-pumped Erbium fibers). Finally, lumped ODN-based in-line amplifiers can be implemented. In principle, only the limitations already known from long-haul transmission research apply, given the respective technologies can be implemented cost-efficiently.

Higher Capacity
Capacity scaling is straightforward in WDM/WDMA-PON as well. WDM-PON already starts with high total bandwidth in cases of, say, 80 wavelength of 1 Gb/s (symmetrical) each. In Section 3.1 it was already discussed how support for 10G backhaul requirements could be provided within WDM-PON. It is relatively simple (as compared to shared TDMA or similar approaches) to scale the per-wavelength bit rate via 2.5 Gb/s into the range of 4.3…5.0 Gb/s. These bit rates are still based on similar transceiver technology. Likewise, they will add relatively small transmission penalties. Further scaling to 10…11 Gb/s per channel is possible. Here, added cost (for example for external modulation and for added FEC) and path penalties (if not compensated by FEC and more sophisticated modulation) need to be considered. Finally, scaling into the region of 25 Gb/s per channel seems feasible from today's perspective. We refer the reader to the EU FP7 project C-3PO where some basic work on low-cost 25-Gb/s transceivers is being done.

Higher Client Count
Client count can be scaled for WDM-PON in two directions. First, the number of wavelengths in a WDMA-PON can be increased within certain limits. Second, shared per-wavelength fan-out may be added later. The latter is analysed within this project under the term of Hybrid PONs.

The number of wavelengths can be increased within certain limits which are set by laser safety and complexity. Complexity includes components' insertion loss which tends to increase with increasing channel count, and issues with temperature stabilization for decreasing channel spacing. Partly, these issues can be counteracted with coherent approaches which then allow UDWDM spacing. For DWDM spacing, a practical limit is reached at 384 clients (or bi-directional channels, equalling 768 wavelengths). This number can be derived, considering eye safety according to Laser Safety Class 1M (i.e., a total launch power of +21.34 dBm for wavelengths >1400 nm), when using the intire S-band, C-band, and L-band of a cyclic 50-GHz AWG in non-co-existence scenarios. The AWG then is a 96-port, 50-GHz device. Two wavelength channels each are interleaved into every AWG port and cyclic order by means of 25-GHz interleavers.

4.2 HYBRID WDM/TDM-PON

This section addresses various challenges faced by different hybrid WDM/TDM PON approaches proposed within the project. One particular challenge concerns resource allocation, especially where it is it is based on dynamic wavelength allocation. Section 4.2.1 describes work related to algorithms for resource allocation and dynamic wavelength allocation. Section 4.2.2 considers resilience and Section 4.2.3 presents in-depth studies of different power saving techniques applicable for hybrid WDM/TDM-PON.

4.2.1 Implementation of resource allocation

Flexible resource allocation is a key element of the hybrid WDM/TDM concept, with flexible allocation primarily in the time domain but potentially also in the wavelength domain. Dynamic wavelength allocation presents particular challenges which are investigated in this section. The OASE hybrid WDM/TDM PON variants are realized with a Tunable Laser (TL)

in each ONU. There exist several types of TLs the slowest of which can switch between wavelengths in times ranging from several seconds to a few microseconds. The fastest can switch in nanoseconds and are therefore called Fast Tunable Lasers. Unfortunately these fast tunable lasers are very costly and energy consuming and thus would not be available for access networks. For hybrid WDM/TDM PON, several DBA algorithms are proposed; however they do not take into account the tuning and switching time of lasers and receivers, leading to a very high wavelength switching at ONUs. A very high switching leads to a high switching latency, which degrades the DBA performance. However, static allocation of wavelengths may also be inefficient. In this section, we try to investigate the optimal ONU switching based on switching and tuning time considerations, and propose an algorithm which switches ONUs based on the tuning and switching latency considerations.

A general approach to decide which wavelength will be assigned is the First Available Wavelength (FAW). In this category, some algorithms are proposed like Earliest Finish Time (EFT) and Latest Finish Time (LFT). In the EFT algorithm, the wavelength with the earliest finishing last transmission is selected and the grant for the new reservation must be delayed accordingly. Another variation of FAW is Latest Finish Time (LFT). Here the selected wavelength must now have the latest finish time among all channels. The problem is that these algorithms are only concerned with delay and therefore allowunlimited switching of wavelengths without considering the laser tuning time. They treat the laser tuning time as negligible.

We propose the Earliest Finish Time - Minimized Wavelength Switching (EFT-MWS) algorithm, which extends the EFT algorithm to make it aware of switching and tuning times. When the OLT receives the request from an ONU, there are four possible outcomes. In the first case, the current wavelength (the one to which an ONU is tuned presently) has the earliest finsishing last transmission time and thus there is no need to switch. In the second case, the OLT may not switch an ONU due to the maximum switching limitations. By switching the ONU to a new wavelength, the switching time per ONU may exceed the maximum switching limit. The maximum switching limit is referred as the maximum switching time and for this study, a maximum switching time of 400 μs (following from a maximum of 2500 switches per second) is adopted. Note that, at a very low load, an ONU may switch maximally according to the round trip time and for a 25 km scenario, this value is 250 μs or 4000 per second. In the third case, the OLT may not switch an ONU as the gains of switching may be limited. The OLT may evaluate the delay decrease or time gain by switching to another wavelength. This number must be large enough. We define the percentage TGmin as the time gain divided by the previous cycle time. We will obtain optimum values for TGmin by extensive simulations. In the fourth case, the OLT may switch the ONU to another value if it does not observe the first three constraints.

In our simulations in OPNET we use a hybrid WDM/TDM PON with 32 ONUs in a 25 km range. We use 4 upstream wavelengths of 1 Gb/s each and a guard band of 1 μs. ONUs generate self-similar best-effort traffic with Hurst parameter 0.8 and exponential frame sizes between 64 and 1518 bytes at a rate of 500 Mb/s. We assume the tuning time ttune as 0.5 μs. This is within the guard band. Figure 27 shows the average queueing delay for static WDM, EFT and EFT-MWS with different values of TGmin. Static WDM is a DBA which doesn't allow switching and therefore an upper bound for our results. EFT is used as the lower bound. The results of EFT-MWS with TGmin equal to 3, 15 and 90 are almost identical to EFT for a network load up to 0.8. Even the delays for TGmin equal to 300 and 1000 are just 340 and 420 μs and thus still be acceptable for some applications. At higher loads the delays are saturating to the same value. This is because the channels are overloaded and switching is not useful anymore.

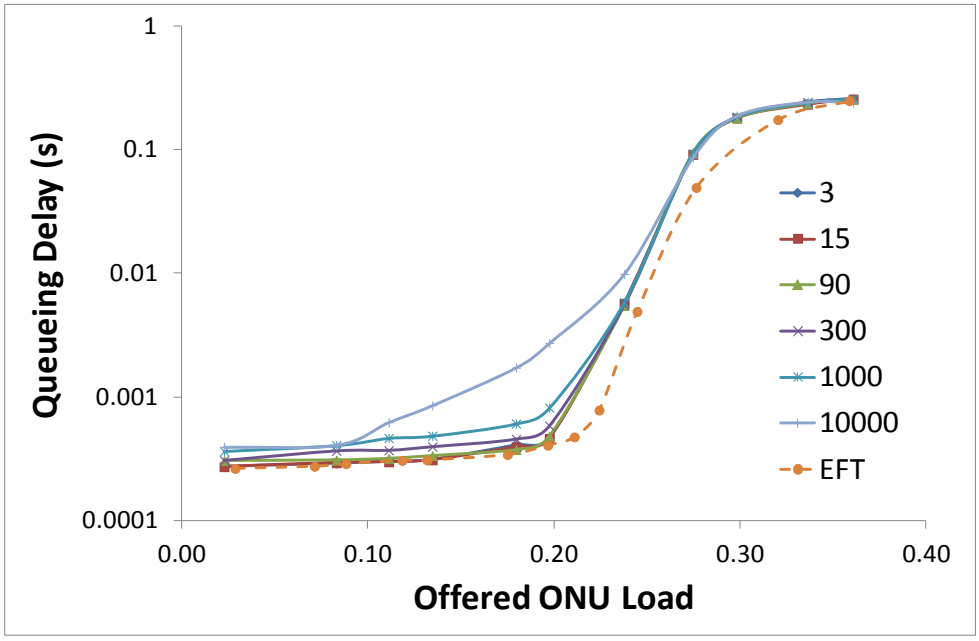

Figure 27: Queueing delays for EFT-MWS with different TGmin compared with EFT and static WDM.

The corresponding number of switching times per ONU is depicted in Figure 28. EFT shows the huge number of switching times due to 74% of all requests are switched to another channel. With our limitations the number drops quickly for TGmin = 90 and higher. With this value 95% of all possible switchings are blocked, mostly because of a limited gain.

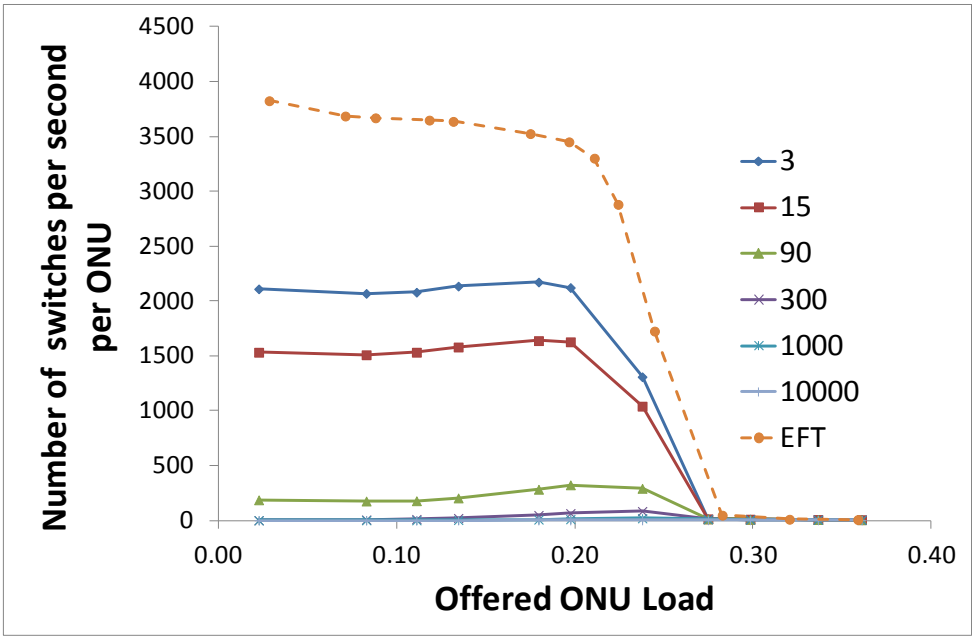

Figure 28: Switching times for EFT-MWS with different TGmin compared with EFT.

When the results on Figure 27 and Figure 28 are considered together, a trade-off between the number of switching times and the queueing delay has to be made. We choose TGmin = 90 as this is the most optimal value from these results. In Section III we suggest the problem of the nonzero tuning time. Figure 29 depicts the influence of larger tuning times ranging from 50 µs up to 10 ms. The results show that realistic tuning times cannot be ignored because the queueing delay becomes problematic. However, EFT-MWS is capable of using TLs with

ttune = 50 μs , which is much larger than the guard band.

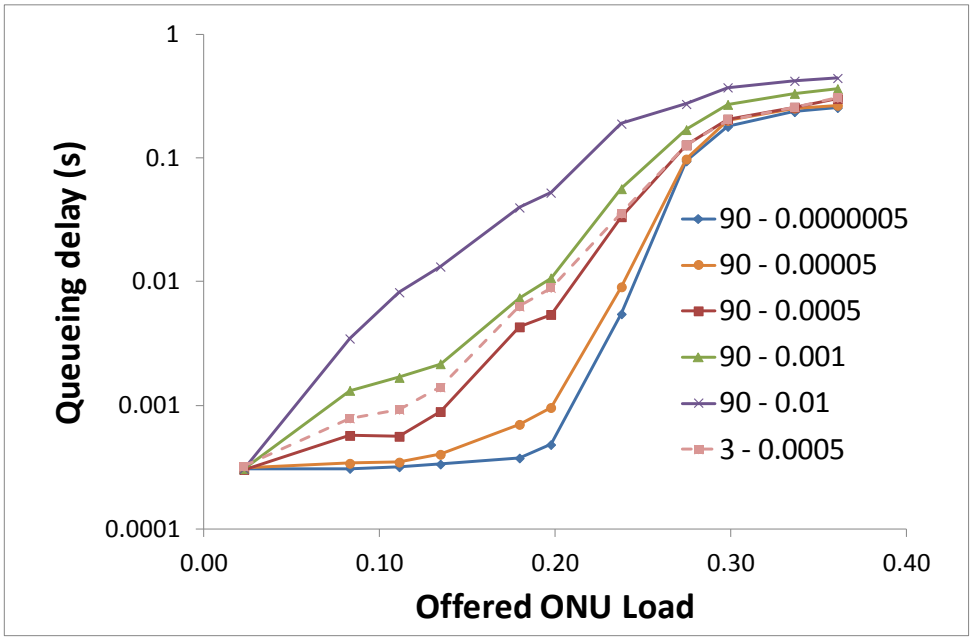

Figure 29: Influence of larger tuning times for EFT-MWS.

4.2.2 Implementation of resource allocation for hybrid WDM/TDM PON in optical test bed: Performance evaluation of AMGAV

Challenges related to resource allocation in the time domain are primarily associated with the increased reach of NGOA systems and the increased system round trip time which degrades performance of conventional DBA algorithms. In the OASE deliverable D3.2, we have proposed the Adaptive Multi-Gate polling with void filling (AMGAV) algorithm, which improves the DBA performance for the Long-reach PON. In this section, we study the comparative performance of the AMGAV algorithm with the traditional DBA algorithm (called the interleaved polling with adaptive cycle time or IPACT). The algorithms are implemented in an optical test bed. Although, WP7 covers the main work related to test-bed activities from a component perspective, this work relates to the implementation of algorithms in real hardware and the actual performance of these algorithms within a hardware implementation (as opposed to a simulation).

The optical test bed used in the study comprises of the following components: 1G Networked Field Programmable Gate Arrays (NetFPGA), media converters, WDM Filters, SFP 1310 and 1550 nm transceivers, power splitters and optical switches. Since the SFP transceivers are over media converters, it does not give us complete freedom to turn on/off transceivers, and thus optical fiber switches are used to perform a virtual TDMA operation. The optical switches will induce additional guard band overheads and thus the performance of algorithms will reduce. However, since the performance degradation will be same for all the compared algorithms, some useful insights can be drawn from the obtained results. Presently, the algorithms are implemented using C, however, the more precise timing control would be obtained by the implementation of the algorithms in Verilog.

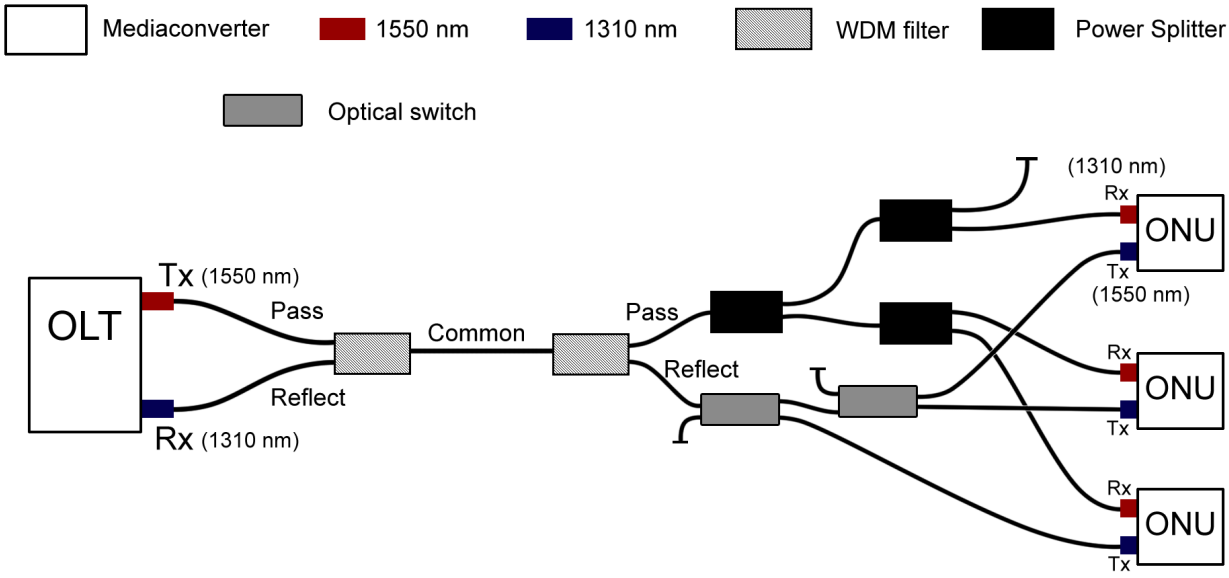

Figure 30: The optical test bed used for the measurement of DBA performance.

To control the network, we make use of two 1G NetFPGAs inserted in a workstation. The picture of a 1G NetFPGA is shown in Figure 31. The 1G NetFPGA consists of a Xilinx Virtex-II Pro FPGA, which can be programmed by using a hardware description language like Verilog. In our project, we configure our NetFPGAs as a Network Interface Card (NIC). The NetFPGA features four gigabit Ethernet network ports. The electric signals coming from the NetFPGAs are coverted into optical signals by using a media converter with an SFP (Small-Form factor Pluggable) inserted. The Media Converter is configured using Telnet. The SFP contains a receiver (PIN photo-diode) and a transmitter (Fabry-Perot laser). A SFP on 1310 nm wavelength for upstream and 1550 nm for downstream is used. Furthermore, WDM filters are used to multiplex/demultiplex the two wavelengths. As the media converters are not able to force the laser shutdown, the optical fiber switches are used to allow only 1 ONU to transmit at a time. By switching the optical switches we are then able to decide which ONU should be connected (in its upstream path) with the common fiber. We make use of the CrystaLatch 2x2 from Agiltron, a fast Solid State fiber optical switch. The switch has 2 input and output fibers. The switch is actuated by applying a voltage pulse on the 2 pins of the switch, which is done by sending a pulse on the parallel port of the workstation. The output fibers are straight or cross connected to the input fibers depending on the polarization of the voltage pulse. The voltage of the pulse must be 2.5 V and the current has to be 200 mA, but as the parallel port delivers 4.3 V and 5 mA, we need to employ an electrical driver circuit to make the parallel port useful. In this circuit, we used 2 microcontrollers to make a perfect and safe (a too long pulse can damage the switch) pulse of 200 µs.

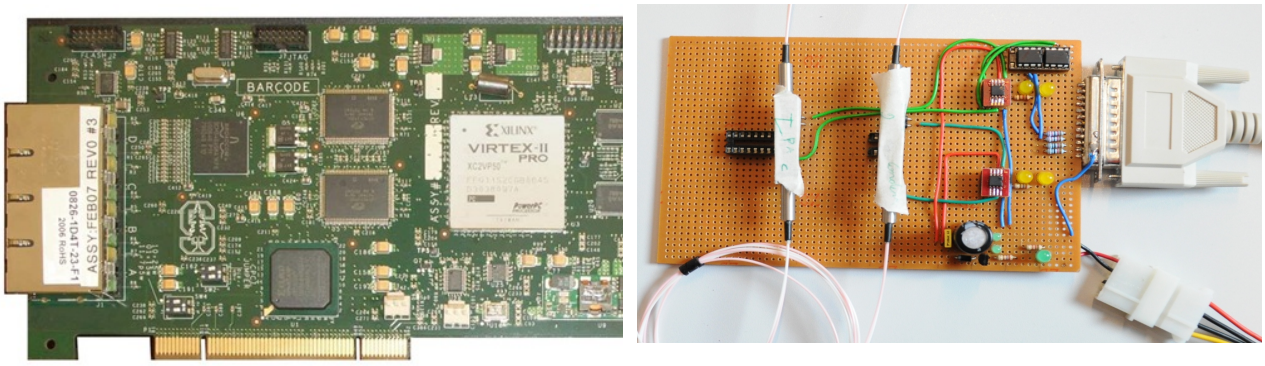

(a) (b)

Figure 31: (a) shows the 1 G NetFPGA (b) shows the electric driver circuit used for buffer simulation

Simulation Results

In this section, we discuss the obtained results. We will study the AMGAV algorithm with IPACT limited service. We have tested the results for 3 ONUs with a guard time of 1.8 ms and a buffer size of 10 MB. The generated user traffic is self-similar by aggregating multiple sub-streams, each consisting of alternating Pareto-distributed on/off periods, with a Hurst Parameter of 0.8. We generate packets in the form of Ethernet frames (64 to1518 bytes) and packets arrive at each ONU from the end user. The linux pktgen kernel module is used to implement the traffic generator. Figure 32 shows the delay performance of the AMGAV algorithm with IPACT-limited when the maximum transmission slot per ONU is chosen as 5 ms and 20 ms. When the transmission slot is chosen to be 5 ms, it will lead to high inefficiency and the delay will saturate when the load exceeds 0.6. In case of transmission slot per ONU as 20 ms, the throughput of about 90% can be achieved in both cases.

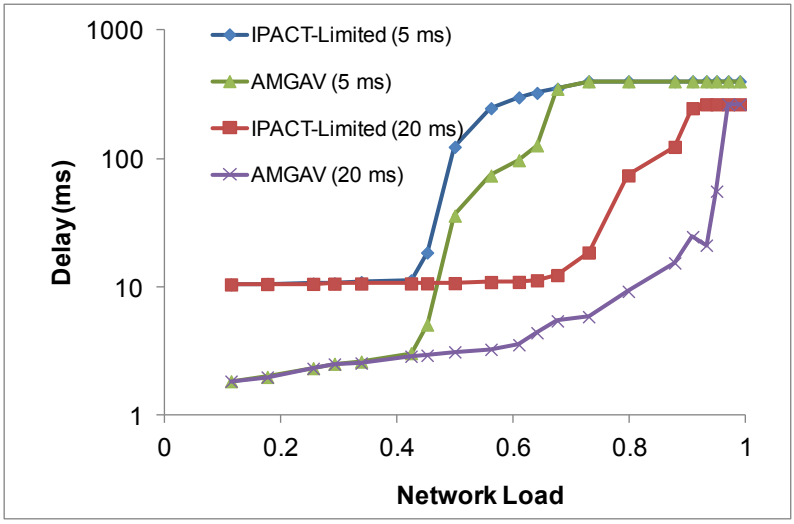

Figure 32: Delay performance of the AMGAV with IPACT-Limited

4.2.3 Implementation of resilience techniques

In this section we will estimate the reliability performance of the various unprotected hybrid WDM/TDM PON systems and identify where resilience is really required.

Figure 33 gives the unavailability of various hybrid WDM/ TDM systems. After a reach of 1 km, feeder fiber (FF) (which is split between the three considered scenarios) is the dominating part. The unavailability of an OLT and a wavelength switched RN1 is relatively high. For high customer satisfaction, the ONU reliability is also crucial. The wavelength selected RN1 has high unavailability, as it always uses an active reach extender (RE). There is a step jump in the unavailability of RN1 - wavelength split due to the need to use a RE after 16 km. The reliability of the remaining elements is not crucial. This evaluation helps us to identify that FF, OLT, wavelength switched RN1, ONU and RN1 with REs are the real difficulties in reaching the satisfactory connection availability.

Figure 34 gives the figure of merit (FOM) (see definition in OASE deliverable D3.2) values for different elements of the considered hybrid WDM/TDM PON variants. Note that we do not show the FOM of DF and LMF as it is expected to be quite high due to the small number of end users affected by a failure occurred at DF or LMF. FF, OLT, wavelength switched RN1, and RN1s with REs are most important to protect. We see that, from an operator perspective, it is not important to protect an individual customer. It is most relevant to protect up to RN1 and not afterwards, as there is no major impact of failure of RN2 and ONU.

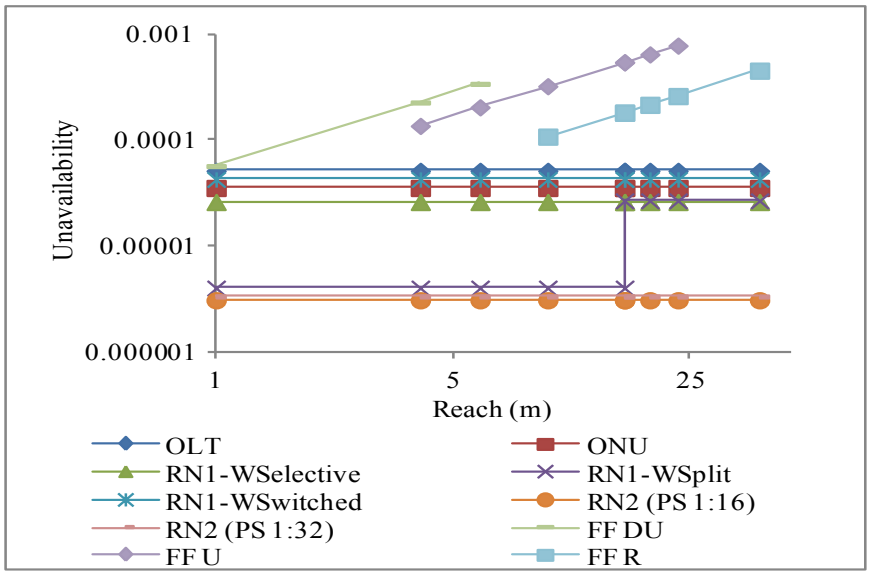

Figure 33: Unavailability of various unprotected systems

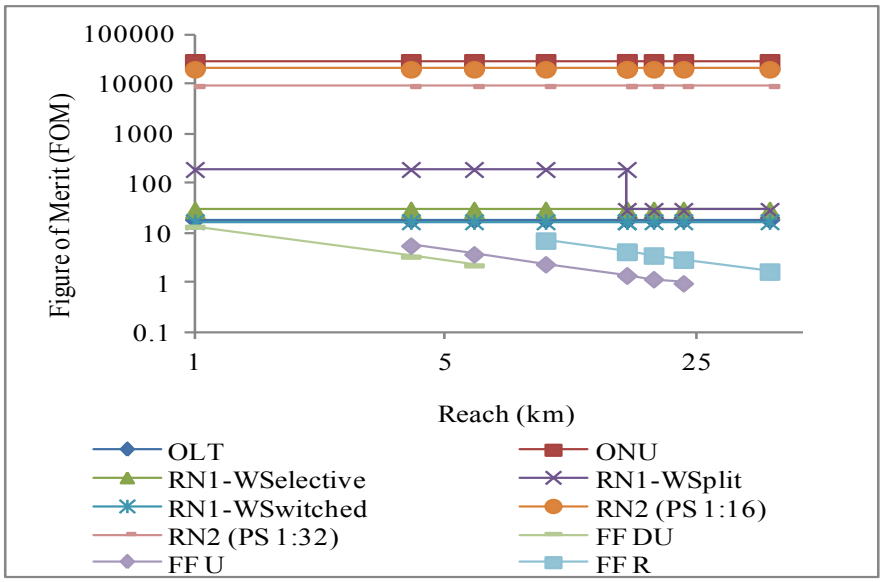

Figure 34: FOM of various unprotected systems

4.2.4 Power saving techniques

The power-saving techniques described Section 3.2.2 in this deliverable are quite generic and applicable to most of the NGOA architectures being investigated in the OASE project. Many of the power-saving modes (sleep/idle/hibernate modes) can be applied to all the NGOA architectures. The hybrid WDM/TDM-PON architecture offers additional (alternative) power-saving/energy-efficiency opportunities because of its active intermediate remote node (located at PCP5) containing the wavelength-selective switch (WSS) or optical switch. In this particular case, the NG AON also shares this property and can also enjoy the same energy-efficiency benefits as the hybrid WDM/TDM-PON. Active remote nodes offer interesting opportunities for lowering the carbon footprint of the overall network architecture, since the power requirements at the RN tend to be quite modest. For example, in the case of the hybrid PON, the WSS is only anticipated to require 10 W of power. This figure is likely doubled (power usage effectiveness, PUE=2) by a suitable environmental conditioning system, so as to maintain an appropriate temperature within the cabinet all year around. Fortunately, in line with the solar power set-up described in section 3.2.3, such modest power requirements enable the active RN to be powered by small-scale renewable energy sources, e.g. photo-voltaic (PV) cells, and/or a wind turbine. In this case, supplying a guaranteed 20 W power requires a PV cell with 200 W capability, which equates to a panel area of 1.67 m^2, for a conversion efficiency of 12%, irradiance of 1 kW/m^2, and a 90% overprovisioning factor. Likewise, a wind turbine with a blade radius of only 0.57 m would also be expected to be able to produce an average 20 W power output, assuming 90% overprovisioning, an average wind speed of 5 m/s, and 59% Betz-limit efficiency factor [16].

For the power-saving modes, the hybrid-PON with its burst-mode operating basis is particularly ideal for energy-saving sleep, idle, and hibernation modes, since the transmitter and receivers are designed to have rapid switching-on and –off times. In this case, the ONTs need to be co-ordinated via the appropriate MAC protocols, as are discussed below. However, as earlier described in Section 3.2.3, we have also been investigating a master-slave mode of operation for those items of equipment which do not necessarily switch as fast as burst-mode devices, and which also tend to exhibit an inelastic power consumption compared with the variation in traffic load presented, for example routers and switching equipment. In the base

of hybrid-PON, the L2 switch at the OLT lends itself to master-slave switching. Here, the estimated power consumption of the L2 switch is up to 800 W for a maximum 800 Gb/s throughput. According to the simulations discussed in section 3.2.3, assuming a Poisson-distributed upstream traffic distribution, with a x50 statistical multiplexing advantage, and a 50% most-likely (modal) peak load, then the master-slave approach can generate potentially up to 26.3% energy savings, i.e. reduce the L2 power consumption to only 589.6 W. In this case, the master L2 switch has a capacity of 800 Gb/s, whereas the slave switches in at 50% load and has a capacity of only 400 Gb/s. Trying to achieve a higher energy-efficiency saving, e.g. 45.7%, would require a 30% modal peak load distribution; but this is likely to be an inefficient use of the CapEx resource, since it would tend to require a lower statistical multiplexing advantage of only about x30 in this case. Here, the master switch would still have a 800-Gb/s capacity, while the slave L2 switch would only have a capacity of 30% of 800 Gb/s, which is 240 Gb/s. In this case, the overall expected power consumption would be 434.4 W (i.e. a saving of 365.6 W as compared to the single device deployment); but in order to offer the same stat-mux QoS and packet-loss ratio (as compared with the x50 stat-mux case) there would need to be 50/30=1.67 times as many master-slave L2 switch units at the OLT head end. Apart from the additional CapEx costs required, the overall power consumption for the same total number of end-users, would also increase by a factor 1.67 to 725.5 W.

In addition to these approaches, the hybrid WDM/TDM PON architectures may further benefit from switching off and on OLT line cards in night and day scenarios. During times when the network load is low, some OLT line cards can be switched off, leading to energy efficiency. The number of line cards that can be turned off depends upon the network load, and the flexibility of the remote nodes. For example, a power splitter based remote node is full flexible as all wavelengths are routed to each customer and an AWG based remote node is completely static. Furthermore, the opportunity to use a minimal number of transceivers can be complemented by the multi-cast functionality of WSSs. In hybrid WDM/TDM PON with power splitters or with AWGs, every wavelength undergoes the same level of splitting. However, the uniform splitting of wavelength is not optimal. For example, the users which are close by can be grouped on the same wavelength and the wavelength can undergo a higher splitting whereas for the users which are far off should be served with a wavelength which undergoes a lower splitting. By using WSSs, we group ONUs on the basis of their distances and this lead to the optimal splitting of the wavelengths. Note that, the grouping of users on a wavelength also depends upon the load of the network, and thus can not be dimensioned from the start. This optimal spltting of the wavelengths lead to the minimal use of transceivers at the OLT and lead to energy efficiency. However, the number of used wavelengths is also influenced by the data rates and the offered load. For example, when the data rate or the network load increases, small number of users can only be served using the same wavelength as otherwise their sustainable bandwidth requirement can no longer be fulfilled.

Figure 35 shows the energy consumption of the OLT when the ONUs are grouped on the same wavelength according to distance while still satisfying the data rate of the users. In this way, we can minimize the use of transceivers and switch them off leading to the savings in energy consumption. The 100 % is the energy consumption when all transceivers are on. Since the power consumption of ONU is much higher than OLT, there is a much smaller effect of power saving techniques at the OLT on the overall savings. However, the power savings at the OLT will also lead to savings for cooling. The power for cooling is typically equal to the system power used (PUE=2).

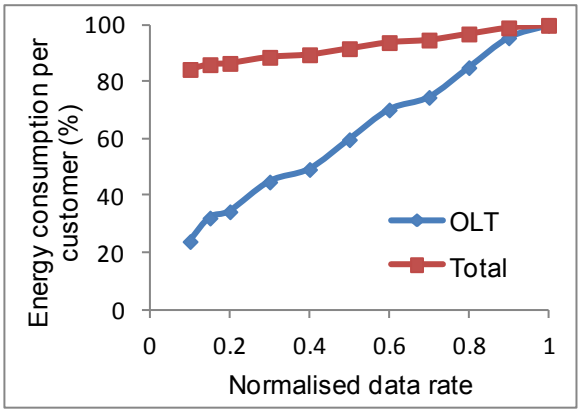

Figure 35: shows the energy consumption of the OLT per customer where the 100 % represents the energy consumption of the OLT in static hybrid WDM/TDM PON

Data link approach for power saving

This section examines a data link approach for power saving applied to passive hybrid WDM/TDM PON. A service-based technique originally proposed for TDM PON is considered and further extended to be utilized in passive hybrid WDM/TDM PON. The scheme can minimize the energy consumption at ONUs while guaranteeing the network requirements (e.g., delay) by using a Sleep and Periodic Wake-up (SPW) control mechanism with variable sleep periods.

In SPW, the OLT manages energy saving at the ONUs through the SPW technique using sleep cycles. The ONUs switch between sleep mode or active mode depending on the OLT's decisions. Our SPW technique is based on the one presented in [17] in which the sleep period is set by an interarrival-based algorithm between two values. Ouridea is to extend the SPW technique to a service-based algorithm in which the sleep period is set in order to maximize the energy savings for ONUs while guaranteeing the required maximum tolerable delay for different services.

Service-based algorithm

The concept of a service-based variable sleep period has been proposed in [18] to save energy in ONUs while avoiding service degradation in the presence of traffic with demanding requirements (e.g., delay). According to this approach, each class of service (CoS) is assigned a specific sleep period. If multiple CoS are received at one ONU, the sleep period of the most demanding class is selected. The feasibility of using the concept of cyclic sleep with adaptable sleep length has also been experimentally proven in [19]. In this work, two methods of estimating packet inter-arrival time are combined with two strategies for choosing the length of the sleep period as a function of the estimated inter-arrival time. As a result, the authors in [19] present four methods for choosing the most suitable sleep period for a certain predicted value of inter-arrival time.

Usually one CoS is characterized by strict and absolute Quality of Service (QoS) constraints that must be met by the service provider to adhere to the Service Level Agreement (SLA) stipulated for users of the ONU. In addition, users (i.e., ONUs) may dynamically modify their service subscriptions (e.g., request a video streaming to watch a movie for some hours), possibly changing the overall delay requirements.

Utilizing the service-based variable sleep period concept, this section proposes a method for maximizing the energy savings for ONUs while guaranteeing the required maximum tolerable delay for different services. The approach differs from the one proposed in [18] because the

chosen sleep period is a function of the maximum allowed delay rather than based on the estimated average inter-arrival time and the highest-priority class. Moreover, it differs from the approach proposed in [18] and [19] because the sleep time is a function of the CoS absolute delay constraints instead of the estimated packet inter-arrival time.

We assume that the OLT is constantly aware of the services subscribed by each ONU by using a certain packet processing technology, such as deep packet inspection. In addition, the OLT has a table in which services are categorized in terms of CoS with specific absolute bandwidths (i.e., data rates) and delay constraints. Such constraints can be derived from ITU-T standards such as [20][21] and statically loaded into the OLT. Leveraging on such information, the OLT dynamically builds a table containing the minimum bandwidth and maximum delay requirement per each registered ONU. The minimum bandwidth is the sum of all the minimum bandwidths (in this work, Poisson arrival process is assumed) while the maximum delay is the minimum of all the average acceptable delays required by the services to which the ONU is subscribed.

Table 3 shows several typical applications with their corresponding delay requirements and data rates. Note that the delays shown in this table are the strict delay requirement for the access segment only that can be inferred from the contributing portion of access network to overall end-to-end delay of an Internet application presented in [21].

Table 3: Applications with their corresponding delay requirements, data rates and service class

Service Class	Service Type	Average Delay [ms]	Data Rate Bi [b/s]
1	Web Browsing	220	30.5K
2	Internet Relay Chat	110	1K
3	Multimedia on Web	84	28.8-500K
4	Voice over IP	56	5.3-64K

The ONU implements a slightly modified version of Sleep and Periodic Wake-up (SPW) (i.e., cyclic sleep) [17] whose behavior is depicted in Figure 36. The main difference from SPW is that no threshold for the frame inter-arrival time is used to set the ONU sleep time. One period of activity T_a of the ONU used for exchanging Confirmation, Request, and ACK messages with the OLT is always followed by sleep period of duration T_{sl}. Moreover, whenever the OLT receives a Confirmation message from the ONU, it sends all data frames received before the Confirmation reception (e.g., frames n-2, n-1, and n in Figure 36) to the ONU. This operation requires a variable time T_{DS}.

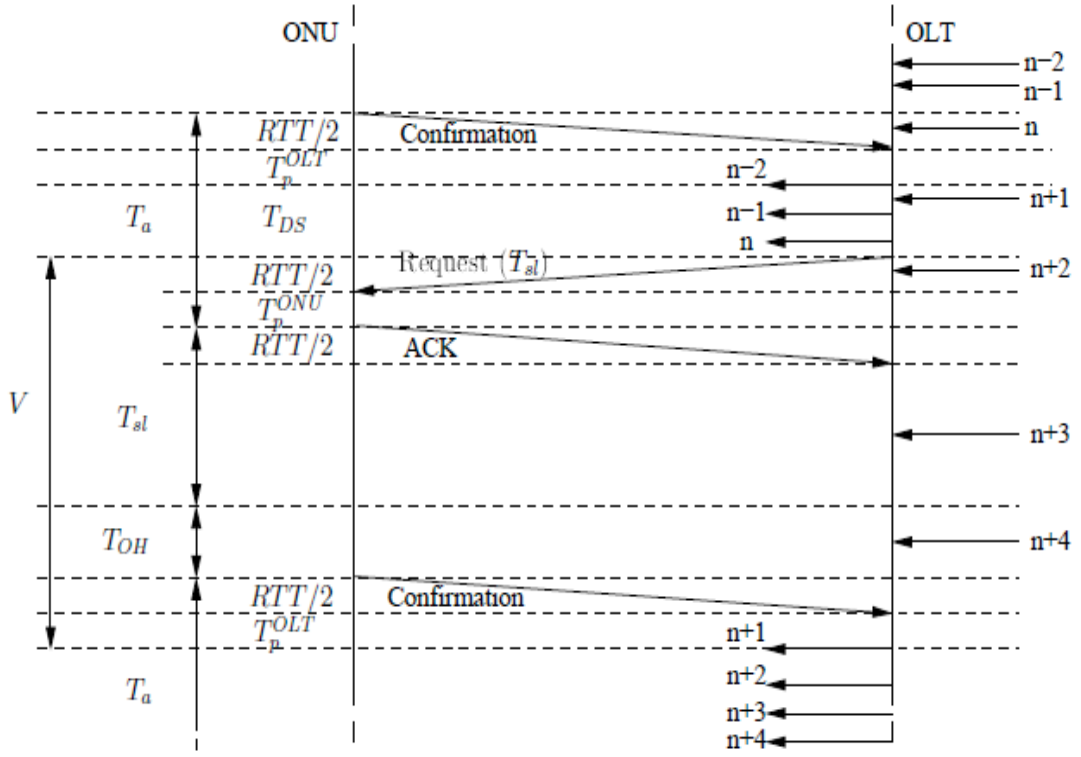

Figure 36: SPW operation with the service-based algorithm

A first approximated model of the system OLT-ONU with the modified SPW is a M/G/1 queue with vacations [22]. The average waiting time of a frame in the queue is expressed by:

$$\overline{W}_{q\ ,MG1} = \frac{\lambda \cdot \overline{S^2}}{2 \cdot \left(1 - \lambda \cdot \overline{S}\right)} + \frac{\overline{V^2}}{2 \cdot \overline{V}} \qquad (1)$$

where $\overline{S}$ is the average service time, $\overline{S^2}$ is the second moment of the service time, λ is the average frame arrival rate, $\overline{V^2}$ is the second moment of the vacation time and $\overline{V}$ is the average vacation time.

A more detailed model that has been considered is a polling system with gated service policy with identical stations [23]. The average waiting time of a frame in the queue $\overline{W}_{q\ ,poll}$ is expressed by:

$$\overline{W}_{q\ ,poll} = \frac{\overline{V^2} - \overline{V}^2}{2 \cdot \overline{V}} + \frac{N \cdot \overline{V} \cdot \left(1 + \lambda \cdot \overline{S}\right)}{2 \cdot \left(1 - N \cdot \lambda \cdot \overline{S}\right)} + \frac{N \cdot \lambda \cdot \overline{S^2}}{2 \cdot \left(1 - N \cdot \lambda \cdot \overline{S}\right)} \qquad (2)$$

where N is the number of ONUs. Assuming negligible processing time T_p at both ONU and OLT and transmission time of the control frames, the vacation can be written $V = T_{sl} + T_{OH} + RTT$, where T_{OH} is the clock and frame synchronization overhead and RTT is the round trip time. For networks in which the service time is significantly smaller than the sleep time and $\lambda \cdot \overline{S} << 1$, Eq. (2) can be approximated as:

$$\overline{W}_{q\ ,poll} \approx \frac{N \cdot \overline{V}}{2} \qquad (3)$$

For example, in a scenario with 1250 byte frames, transmission rate of 10Gb/s, frame arrival

rate λ = 62.5 frame/s (i.e., 625 kb/s), T_{sl} = 1 ms, T_{OH} = 2 ms,

N = 1, and RTT = 0.4 ms the three contributions to $\overline{W_{q,poll}}$ in Eq. (2) are 0, $1.7\text{x}10^{-3}$, $3.125\text{x}10^{-11}$, respectively. Because V is constant, it is possible to write:

$$\overline{W_{q,poll}} \approx \frac{V}{2} = \frac{T_{sl} + T_{OH} + RTT}{2} \qquad (4)$$

Solving the equation (2) and considering only one station (N = 1), (2) can be written:

$$\overline{W_{q,poll}} = \overline{W_{q,MG1}} + \frac{\overline{V} \cdot \lambda \cdot \overline{S}}{1 - \lambda \cdot \overline{S}} \qquad (5)$$

The average queuing delay of the two systems can be approximately the same only if $\lambda \cdot \overline{S} << 1$ and $\overline{S} << T_{sl}$ with V constant. Then:

$$\overline{W_{q,poll}} \approx \overline{W_{q,MG1}} \qquad (6)$$

Figure 37 shows the algorithm for the OLT to determine the sleep period for an ONU. The algorithm is based on substituting $\overline{W_{q,poll}}$ with the maximum delay D_{max} and deriving T_{sl} as a function of the other quantities in Eq. (4).

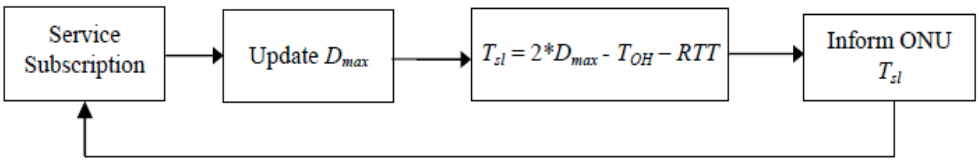

Figure 37: Algorithm for the service-based method

The algorithm starts with the service subscription of each ONU. The OLT builds or updates the table for each ONU in which the services subscribed are categorized in terms of CoS with specific absolute bandwidths and constraint delay. Thus the maximum delay D_{max} of a service composition is calculated from the table and used in input to derive T_{sl}. The last step is to inform the ONU about the sleep period through a Request message.

Simulation scenarios

We built a model in OPNET Modeler, a network modeling and simulator tool, to evaluate different energy saving techniques, in particular using sleep cycles in the ONU.

OPNET has a hierarchical architecture in a manner that emulates real network systems. Specialized editors address issues at different levels of the hierarchy. This provides an intuitive modeling environment and also permits re-use of lower level models.

The bidirectional transmissions in a PON are performed by a point-to-multipoint (P2MP) network between an OLT placed in the Central Office (CO) and an ONU interfaced to the client network.

A single fiber is used to serve multiple premises, exploiting passive components like optical splitters, by a bus topology with 1x2 optical tap couplers to attach the nodes to the bus as shown in the Figure 38.

Figure 38: Bus topology of the PON model

The bus topology is chosen to simplify our model. The bidirectional communication is the same as a tree topology with a passive splitter following the same policy in which the ONUs can transmit frames only to the OLT sharing the optical fiber and the OLT sends traffic in broadcast to all the ONUs using the logical link ID LLID.

We set the distance between the OLT and the ONU in terms of propagation delay T_{pr} to 0.2 ms. Since we are studying a 10G peak data rate, the transmission capacity of the bus link and the optical tap couplers is set to 10 Gb/s.

The traffic flows downstream (from the network to users) and upstream (from the users to the network) using two different wavelengths. All the upstream signals can operate in the same wavelength in a Time Division Multiple Access (TDMA) managed by the Multi-Point Control Protocol (MPCP) assigning to the ONUs the transmission windows. There is no frame loss, since all downstream frames coming when the ONU could not receive them are buffered at the OLT. For sake of simplicity, only downstream traffic from one OLT to one ONU is considered in simulation.

In the SPW technique, the ONU can switch between the active mode and sleep mode. Depending on which mode is enabled, the unit consumes different amounts of power, in particular, P_a equal to 10 W in active mode and P_s equal to 1 W in sleep mode. The time that the ONU needs to trigger the active mode from the sleep mode is T_{OH} that is set to 2 ms.

The data frames arrive at the OLT according to a Poisson process with arrival rate λ frames/s depending on the ONU service composition. We run two sets of simulations. In the first set a source is used to generate traffic with the bandwidth of a single service composition, while in the second a source generates traffic for each service composition.

In both the sets, the simulations are run twice with different frame size f_s , one is constant and equal to 1250 bytes, the second one is uniformly distributed between 72 and 1526 bytes - the Ethernet minimum and maximum frame size respectively.

Without loss of generality, this work limits the number of traffic classes to 4 and considers several class combinations as shown in the left part of Table 4. For classes with a range of data rates, the maximum one has been considered to compute λ. The values of λ^{-1} reported in Table 4 have been computed by following formula:

$$\lambda^{-1} = \frac{8f_s}{\sum_{i \in S} B_i} \quad (7)$$

where S is the service composition.

The bandwidth for a service composition is the sum of the bandwidth B_i of all the services that are part of it, assuming frames arrive following a Poisson process.

The evaluated performance metrics are the frame queuing delay D and the energy efficiency

η. Here, the efficiency is defined as

$$\eta = 1 - \frac{E_{sleep}}{E_{nosleep}} \quad (8)$$

where E_{sleep} is the energy consumed by the ONU implementing the proposed sleep mode and $E_{nosleep}$ is the energy consumed by the ONU if it is always active.

The results are collected by post processing operations setting as input the T_{sl} and the average inter-arrival time values in input to the simulator for a specific service composition. The T_{sl} is calculated as

$$T_{sl} = 2 * D_{max} - T_{OH} - RTT$$

where D_{max} is the maximum constraint delay of a service composition taken from the table that the OLT built for each registered ONU; T_{OH} is the time of overhead in which the ONU switches from the sleep mode to active mode; RTT is the round-trip time between OLT and ONU. The inter-arrival time is calculated as in (7).

The output parameters of the system are the queuing delay for the frames with constant and uniform distributed size and the energy efficiency calculated as in (8). Moreover the confidence interval with confidence level of 0.9 is calculated for both output parameters.

The results from the first set of simulations are shown in the Table 4. In the right part of the table it is shown that in any service composition, ONU can save up to around 89% of energy while not violating any delay requirements. The advantage comes from the method of determining the sleep time that allows the ONU to maximize the sleep time, thus maximizing the energy savings, without violating the service delay constraints.

Table 4: Results per service composition with one generator of traffic

Input Parameters				**Output Parameters**	
Service Composition	λ^{-1} [ms/frame]	D_{max} [ms]	T_{sl} [ms]	D_{const} , D_{uni} [ms]	Efficiency η [%]
1+2+3+4	17	56	109	55.7 (± 1.8 x 10^{-1})	88.01 (± 3.0 x 10^{-4})
1+2	317	110	217	109.7 (± 3.7 x 10^{-1})	89.01 (± 1,3 x 10^{-4})
2+3	20	84	165	83.7 (± 0.7 x 10^{-1})	88.66 (± 3.2 x 10^{-4})

The reliability of the formula used for this system is compared with our simulations. The results are taken with a T_{sl} set and changing the average bandwidth of the traffic generated:

$$B = \frac{10}{2^x} Gbit/s \quad (9)$$

with x = {0, 1, 2, 3, 4, 5, 6}.

The average inter-arrival time is calculated as in (7).

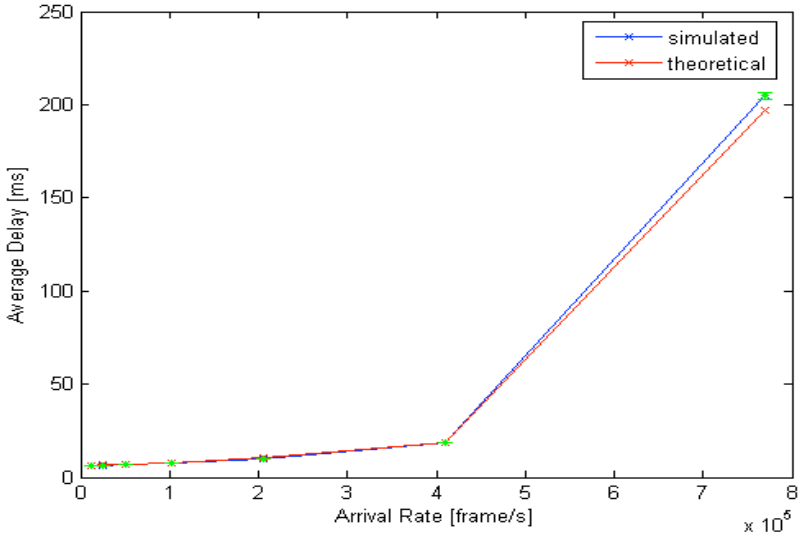

Figure 39: Comparison between the theoretical and simulated average delay

As Figure 39 shows, the curves of the theoretical average delay and the simulated average delay are exactly the same until close to the limit of transmission rate of 10Gb/s.

The last step is to verify that the results collected about the average delay D, considering only one generator, are the same considering one generator per service.

The second set of simulations were run to verify that the simplification of using only one generator with the bandwidth of a service composition was correct and if the service with the maximum constraint still respect the acceptable delay. The results are shown in the Table 5, Table 6 and Table 7.

Table 5: Results for a service composition 1+2+3+4 with a generator of traffic per service

Service Composition: 1+2+3+4 with T_{sl} = 109 ms					
Input parameters			**Output parameters**		
Service	λ^{-1} [ms/frame]	D_{max} [ms]	D_{const} [ms]	D_{unif} [ms]	Effic. η [%]
1	328	220	55.9 (± 7.8 x 10^{-1})	55.6 (± 7.8 x 10^{-1})	88.01 (± 3.0 x 10^{-4})
2	10000	110	55.3 (± 4.9)	55.1 (± 5.3)	
3	20	84	55.7 (± 1.9 x 10^{-1})	55.7 (± 1.9 x 10^{-1})	
4	156	56	55.9 (± 5.4 x 10^{-1})	55.7 (± 5.4 x 10^{-1})	

Table 6: Results for a service composition 1+2 with a generator of traffic per service

Service Composition: 1+2 with T_{sl} = 217 ms					
Input parameters			**Output parameters**		
Service	λ^{-1} [ms/frame]	D_{max} [ms]	D_{const} [ms]	D_{unif} [ms]	Effic. η [%]
1	328	220	109.7 (± 3.8 x 10^{-1})	109.7 (± 3.8 x 10^{-1})	89.01 (± 1.3 x 10^{-4})
2	10000	110	109.7 (± 2.1)	109.6 (± 2.1)	

Table 7: Results for a service composition 2+3 with a generator of traffic per service

Service Composition: 2+3 with T_{sl} = 165 ms					
Input parameters			**Output parameters**		
Service	λ^{-1} [ms/frame]	D_{max} [ms]	D_{const} [ms]	D_{unif} [ms]	Effic .η [%]
2	10000	110	83.5 (± 1.6)	83.7 (± 1.6)	88.66 (± 1.9 x 10^{-4})
3	20	84	83.7 (± 0.7 x 10^{-1})	83.7 (± 0.7 x 10^{-1})	

The results in the tables show the correctness of our previous assumption that we may consider the bandwidth of a service composition as the sum of the bandwidth of each service. We obtained values of the average delay in both situations of constant and uniform distributed packet size in accordance with the delay constraints for each service in all combinations. The average delay for each service respects its own constraint delay. Besides, the energy efficiency of each combination is the same as in the case of where only one generator is being used and so reaches a value of around 89%.

4.3 NEXT-GENERATION AON

The OASE project has set an ambitions long term goal of up to 300Mb/s - 500Mb/s sustainable bandwidth per customer with a minimum peak rate of 1Gb/s. This extraordinary bandwidth goal is meant to enable delivery of future services, especially future high definition TV steams and other high bandwidth services.

This, combined with a high customer density, leads to very high bandwidths higher up in the access and aggregation network. For example, every OLT in NGOA architectures will generate at least 300 Gb/s traffic in this long term scenario. This traffic is then aggregated into streams at even higher bandwidths on each aggregation step. This leads to a network where the core nodes would be required to handle hundreds of Tb/s, which would create immense challenges. It is therefore desirable to minimize the traffic reaching these higher aggregation nodes, and keep the network traffic local in the network. This could, if successful, reduce the load of higher aggregation nodes and therefore reduce the dimensioning requirements for the higher aggregation nodes, which in turns reduces costs for the network operator. It would also lead to higher degree of quality of service for such flows, due to (for example) lower latency and lower contention probability through lower hop count.

Deliverable 3.3 presents traffic measurements and analysis of content distribution in current FTTH networks. This work analysed the content locality of transported content, i.e. how many end customers were interested in the same content during a certain time window and how close they were located in the network topology. The content was distributed via the BitTorrent protocol, a content distribution protocol selected because of its popularity in the networks measured. The study looked into how much of the content could be distributed via a

more local route between end customers instead of forcing the traffic to go via more centrally located nodes. This also provides an initial analysis of the benefits which may be obtained from content caching servers placed at the customer premises or in the access and aggregation network. It was found that as much as 24% of the traffic could be kept local in the network if customers would exchange the specific content in a more local manner. This amount could be as much as 50% if a caching node is introduced into the network. The amount of active customers in these networks were relatively low, 500 and 1200 respectively. This represents fewer customers than will be expected from one CO in an urban scenario. This means that local traffic flows, because of peer-to-peer traffic or local caches, are possible even in the lowest aggregation steps. It is also likely that CDN nodes would become more common even at lower aggregation levels in the network as traffic demands increases.

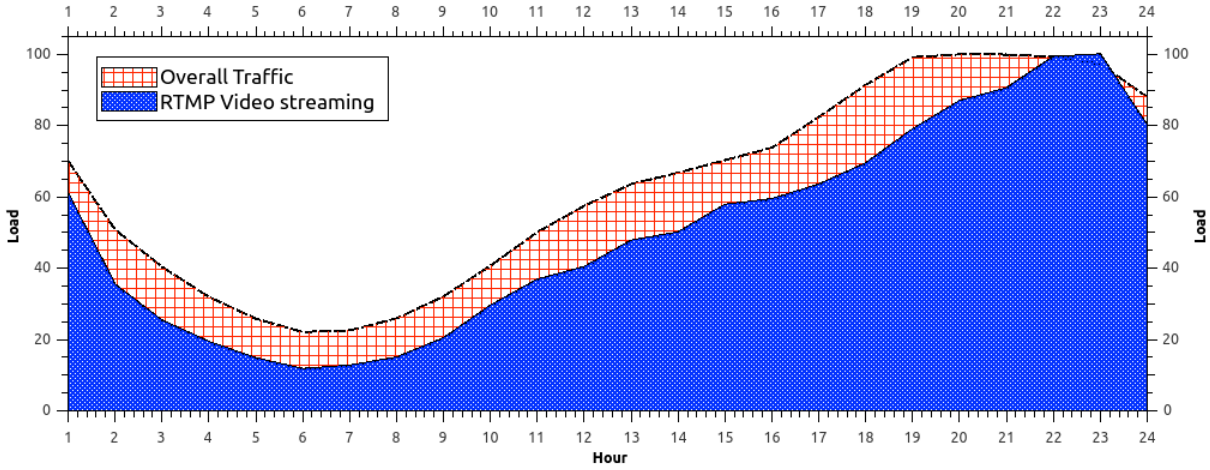

Figure 40: Average traffic load per hour in FTTH network in southern Sweden.

The future high bandwidth services, for example high quality streaming services, might also change the traffic load of the network to be more concentrated during the evening where these kind of services are often consumed. Figure 40, which presents the average network load per hour for a FTTH network, presents the overall network load and the load from the Real Time Messaging Protocol (RTMP). The RTMP protocol is a common protocol for video distribution on the Internet, used by most of the commercial TV and movie offerings available in the country where the network is located. From this figure it can be be seen that the load is more concentrated to the parts of the day when entertainment is typically consumed. The majority of current users of these services are young and experienced computer users' whose consumption patterns probably differ from the average TV consumer. It is therefore likely that more of the network traffic will be concentrated to the evenings when common users get their TV content via their broadband network connection. This would lead to even less network traffic during off-hours relative to the peak hours. This provides an opportunity to change the network configuration during these off-hours to reduce the energy use, while still provide the bandwidth necessary for the active customers. The network performances required to handle the off-hours network traffic is only a fraction of the performance needed during peak usage; it is therefore possible to scale down the network during off-hours by putting the network in to a low power state. This low power state includes moving the electrical functions of the OLT higher up in the network hierarchy by bypassing normal the OLT on the optical level and shutting down the electrical forwarding of these OLTs. This is possible as aggregating on the lower levels is not necessary as the bandwidth need is low during off-hours. This is not possible in other system candidates as the OTL is the first equipment where active routing decisions can be made.

In this chapter a solution is presented which reduces the load on the higher aggregation levels as well as improving the energy use of NG-AON by reconfiguring the network during off-hours.

4.3.1 Overview of the end-to-end NG-AON network

The proposed NG-AON architecture, described in detail in D3.2 and D4.3, consists of the access architecture with an active remote node and the more advanced longer term aggregation network.

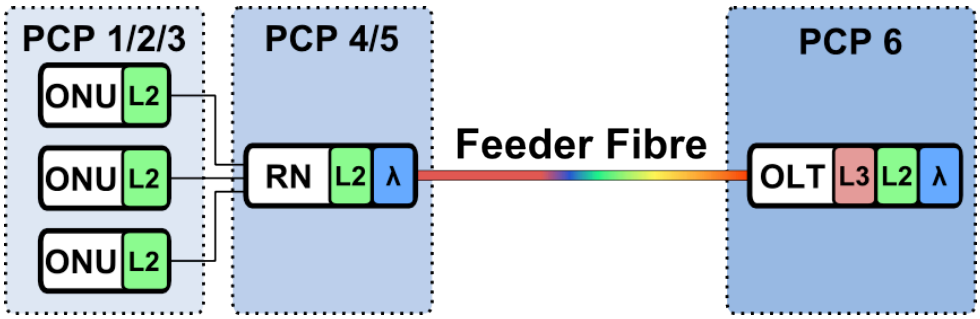

Figure 41: The NG-AON access architecture, with an active remote node. The remote node is capable of layer-2 based forwarding and has a WDM based uplink the OLT. The OTL needs to support layer-2 based forwarding but could also support layer-3 forwarding or wavelength switching.

Access architecture

In the NG-AON architecture each ONU is connected to a remote node via a dedicated fibre using a point-to-point layer-2 connection as seen in Figure 41. The remote node forwards the traffic on layer two and is using a WDM based point-to-point link to the OLT. This architecture could also be modified to use WDM-PON for backhauling, or connecting the remote node directly to an aggregation node in PCP7. The OLT needs to support layer-2 based forwarding but could also support layer-3 forwarding or wavelength switching. The system described bellow augments the OLT with WSS capabilities, which gives the possibility to optically switch a wavelength from the remote node to an aggregation node without terminating the wavelength in the OLT.

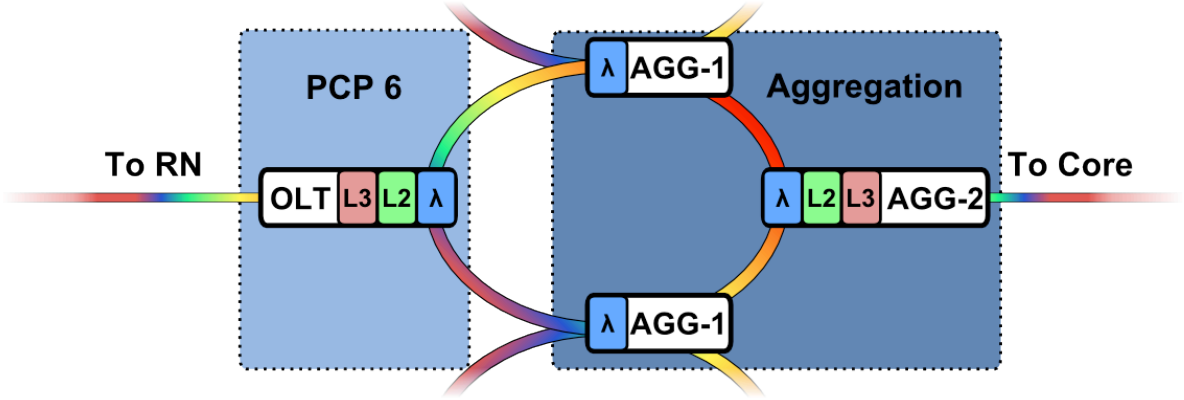

Figure 42: Advanced WDM based aggregation architecture

Aggregation architecture

A result of the OASE long term goal of 300Mb/s sustainable bandwidth is the proposal of a WDM based aggregation network together with WDM based uplink for AON network nodes. This long term advanced network architecture requires an access/aggregation network where the forwarding capabilities of the nodes are mixed, utilising both electronic and optical forwarding. This means, for example, that an aggregation node, connected with other aggregation nodes in a ring, can optically switch wavelengths and, for selected ones, do packet forwarding. The nodes therefore include both WSS and L2/L3 functionality, which is required to handle the large traffic requirements that the long term OASE vision implies.

4.3.2 Flow based network configuration

Traditionally a network configuration is static; at installation time the network is statically configured to handle the current state of the network and certain security requirements. This leads to a network configuration which handles the maximum load in the network and a routing solution where all traffic is pushed up to the network core. Local traffic flows, e.g. traffic between two neighbours, is routed in a very inefficient ways since the traffic needs to traverse all the way to the network core and then be routed back to the same region of the network. Furthermore this type of static network configuration does not handle the daily change in network traffic during a given day, and is instead configured only for the peak usage. This means that most network elements will he heavily underutilized for most of the time, and this underutilization will likely grow which the introduction of more video consumption in the network.

It would therefore be desirable to have a network configuration that can change over time and can handle large local network flows in an efficient way. This could lead both to a reduction in power use as well as a reduction in the load on the higher aggregation nodes, leading to more-efficient dimensioning and therefore lower cost. A solution to these issues is to allocate resources dynamically when needed and shutting down part of the network when the resources are not needed. One way to accomplish this is to allocate resources in the network based on the actual traffic flows in the network. The flows in the network can be analysed at key points in the network, and can then be acted upon by a central traffic-engineering system.

This implementation monitors the traffic at key points, for example at selected aggregation nodes, and based on these flows then optimizes the network state to reduce the impact of these network flows based on certain key parameters. E.g. this could both reduce the network load at higher aggregation levels and reduce the overall power use of the network. The overall procedure is:

1. Monitor and collect flow information at key nodes
2. Identify where these flow originate and terminate
3. Identify problematic path segments, for example:
    a. Flow that could be routed more locally
    b. Flow that can be routed in a more power efficient layer (e.g. optical layer)
    c. Add resources to network nodes with high network load
4. Calculate a more efficient replacement path(s)
5. Allocate the more efficient replacement path(s)
6. Reroute traffic onto new path, while keeping routing entries for the old network path
7. Once flow is reduced or finished, remove new path, traffic flows back on original route.

A side of effect of this procedure is that the network will automatically scale the resources need also for primary path, i.e. path from customer to the core. This means that the network

can be configured for the lowest energy state, where limited resources used, and then let the system allocate more resources, and therefore more energy, as the load of the network goes up. As can be seen, procedure steps 5-7 indicate that resources are allocated in a make-before-break manner, later described in more detail.

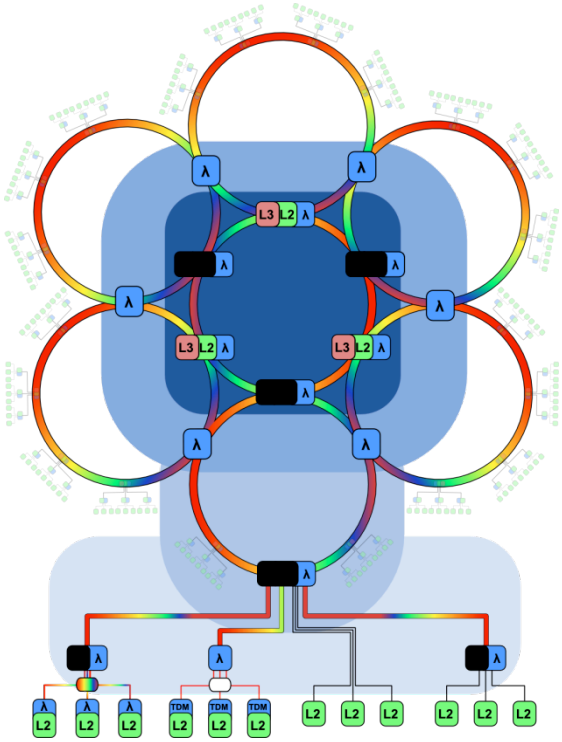

Figure 43: Holistic view of a network in a lower power state, where most forwarding is done on the optical layer

Low power state

The first step in creating the NG-AGON system is to configure the network in a low power state, which provides network connectivity to all customers. This low power state is possible since the bandwidth requirement should only represent the lowest baseline bandwidth requirement. According to Figure 40 this is likely to occur during the nights and early mornings. Much of the electrical-based forwarding can then be bypassed and shut down, and most of the data transport may done on the optical layer. This means, for example, that a single WDM wavelength can be used to transport all traffic from a remote node as high as possible in the aggregation hierarchy. Intermediate nodes will therefore only do optical switching, while the electrical parts of these nodes are shutdown.

How high up the aggregation hierarchy a RN wavelength can be created/terminated depends on the amount of OLTs and RNs in the system and the WDM system used. For example, 5 OLTs which in turn connect to 10 RNs each would require 50 wavelengths to be terminated in the first aggregation node. Some amount of wavelength reuse can be preformed for wavelengths allocated in the WDM rings to improve scalability.

Network flow information

The second step in the architecture is to collect network flow information. Two categories of network information are needed, IP flow information and interfaces/label statistics. The former is needed for identifying the source and destination of customer's network traffic, which is then potentially used to allocate new resources in the network. The latter is need for

monitoring of allocated paths in the network, which is used to decide if a resource should be released.

Monitoring of IP flows can be performedonly at selected nodes, preferably central nodes where traffic flows in the default case. The source/destination addresses as well as the size of the flow is required to be collected or sampled on these nodes. This will give the system the necessary information to calculate the flow's end-points in the topology as well as the size of the flow.

This can be accomplished with today's hardware using primarily two different standardized approaches, NetFlow [24] and sFlow [24]. NetFlow, originally developed by Cisco, provides IP traffic information and m vendors provide compatible solutions under their own names. It may therefore be considered a de facto standard for traffic flow monitoring. sFlow is developed in an open consortium and is based around sampling the network traffic, and is therefore more scalable than the original NetFlow implementation. It would also be partly possible to collect the necessary information from OpenFlow [25] based switches, but more information processing could be required.

Each allocated resource needs to be occasionally monitored so unused resources can be released. For example, once a large flow is detected a wavelength may be allocated to more-effectively route the data. Each end-point of the wavelength is monitored and when the usage of the wavelength falls down below a certain threshold the resource is released. The usage information, for example number of bits/s, only needs to be sampled and only requested occasionally. Much of today's hardware provides this kind of information, Juniper for example provides the "*mpls statistics label*" to enable collection of the number of incoming packets, and it's probable the similar capability exists from most vendors. This information can also be collected from OpenFlow capable switches via "*ofp_flow_stats_request*" messages.

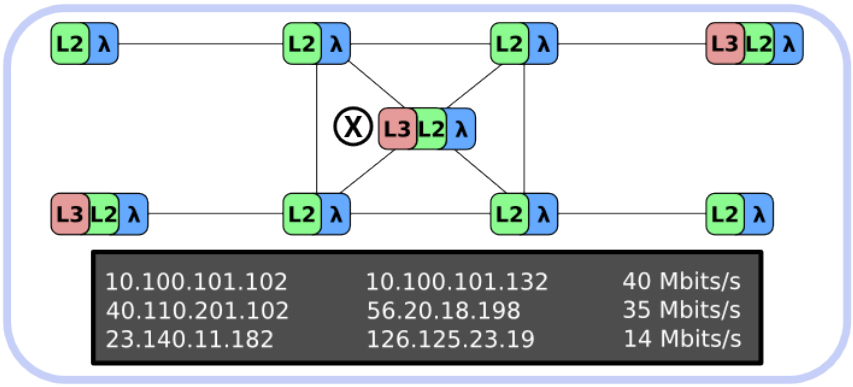

Figure 44: Example network with nodes capable switching on optical layer (lambda symbol), layer two (L2) and on layer three (L3). The flow information is captured at node X, and presented in the dark box.

Flow topology mapping and analysis

The flow information, collected from key nodes in the topology, needs to be processed to determine which nodes in the topology connect between the end-points of the flows. Figure 44 depicts a simple demonstration network topology where nodes have a mix of switch capabilities, from wavelength switching to L3 switching, and set of collected flow information. The flow information has been collected in the central node (node X), which could be the exit point to the rest of the operators network. The system must now determine

the path of the flow through the network. This requires that the system has access to the full topology information, which can be collected via OSPF, SNMP, OpenFlow, or NMS solutions. This must contain information about current allocations in the network, for example forwarding table configurations and wavelength assignments.

Using the topology information the system processes each flow entry (e.g. IPv4 SRC, IPv4 DST, and bandwidth) according to the following procedure:

1. Identify from which node the IPv4 SRC originated from, this will always be a local node in the network (e.g. an ONU).
2. Identify which outgoing interface depending on the type of node:
    a. If IPv4 router, lookup forwarding table based on DST.
    b. If MPLS router, lookup outgoing label and interface based on incoming interface and previous label.
    c. If WDM determine outgoing interface based on incoming interface and wavelength.
3. Remember current path information (label, wavelength, etc.) and go to next node
4. Go to 2.

Based on this procedure a full path through the network is created, including the resources used by the path (wavelengths, forwarding entries etc.). This solution is computationally simple as no searching in the topology is needed and complexity will be linear. If this is done for all flows in Figure 44, then the resulting topology will be composed of the flows shown in Figure 45.

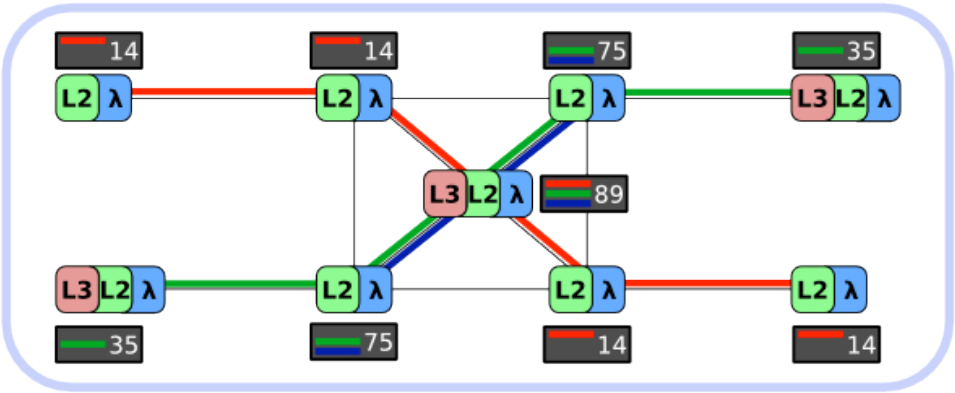

Figure 45: Final flow layout after all flow has been processed

Based on these paths of the flows the interfaces and nodes are annotated with the cumulated bandwidth that is used.

Creating new, better paths

The next step after mapping all the flows to the topology is then to calculate potentially more optimized paths for these segments, using an locality aware PCE. This involves central processing of the flows passing through each node, finding common segments for the flows in the node, and finally calculating a new path for these flows. The processing of each node is done in an ordered fashion based on its locations in the topology (i.e. nodes higher up in the aggregation hierarchy).

If a calculated path is more efficient (based on a policy threshold), or is necessary to fulfil network load, the new path is deployed into the network. Specifically, we use the following

procedure:

1. Calculate a priority metric for each node, based on:
    a. Power use. (High power use)
    b. Placement in topology. (Central > edge)
    c. Current load. (High load, Low load, average load)
    d. Switching capabilities. (Layer 3 > layer 2)
2. Based on metric in **1**, start analysis of flows in node with highest priority.
3. Iterate over the flows in that node.
    e. Try to find common segments for the flows.
    f. Check that the common segment fits the policies.
    g. Adjust the segments based on topology.
    h. Request a path between the end-point of the segment, optimized for power used and path locality.
    i. Deploy the new path in the network if more efficient.
    j. Adjust topology information with the new path, including removal of affected flows from affected nodes.
4. Process flow on next node.
5. Restart when new flow data is fetched.

A couple of aspects of the procedure require further explanation. Step **3e** finds common path segment of the flows in a given node. Finding common segments involves comparing the path taken by each flow, grouped by the layer (i.e. forwarded on the same forwarding layer e.g. lambda, MPLS, VLAN etc). For example consider two paths, A and B, where A uses nodes {1,5,6,9,12} and B nodes {3,5,6,9,17}. First both these paths should to be operating on the same forwarding layer, and then the intersection of the two is calculated, which in this case would be the path {5,6,9}. This means that both paths can be routed through same allocation, for example an optical wavelength, between node 5 and 9.

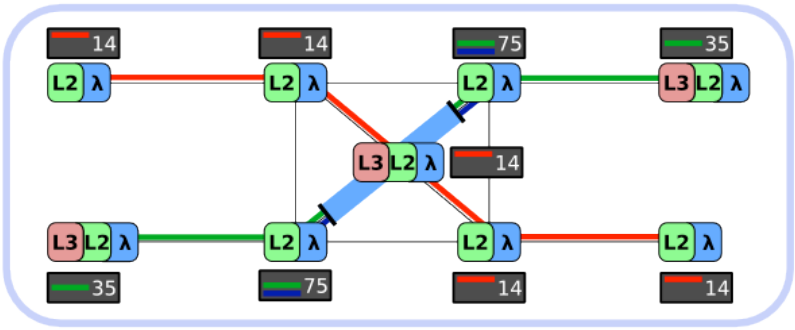

Figure 46: The final topology where an optical channel has been created to reduce electrical processing load on core node, i.e. it is bypassed on the optical level.

If this procedure is applied to the example topology in Figure 46, the system would find that a better resource allocation can be done between the core node and its two neighbours by creating an optical tunnel between the two neighbours and thereby bypassing electrical processing in the central node. This leads to reduced load for the central node as well as reduced power use as the optical transport is more power efficient.

4.3.3 Implementation overview

The system consists of three parts: the collection of traffic flow information, the analysis of

the collected flows and the network allocation infrastructure. The traffic flow information should, in real life, be collected via the previously described NetFlow or sFlow, but was for this work implemented as a piece software running on a server. The software, written in C++, uses a raw socket to collect all received packet on preconfigured interfaces. The source, destination and the size of the packet is parsed and stored to an in-memory table. Each time period (for example 1 second) the information is processed and the flow bandwidth is calculated and sent to the analysis component.

The analysis and optimization of the network is handled by a second software component (written in C++), which contains a flow analysis module, a path computation module and a traffic-engineering database. The core loop of this component is as follows:

1. Receive flow information.
2. Each flow is processed where the network path for each flow is calculated.
3. Group and calculate the intersections of the flows.
4. Calculate replacement path using the path computation module.
5. Allocate new paths in the network

The path computation and traffic-engineering database are specifically implemented as libraries which the component uses. The path computation algorithm is based upon Dijkstra's and is based on three steps, request validation, topology pruning and path computation.

For testing purposes a small testbed was created where each node runs in its own isolated environment, providing separation between other emulated nodes. The software virtualization technique used in the testbed is LXC, short for Linux Containers, which in turn runs on Ubuntu Linux. This virtualization technique provides a light-weight separation between instances, and therefore scales better than most other virtualization solutions.

Each instance is connected to other instances via emulated network interfaces implemented using a Linux kernel module. Each virtual interface can be connected to another virtual interface, and the association between the interfaces can be changed dynamically. On each LXC instance, we run a set of control plane software, including RSVP-TE and a NMS client. The data plane for each node depends on the desired capacities of the node. An OpenFlow 1.1 capable switch was used for nodes with packet forwarding capacities. Wavelength forwarding is accomplished using a WSS "client", which reconfigures the underlying emulated wavelength data plane, which in turn changes how the virtual interfaces are connected.

4.3.4 Practical implications

Several important issues need to be addressed when dealing with the real world implementation of such a system. The QoS of customers traffic must be maintain at all times, which means that any change in network topology, such as new resource allocations, cannot affect the QoS of the traffic in a negative way. In this system a new allocation, for example a new more-direct allocation between two RNs, is allocated first in the network. When the resource is up and running the forwarding tables of the ingress and egress side of the path are changed to route the traffic to the new resource. This approach is known as "make before break" and provides a safe way to make changes to the network, but requires that there are sufficient resources in the network to facilitate both states concurrently. In this system one potential QoS side-effect could be that a few packets arrive out of order when the packet flow is switched to the new path. This could happen since the transmission time for the new path might be lower than the existing path, which could lead to situation where the packets sent just before the switch arrive at the destination after those send directly after the switch. Packet reordering is common on the Internet and most protocols therefore handle this case meaning it should have a limited affect of the customer perceived QoS. All protocols running over TCP

or video stream using buffered playback will handle this case without customer awareness.

The scalability of the system is another important aspect to consider, as future access/aggregation networks may consist of a large amount of nodes. The two major scalability factors that need to be considered are performance of the system computation scalability, and the scalability of the flow collection. The amount of flows that need to be handled by the system may become an issue if all possible flows need to be considered. It might therefore be required to filter out flows which are short lived or small in terms of bandwidth. This could, for example, be performed by the hardware which collects the flow information; such hardware can already today handle millions of flows [26].

The scalability of computational size will, to a large extent, be limited by the computational need of the PCE, which will need to compute the alternate paths of the flows. The reason for this is that the other steps of the procedure are computationally linear or/and may be performed in parallel. For example the processes of tracing how a flow goes through the network can be performed in parallel and the computational requirement will scale with the length of the path.

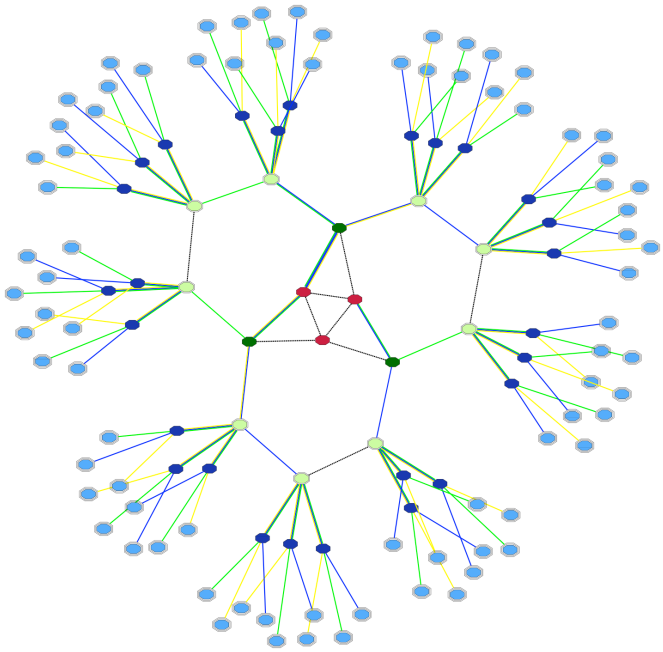

Figure 47: Virtual topology used when performing tests on PCE, leaf nodes represent RN and dark blue node represent OLTs

The PCE implementation, based on dijkstra's algorithm, was therefore benchmarked. It is important to nove that the system will not calculate the path from the ONU during normal use by the system and can therefore be pruned out from the topology. Virtual topologies were generated using the same topology structure as shown in Figure 47, and the number of RN and OLT where changed to scale the topology. A PCE client then made one thousand requests to the PCE, with random source and destination nodes, and the time to path response was collected. Figure 48 shows the result of the benchmark, the number of RN range from 1080 to 17280. Even with 17280 RN in the network, each representing many hundreds of customers, the PCE could still calculate paths in less than 300ms on average.

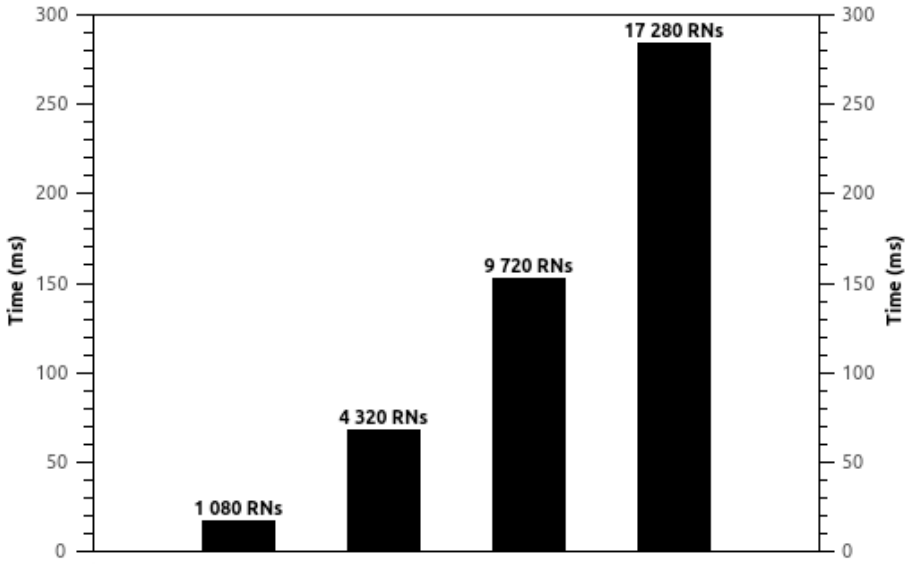

Figure 48: Average computation time for path in topologies different number of RNs

4.3.5 System Techno-economic impact

This proposed system has three major effects on the network: 1) reduction of energy used by shutting down network elements during off hours, 2) reduction of load in higher aggregation levels, and 3) reduction of IP upstream transit cost because of increase of local traffic flows. The impact of these aspects is non-trivial to estimate as they depend heavily on the size of operator (global, large and minor), the topology of the network, and the traffic patterns of future internet use. Therefore only major possibilities and trends will be presented.

Energy reduction

The system will automatically allocate new resources, for example new wavelengths, to accommodate increases in traffic demand. This leads to an architecture where the electrical processing of certain aggregation steps can be disabled during off-hours. This will therefore also affect all part of the access/aggregation network, but in this work the focus will be on the NG-AON access.

The largest impact on energy use will be during offpeak-hours and it is therefore important to understand how the load characteristic changes over a day. Figure 49 which contains the average traffic load per hours collected over a month for streaming based services, captured from a FTTH based network in southern Sweden. From the figure it can be observed that during eight hours the incoming load (i.e. traffic to customers) is under 35 %, and under 20% during approximately four hours.

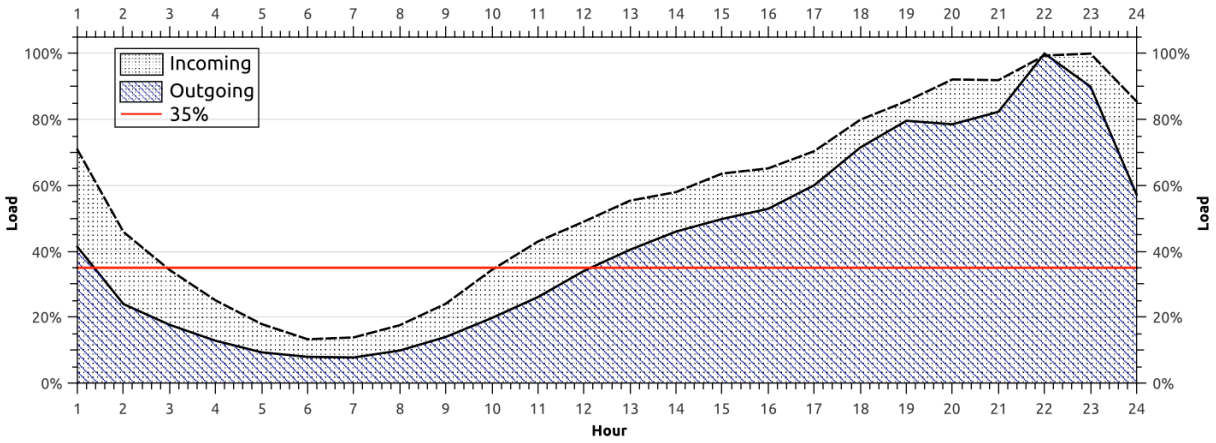

Figure 49: Average network load per hour for streaming services, which include for example HTTP video download and RTMP

During these off-hours it would be possible to completely shut down the electrical forwarding on the NG-AON OLT, and only use the WSS capability of the OLT, and thereby move the OLT function higher up in the network. The long term OASE goal is 300 Mb/s sustainable bandwidth, combined with minimum of 1000 user each feeder fibre. This would lead to an AON RN having an outgoing bandwidth of 60 Gb/s at 20% load and 105 Gb/s at 35% load. Both of these cases could be handled by a single 100G wavelength, which means that the electrical forwarding of the OLT could be shut down for eight hours of each day, i.e. 33% of the time.

Reduction in core load

The local traffic in the network will be kept as low down in the network's aggregation hierarchy as possible, which reduces the load on the higher aggregation levels, and especially the core network. This could keep back the gradual build out of the capacity of these levels. Furthermore this will also reduce the amount of resources used in the network elements, which may reduce the energy use, given that the network elements energy used scales with network load. These aspect are however hard to estimate as the design and equipment used affects the cost reduction and will therefore be considered in potential future work.

Reduction in transit costs

Traffic that is sent to a destination outside of the operator's network can be associated with a transit cost, where the operator needs to pay a fee per amount sent. How much an operator will need to pay depends heavily on size of an operator, where a large operator can exchange most of its traffic freely compared to smaller operators who may need to pay for most of its external traffic. Estimations of transit costs range from 3-30 USD per Mb/s per month in 2011, depending on region and source of the information [27][28][29]. The same sources also indicate that the price for the bandwidth will go down in the future. It is therefore hard to estimate the bandwidth cost for the long term OASE timeline. This system could reduce the amount of transit costs with as much as 20-30% in the long term, based on the locality of content study in D3.3, but estimating this in absolute numbers will depend on the operator and the evolution of future services and protocols and are subject to potential future work.

4.4 WDM-PON BACKHAUL

The WDM-PON backhaul architecture provides an architecture alternative where a WDM-PON system is used as long-reach backhaul to provide consolidation of aggregation nodes rather than access nodes. The WDM-PON system serves a larger number of remote nodes

which holds the first mile system. One particular advantage of the WDM-PON backhaul architecture is in a future converged fixed mobile scenario where the WDM-PON system is used simultaneously to cater for the transport requirements of radio access.

One potential trend in radio access is the centralization of base band processing where the baseband unit of the base station is placed in a central location where it can be shared by several remote radio units (i.e. CRAN or Cloud-RAN). This solution provides large cost and energy saving opportunities in the radio access. However, it comes at the cost of large capacity requirements in the transport between the base band unit and the radio remote unit. The WDM-PON backhaul architecture can cater for such a scenario. As part of understanding the future advantages of the WDM-backhaul architecture we investigate the concept of centralized base band processing in the WDM-PON backhaul scenario based on WDM-PON technology investigated in WP7.

4.4.1 CRAN over WDM-PON

RAN centralization is a new approach for RBS implementation where RF and processing equipment of the Radio base station are split in two parts. The processing is centralized in a MU (Main Unit), which offers processing resources for multiple cells. Each cell is covered by antennas driven by RRU (Radio Remote Unit).

Shortly, the aim is to apply some cloud computing concepts to RAN. A pool of processing resources is dynamically shared among many cells. A first bunch of benefits consists of a cutback in the power consumption, improvements in radio link reliability, and in the possibility to consolidate radio base stations.

The main drawback comes from the needs of low cost, dedicated and ultra high speed links between MUs and RRUs. The protocol used to connect MU and RRU is the CPRI.

Conventional CPRI transport on fiber is operated using P2P (point to point) connections between MUs and RRUs. This approach guarantees high bit rates, low cost optical interfaces and good reliability. A simple optical layer also fit the strict requirements of CPRI in terms of latency and in particular in terms of differential delay between UL and DL.

WDM-PON could offer a big opportunity because it is an ultra high bandwidth access (PON) technology that at the same time is also able to offer segregation, transparency and end to end connectivity. Its aim is to combine low cost with optical transmission performance.

Using WDM-PON to transport CPRI traffic is appealing from many points of view:

- High bit-rate: CPRI Option 7 also supported with multiple CPRI streams per fiber
- CPRI channels segregation and protocol transparency: coexistence on the same PON of CPRI links at different bit-rate and also CPRI links together with wire line conventional WDM-PON channels.
- High spectral efficiency: MU consolidation and cost reduction in the fiber deployment.

A novel non hierarchical WDM-PON system has been realized to be used in a C-RAN scenario and used to set-up an LTE cell over WDM-PON. This system is able to auto-configure itself, finding the proper wavelengths.

In Figure 50 is the demonstration setup between MU and RRU is shown.

For each CPRI link, Ericsson demonstration equipment is able to look for a pair of suitable wavelengths (UL and DL) along the whole C-Band: 16 CPRI links supported (100GHz wavelength spacing). Again any CPRI option is supported: starting from Option1 (614.4

Mb/s) up to the recent Option7 (9830.4 Mb/s). A combination is also possible without any hardware or infrastructure upgrade: full channel segregation and bit-rate transparency are features of WDM backhaul. A combination of "C+L band" is also possible, offering the transport of 48 different CPRI links per fiber.

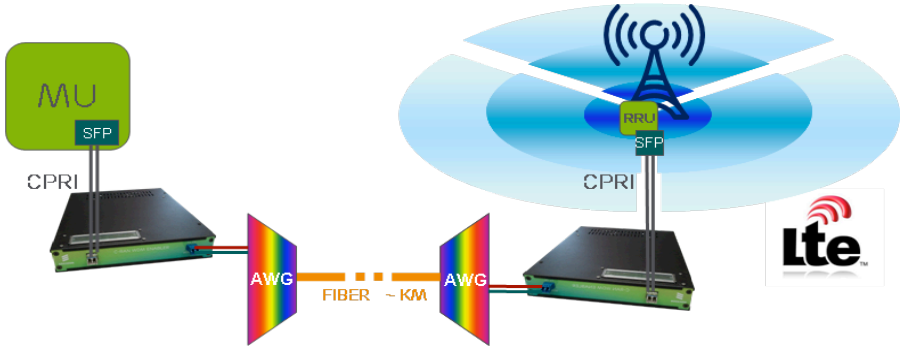

Figure 50: LTE C-RAN over WDM (just one link is shown)

The radio part (MU/RRU) is built with an Ericsson RBS6000 system able to generate an LTE radio base station. The WDM appliances have been used to carry CPRI links between MU and RRU and with a final handheld LTE device (able to operate up to 60Mb/s). Tests have been performed on the bandwidth available from the generated cell in different working conditions. We had maximum flexibility on the chosen couple of wavelengths, because they depend on the port used in the AWGs.

We changed both the fiber lengths between MU/RRU and the wavelength distance between uplink and downlink. Changing the distance between the wavelengths permits to test different unbalanced delays in the CPRI links due to the use of different wavelengths for the two directions.

Using adjacent wavelengths for uplink and downlink we are able to minimize the unbalanced delay and obtain maximum performance, in terms of LTE cell throughput, up to 20km.

Choosing the maximum wavelengths distance, using the two edges of the C-Band, we intentionally explore the worst condition in terms of unbalanced delay. In any case we are still able to reach the maximum cell throughput up to 10km of fiber length.

5. System implementation

Detailed NGOA system models are described in deliverables D4.2.2 and D4.3.2 which define the different system alteratives and required components. For techno-economic evaluation of NGOA scenarios further implementation assumptions are needed. The basic hardware units handled in the TCO processes must be defined. The fault management and service provisioning processes are based on handeling of units such as fiber, slot cards, chassis, etc. rather than individual components Hence each system description must be remapped from a component description to an equipment description that displays the basic equipment units (e.g. chassi, slot cards, etc) which are the modular units of the network equipment.

This remapping involves defining the main composition of the basic equipment units in terms of components and calculating aggregated values for e.g. cost, power and MTBF for these units. Furthermore, in collaboration with WP5, further estimates regarding parameters for different OPEX processes and costs were made for the different equipment units. This includes aspects such as average repair/replacement time, number of required personnel for

repair, maintenance costs, etc.

Table 8 in the Appendix presents the resulting equipment description for the different system concepts in terms of equipment units that are available in a real system. This table serves as the main input from the system design to WP5 and calculation of TCO. The general approach for defining the equipment units was to keep the number of different types of units small.

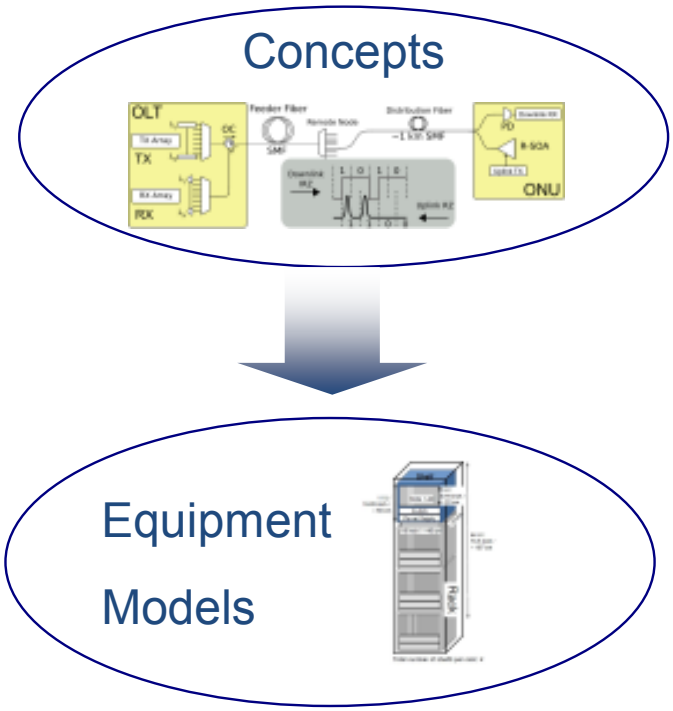

Figure 51: From concepts to equipment models

6. Summary

This deliverable D4.4 provides an in-depth study of selected challenges of the OASE system concepts for next-generation optical access (NGOA).

For mobile/business backhaul it has been shown that the initial requirements defined in D2.1 can be supported within all the presented concepts with limited or some additional effort, where some additional effort may at most consist of manual patching work for service provisioning.

For the effect of power saving techniques a comparision was made of ONU power saving modes for the different system concepts. The ONU represents the dominating contribution to access network power. Although results rely heavily on assumptions on traffic, it can generally be said that power saving modes can reduce average ONU power consumption by about 90% when it is applied to NGOA system concepts with a burst mode transmission and reception like high bit rate TDMA-PONs and about 80% in hybrid TWDM-PONs. Moderate savings between 35 to 41% are found for WDM-PON, AON and PtP systems. We have also described an innovative master-slave scheme that can enable significant energy-efficiency savings across a range of equipment and system types in the next-generation access network area. In particular, the master-slave approach offers a generic scheme to enable devices and

equipment (e.g. optical amplifiers, wavelength-selective switches, routers, port aggregators etc.) to have a quasi-elastic power consumption profile with respect to the offered traffic load. Whereas on their own, these types of equipment tend to have a high, fixed power consumption, so that the overall energy dissipated during operation is inelastic with varying incoming traffic load, when configured into a master-slave scheme, the overall power dissipation is more elastic with respect to traffic load, and enables useful power saving. Offering a degree of equipment redundancy, this also has the advantage of making the overall architecture/system more resilient and robust. Although this may have higher CapEx implications, the combined higher resilience and improved energy-efficiency should offer OpEx savings. In addition, we have identified an innovative upgrade trajectory solution, which re-uses master units as slave units in a subsequent generation upgrade, so saving on CapEx and offering still more TCO savings. These master-slave schemes are applicable to all the NGOA architectures discussed in the OASE project, and are complementary to the more conventional sleep/idle/hibernation modes that can also be employed to reduce the overall carbon footprint of NGOA architecture solutions.

For the WDM-PON architecture, work related to implementation of efficient ODN fault-localization was presented. The development enables accurate identification of faults in a wave-length routed ODN providing operational advantages for this particular ODN with respect to ODN fault localization and repair costs.

For the hybrid WDM/TDM-PON architecture resource allocation is a critical point. The deliverable presents work related to development of efficient TDMA resource allocation in the long-reach limit where the large round-trip-time presents a challenge. The deliverable also presents work related to dynamic wavelength allocation and expected efficiency of different wavelength allocation schemes. Regarding power saving techniques a scheme for sleep mode control based on service requirements was delevloped and evaluated in a simulation demonstrating some of the assumed energy saving opportunities within this architecture.

For the NG-AON architecture a control plane implementation was implemented in order to demonstrate intelligent control mechanisms which enable reduction of network energy consumption, reduction in core load and reduction in transit costs.

Finally, for the WDM-PON backhaul architecture to which much of the work associated with the WDM-PON architecture and NG-AON applies, the deliverable reports work related to future developments in mobile networks and support for CPRI transport.

7. Appendix

As described in Section 5, Table 8 presents the equipment description for the different system concepts in terms of equipment units that are available in a real system. This table serves as the main input from the system design to WP5 and calculation of TCO.

Table 8: Equipment units for the OASE NGOA system concepts

Network component	Power consumption [W]	Cost [a.u.] 2020	MTBF [hours] 25° for indoor
G-PON system			
OLT Shelf / Backplane (18 tributary slots)	90,00	100,00	1 500 000
OLT Power unit	0,00	incl in shelf	500 000
OLT Switch/Route processor (~200G)	200,00	20,00	430 000
OLT Control and management plane	0,00	incl in shelf	not considered
OLT Software	0,00	incl in shelf	not considered
OLT Downlink line card 8-Port GPON (not incl pluggables) (occupies 2 tributary slots)	24,00	12,40	1 333 333
OLT Pluggable B+	1,20	2,00	1 000 000
OLT Pluggable C+	1,50	3,00	750 000
RN2 Outdoor cabinet (for max 10 RE)	50,00	150,00	1 500 000

RN2 Reach extender 8-Port GPON (not incl pluggables)	40,00	8,00	1 090 909
RN2 Reach extender Pluggable B+	1,20	2,00	1 000 000
RN2 Reach extender Pluggable C+	1,50	3,00	750 000
RN1 Passive RN chassis (not incl splitter)	0,00	0,00	2 000 000
RN1 Optical power splitter (1:32)	0,00	6,60	6 000 000
RN1 Optical power splitter (1:16)	0,00	3,40	7 500 000
RN1 Optical power splitter (1:8)	0,00	1,80	9 000 000
RN1 Optical power splitter (1:4)	0,00	1,00	10 500 000
GPON-ONT (hardware + software failures)	4,00	1,00	281 250
XG-PON1 system			
OLT Shelf / Backplane (18 tributary slots)	90,00	100,00	1 500 000
OLT Power unit	0,00	incl in shelf	500 000
OLT Switch/Route processor (~600G)	600,00	60,00	390 000
OLT Control and management plane	0,00	incl in shelf	not considered
OLT Software	0,00	incl in shelf	not considered
OLT Downlink line card 6-Port XG-PON (not incl pluggables) (occupies 2 tributary slots)	46,00	19,80	800 000
OLT Pluggable Nom1	2,00	3,40	1 000 000
OLT Pluggable Nom2b	2,50	5,20	750 000
OLT Pluggable Ext2	3,00	6,80	500 000
RN2 Outdoor cabinet (for max 10 RE)	50,00	150,00	1 500 000
RN2 Reach extender 8-Port XG-PON (not incl pluggables)	40,00	20,00	1 090 909
RN2 Reach extender Pluggable Nom2b	4,00	8,00	500 000
RN1 Passive RN chassis (not incl splitter)	0,00	0,00	2 000 000
RN1 Optical power splitter (1:32)	0,00	6,60	6 000 000
RN1 Optical power splitter (1:16)	0,00	3,40	7 500 000
RN1 Optical power splitter (1:8)	0,00	1,80	9 000 000
RN1 Optical power splitter (1:4)	0,00	1,00	10 500 000
XG-PON ONT Nom1 / Nom2a (hardware + software failures)	5,50	2,40	236 842
XG-PON ONT Nom 2b (hardware + software failures)	5,00	1,80	257 143
P2P system			
OLT Shelf / Backplane (18 tributary slots)	90,00	100,00	1 500 000
OLT Power unit	0,00	incl in shelf	500 000
OLT Switch/Route processor (~100G, 300Mb/s per client)	100,00	10,00	440 000
OLT Switch/Route processor (~200G, 500Mb/s per client)	200,00	20,00	430 000
OLT Control and management plane	0,00	incl in shelf	not considered
OLT Software	0,00	incl in shelf	not considered
OLT Downlink line card optical 48Port x1G (not incl pluggables) (occupies 3 tributary slots)	34,00	12,00	800 000
OLT Pluggable 2x1G (compact SFP)	1,00	0,72	3 000 000
P2P-ONT 1G (hardware + software failures)	3,50	0,96	310 345
WR-DWDM PON (tunable lasers - APD)			
OLT Shelf / Backplane (18 tributary slots)	90,00	100,00	1 500 000
OLT Power unit	0,00	incl in shelf	500 000
OLT Switch/Route processor (~200G, 300Mb/s per client)	200,00	20,00	430 000
OLT Switch/Route processor (~300G, 500Mb/s per client)	300,00	30,00	420 000
OLT Control and management plane	0,00	incl in shelf	not considered
OLT Software	0,00	incl in shelf	not considered
OLT Basic Downlink line card DWDM-PON port card 80 channels (for use in 80 config) (incl 80x1G Laser/Rx Array C-band, 1 diplexer) not incl EDFA preamp.	98,00	72,10	214 286
OLT Basic Downlink line card DWDM-PON port card 80 channels (for use in 160 config) (incl 80x1G Laser/Rx Array C/S-band, 1 diplexer) not incl EDFA or TDFA preamp	98,00	73,70	214 286
OLT Basic Downlink line card DWDM-PON port card 80 channels (for use in 360 config) (incl 80x1G Laser/Rx Array C/S-band, 1 diplexer, 2 interleavers) not incl EDFA or TDFA preamp	98,00	85,70	200 000
OLT EDFA Preamp	12,00	15,00	1 000 000
OLT TDFA Preamp	12,00	18,80	1 000 000
RN Passive RN chassis (not incl AWG, etc)	0,00	0,00	2 000 000
RN 80 channels (80:1 AWG)	0,00	24,00	4 000 000
RN 80 channels protection (80:2 AWG)	0,00	28,80	4 000 000
RN 160 channels (2x 80:1 AWG, diplexer)	0,00	48,30	1 714 286
RN 160 channels protection (2x 80:2 AWG, 2 diplexers)	0,00	58,20	1 500 000
RN 320 channels (4x 80:1 AWG, 7 diplexers, interleavers 320 ch)	0,00	98,10	800 000
RN 320 channels protection (4x 80:2 AWG, 7 diplexers, interleavers 320 ch)	0,00	157,80	500 000
DWDM-PON-ONT 1G tunable (APD, C-band) - for 80	4,70	2,20	236 842

ch DWDM-PON-ONT 1G tunable (APD, C/S-band) - for 160, 320 ch	4,70	2,24	236 842
WS-DWDM PON (tunable lasers - APD)			
OLT Shelf / Backplane (18 tributary slots)	90,00	100,00	1 500 000
OLT Power unit	0,00	incl in shelf	500 000
OLT Switch/Route processor (~100G, 32ch, 32ch 300Mb/s preamp)	100,00	10,00	440 000
OLT Switch/Route processor (~200G, 64ch, 32ch 500Mb/s preamp, 64ch 300Mb/s preamp)	200,00	20,00	430 000
OLT Switch/Route processor (~300G, 128ch 300Mb/s per client, 64ch 500Mb/s preamp, 128ch 300Mb/s preamp)	300,00	30,00	420 000
OLT Switch/Route processor (~400G, 128ch 500Mb/s per client)	400,00	40,00	410 000
OLT Control and management plane	0,00	incl in shelf	not considered
OLT Software	0,00	incl in shelf	not considered
OLT Basic Downlink line card DWDM-PON port card 32 channels (for use in 32 config) (incl 32x1G Laser/Rx Array C-band, 1 diplexer) not incl EDFA preamp.	45,00	29,50	214 286
OLT Basic Downlink line card DWDM-PON port card 64 channels (for use in 64 config) (incl 64x1G Laser/Rx Array C-band, 1 diplexer) not incl EDFA preamp	80,00	57,50	214 286
OLT Basic Downlink line card DWDM-PON port card 128 channels (for use in 128 config) (incl 2x64x1G Laser/Rx Array C-band, 1 diplexer) not incl EDFA preamp	150,00	113,90	125 000
OLT EDFA Preamp	12,00	15,00	1 000 000
RN2 Passive RN chassis (not incl band filter)	0,00	0,00	2 000 000
RN2 Band filter (1:4)	0,00	1,50	4 000 000
RN1 Passive RN chassis (not incl splitter)	0,00	0,00	2 000 000
RN1 Optical power splitter (1:32)	0,00	6,60	6 000 000
RN1 Optical power splitter (1:64)	0,00	13,00	6 000 000
DWDM-PON-ONT 1G tunable (APD, C-band) - for 80 ch	4,90	3,20	227 848
WR-DWDM PON (tunable lasers - PIN)			
OLT Shelf / Backplane (18 tributary slots)	90,00	100,00	1 500 000
OLT Power unit	0,00	incl in shelf	500 000
OLT Switch/Route processor (~300G, 300Mb/s per client)	300,00	30,00	420 000
OLT Switch/Route processor (~400G, 500Mb/s per client)	400,00	40,00	410 000
OLT Control and management plane	0,00	incl in shelf	not considered
OLT Software	0,00	incl in shelf	not considered
OLT Downlink line card DWDM-PON port card 80 channels (for use in 80ch config) (incl 80x1G Laser/Rx Array C-band, 1 diplexer)	98,00	72,10	214 286
OLT Downlink line card DWDM-PON port card 80 channels (for use in 160ch config) (incl 80x1G Laser/Rx Array C/S-band, 2 diplexers)	98,00	74,00	210 526
RN Passive RN chassis (not incl AWG, etc)	0,00	0,00	2 000 000
RN 80 channels (80:1 AWG)	0,00	24,00	4 000 000
RN 80 channels protection (80:2 AWG)	0,00	28,80	4 000 000
RN 160 channels (2x 80:1 AWG, diplexer)	0,00	48,30	1 714 286
RN 160 channels protection (2x 80:2 AWG, 2 diplexers)	0,00	58,20	1 500 000
DWDM-PON-ONT 1G tunable (PIN, C-band) - for 80 ch	4,20	1,60	257 143
DWDM-PON-ONT 1G tunable (PIN, C/S-band) - for 160, 320 ch	4,20	1,64	257 143
WR-DWDM PON (seeded reflective - MFL)			
OLT Shelf / Backplane (18 tributary slots)	90,00	100,00	1 500 000
OLT Power unit	0,00	incl in shelf	500 000
OLT Switch/Route processor (~100G, 300Mb/s per client)	100,00	10,00	440 000
OLT Switch/Route processor (~200G, 500Mb/s per client)	200,00	20,00	430 000
OLT Control and management plane	0,00	incl in shelf	not considered
OLT Software	0,00	incl in shelf	not considered
OLT Downlink line card DWDM-PON port card 80 channels (incl 80x 1G Laser/Rx Array C-band, 1 diplexer)	98,00	72,10	214 286
OLT Circulator	0,00	2,00	1 000 000
OLT MFL	10,00	16,00	1 000 000
RN Passive RN chassis (not incl AWG, etc)	0,00	0,00	2 000 000
RN 80 channels (80:1 AWG)	0,00	24,00	4 000 000
RN 80 channels protection (80:2 AWG)	0,00	28,80	4 000 000
DWDM-PON-ONT 1G RSOA/APD (APD, C-band) - for	4,70	1,86	236 842

80 ch			
DWDM-PON-ONT 1G RSOA/PIN (PIN, C-band) - for 80 ch	4,20	1,26	257 143
WR-DWDM PON (seeded reflective - wavelength reuse)			
OLT Shelf / Backplane (18 tributary slots)	90,00	100,00	1 500 000
OLT Power unit	0,00	incl in shelf	500 000
OLT Switch/Route processor (~200G, 300Mb/s per client)	200,00	20,00	430 000
OLT Switch/Route processor (~300G, 500Mb/s per client, 80ch, 160ch)	300,00	30,00	420 000
OLT Switch/Route processor (~400G, 500Mb/s per client, 320ch)	400,00	40,00	410 000
OLT Control and management plane	0,00	incl in shelf	not considered
OLT Software	0,00	incl in shelf	not considered
OLT Downlink line card DWDM-PON port card 80 channels (for use in 80ch config) (incl 80x 1G Laser/Rx Array C-band, 1 diplexer)	98,00	72,10	214 286
OLT Downlink line card DWDM-PON port card 80 channels (for use in 160ch config) (incl 80x 1G Laser/Rx Array C/S-band, 1 diplexer)	98,00	73,70	214 286
OLT Downlink line card DWDM-PON port card 80 channels (for use in 320ch config) (incl 80x 1G Laser/Rx Array C/S-band, 2 diplexers)	98,00	74,00	210 526
OLT Downlink line card DWDM-PON port card 96 channels (for use in 96ch config) (incl 2 48x 1G Laser/Rx Array C-band, 2 diplexers)	134,00	61,00	123 711
OLT Circulator	0,00	2,00	1 000 000
RN Passive RN chassis (not incl AWG, etc)	0,00	0,00	2 000 000
RN 80 channels (80:1 AWG)	0,00	24,00	4 000 000
RN 80 channels protection (80:2 AWG)	0,00	28,80	4 000 000
RN 160 channels (2x 80:1 AWG, diplexer)	0,00	48,30	1 714 286
RN 160 channels protection (2x 80:2 AWG, 2 diplexers)	0,00	58,20	1 500 000
RN 320 channels (4x 80:1 AWG, 7 diplexers, interleavers 320 ch)	0,00	98,10	800 000
RN 320 channels protection (4x 80:2 AWG, 7 diplexers, interleavers 320 ch)	0,00	157,80	500 000
RN 96 channels (96:1 AWG)	0,00	19,50	1 714 286
RN 96 channels protection (48:2 AWG, 2 diplexers)	0,00	23,64	1 500 000
DWDM-PON-ONT 1G RSOA/APD (APD, C-band) - for 80, 160, 320, 96 ch	4,70	1,86	236 842
WS-DWDM PON (seeded reflective - wavelength reuse)			
OLT Shelf / Backplane (18 tributary slots)	90,00	100,00	1 500 000
OLT Power unit	0,00	incl in shelf	500 000
OLT Switch/Route processor (~100G, 32ch)	100,00	10,00	440 000
OLT Switch/Route processor (~300G, 300Mb/s per client, 128ch)	300,00	30,00	420 000
OLT Switch/Route processor (~400G, 500Mb/s per client, 128ch)	400,00	40,00	410 000
OLT Control and management plane	0,00	incl in shelf	not considered
OLT Software	0,00	incl in shelf	not considered
OLT Downlink line card DWDM-PON port card 32 channels (for use in 32ch config) (incl 32x 1G Laser/Rx Array C-band, 1 diplexer)	45,00	29,50	214 286
OLT Downlink line card DWDM-PON port card 128 channels (for use in 128ch config) (incl 2x64x 1G Laser/Rx Array C-band, 1 diplexer)	150,00	113,90	125 000
OLT Circulator	0,00	2,00	1 000 000
RN2 Passive RN chassis (not incl band filter)	0,00	0,00	2 000 000
RN2 Band filter (1:4)	0,00	1,50	4 000 000
RN1 Passive RN chassis (not incl splitter)	0,00	0,00	2 000 000
RN1 Optical power splitter (1:32)	0,00	6,60	6 000 000
DWDM-PON-ONT 1G RSOA/APD TF (APD, C-band)	4,90	2,86	227 848
Hybrid active Ethernet PtP (with DWDM backhaul)			
OLT Active Shelf / Backplane (18 tributary slots)	90,00	100,00	1 500 000
OLT Power unit	0,00	incl in shelf	500 000
OLT Switch/Route processor (~800G)	800,00	80,00	370 000
OLT Control and management plane	0,00	incl in shelf	not considered
OLT Software	0,00	incl in shelf	not considered
OLT Passive RN chassis (not incl AWG, etc)	0,00	0,00	2 000 000
OLT 40 channels dual fiber (2 x 40:1 AWG)	0,00	24,00	2 000 000
OLT Downlink line card DWDM-PON port card 8x10G channels (incl 8x10G TRx)	43,00	8,00	57 971
RN2 Passive RN chassis (not incl AWG, etc)	0,00	24,00	1 000 000
RN2 40 channels dual fiber (2 x 40:1 AWG)	0,00	12,00	4 000 000
RN1 Outdoor cabinet (for max 12 Eth PtP monolithic shelfs)	100,00	150,00	1 500 000
RN1 Monolithic shelf PtP 300 Mbps/client 33xGE + 1x10G uplink (not incl pluggables)	43,00	10,55	521 739

RN1 Monolithic shelf PtP 500 Mbps/client 20xGE + 1x10G uplink (not incl pluggables)	30,00	7,30	705 882
RN1 10G TRx pluggable (coloured dual fiber)	3,50	8,00	500 000
RN1 Pluggable 2x1G (compact SFP)	1,00	0,72	3 000 000
P2P-ONT 1G (hardware + software failures)	3,50	0,96	310 345
Hybrid active GPON (with DWDM backhaul)			
OLT Active Shelf / Backplane (18 tributary slots)	90,00	100,00	1 500 000
OLT Power unit	0,00	incl in shelf	500 000
OLT Switch/Route processor (~800G)	800,00	80,00	370 000
OLT Control and management plane	0,00	incl in shelf	not considered
OLT Software	0,00	incl in shelf	not considered
OLT Passive RN chassis (not incl AWG, etc)	0,00	0,00	2 000 000
OLT 40 channels dual fiber (2 x 40:1 AWG)	0,00	24,00	2 000 000
OLT Downlink line card DWDM-PON port card 8x10G channels (incl 8x10G TRx)	43,00	8,00	57 971
RN3 Passive RN chassis (not incl AWG, etc)	0,00	0,00	2 000 000
RN3 40 channels dual fiber (2 x 40:1 AWG)	0,00	24,00	2 000 000
RN2 Outdoor cabinet (for max 24 GPON monolithic shelfs)	100,00	150,00	1 500 000
RN2 Monolithic shelf GPON 4xGPON + 1x10G uplink (not incl pluggables)	19,00	8,20	521 739
RN2 10G TRx pluggable (coloured dual fiber)	3,50	8,00	500 000
RN2 Pluggable GPON B+	1,20	0,72	1 000 000
RN1 Passive RN chassis (not incl splitter)	0,00	0,00	2 000 000
RN1 Optical power splitter (1:32)	0,00	6,60	6 000 000
RN1 Optical power splitter (1:16)	0,00	3,40	7 500 000
RN1 Optical power splitter (1:8)	0,00	1,80	9 000 000
RN1 Optical power splitter (1:4)	0,00	1,00	10 500 000
GPON-ONT (hardware + software failures)	4,00	1,00	281 250
Hybrid active XG-PON (with DWDM backhaul)			
OLT Active Shelf / Backplane (18 tributary slots)	90,00	100,00	1 500 000
OLT Power unit	0,00	incl in shelf	500 000
OLT Switch/Route processor (~800G)	800,00	80,00	370 000
OLT Control and management plane	0,00	incl in shelf	not considered
OLT Software	0,00	incl in shelf	not considered
OLT Passive RN chassis (not incl AWG, etc)	0,00	0,00	2 000 000
OLT 40 channels dual fiber (2 x 40:1 AWG)	0,00	24,00	2 000 000
OLT Downlink line card DWDM-PON port card 8x10G channels (incl 8x10G TRx)	43,00	8,00	57 971
RN3 Passive RN chassis (not incl AWG, etc)	0,00	0,00	2 000 000
RN3 40 channels dual fiber (2 x 40:1 AWG)	0,00	24,00	2 000 000
RN2 Outdoor cabinet (for max 24 XG-PON monolithic shelfs)	100,00	150,00	1 500 000
RN2 Monolithic shelf XG-PON 4xXG-PON + 4x10G uplink (not incl pluggables)	34,00	15,20	521 739
RN2 10G TRx pluggable (coloured dual fiber)	3,50	8,00	500 000
RN2 Pluggable Nom2b	1,50	0,72	1 000 000
RN1 Passive RN chassis (not incl splitter)	0,00	0,00	2 000 000
RN1 Optical power splitter (1:32)	0,00	6,60	6 000 000
RN1 Optical power splitter (1:16)	0,00	3,40	7 500 000
RN1 Optical power splitter (1:8)	0,00	1,80	9 000 000
RN1 Optical power splitter (1:4)	0,00	1,00	10 500 000
XG-PON ONT Nom 2b (hardware + software failures)	5,00	1,80	257 143
UDWDM PON			
OLT Shelf / Backplane (18 tributary slots)	90,00	100,00	1 500 000
OLT Power unit	0,00	incl in shelf	500 000
OLT Switch/Route processor (~100G, 300Mb/s per client)	100,00	10,00	440 000
OLT Switch/Route processor (~200G, 500Mb/s per client)	200,00	40,00	430 000
OLT Control and management plane	0,00	incl in shelf	not considered
OLT Software	0,00	incl in shelf	not considered
OLT Basic Downlink line card DWDM-PON port card 32 channels (for use in 320, 640) - incl TRX, ASIC, but not TFF or circulators	49,20	48,40	173 913
OLT TFF (10 ports)	0,00	3,00	6 000 000
OLT Circulator	0,00	2,00	6 000 000
OLT EDFA Booster	12	15,00	1 000 000
RN3 Outdoor cabinet (for max 8 RE)	40	150,00	1 500 000
RN3 EDFA based reach extender	100	40,00	1 000 000
RN2 Passive RN chassis (not incl AWG, TFF)	0	0,00	2 000 000
RN2 TFF (1:20)	0	6,00	6 000 000
RN2 AWG (1:40)	0,00	12,00	4 000 000
RN2 AWG protection (2:40)	0,00	14,40	4 000 000
RN2 AWG (1:80)	0,00	24,00	4 000 000
RN2 AWG protection (2:80)	0,00	28,80	4 000 000
RN1 Passive RN chassis (not incl splitter)	0,00	0,00	2 000 000
RN1 Optical power splitter (1:8)	0,00	1,80	9 000 000
RN1 Optical power splitter (1:32)	0,00	6,60	6 000 000
UDWDM-PON-ONT 1G tunable (UDWDM)	5,60	3,07	204 545

Hybrid DWDM / TDMA PON			
OLT Shelf / Backplane (18 tributary slots)	90,00	100,00	1 500 000
OLT Power unit	0,00	incl in shelf	500 000
OLT Switch/Route processor (~600G)	600,00	60,00	390 000
OLT Switch/Route processor (~700G)	700,00	70,00	380 000
OLT Control and management plane	0,00	incl in shelf	not considered
OLT Software	0,00	incl in shelf	not considered
OLT EDFA Booster	12,00	15,00	1 000 000
OLT EDFA Preamp	12,00	15,00	1 000 000
OLT Downlink line card Hybrid-PON (10 x 10G)	95,00	57,80	440000
OLT Diplexer card (7)	0,00	2,10	1 714 286
OLT Diplexer card (15)	0,00	4,50	800 000
RN3 Outdoor cabinet (for max 8 RE)	40	150,00	1 500 000
RN3 EDFA based reach extender	100	40,00	1 000 000
RN2 Passive RN chassis (not incl AWG,..)	0,00	0,00	2 000 000
RN2 AWG (1:40)	0,00	12,00	4 000 000
RN2 AWG protection (2:40)	0,00	14,40	4 000 000
RN2 AWG (1:80)	0,00	24,00	4 000 000
RN2 AWG protection (2:80)	0,00	28,80	4 000 000
RN1 Passive RN chassis (not incl splitter)	0,00	0,00	2 000 000
RN1 Optical power splitter (1:32)	0,00	6,60	6 000 000
RN1 Optical power splitter (1:16)	0,00	3,40	7 500 000
Hybrid-PON ONT 10G tunable PIN (hardware + software failures)	5,00	2,20	236 842
Hybrid-PON ONT 10G tunable APD (hardware + software failures)	5,50	3,10	204 545
Wavelength-Switched Hybrid DWDM / TDMA PON			
OLT Shelf / Backplane (18 tributary slots)	90,00	100,00	1 500 000
OLT Power unit	0,00	incl in shelf	500 000
OLT Switch/Route processor (~400G)	400,00	40,00	410 000
OLT Switch/Route processor (~800G)	800,00	80,00	370 000
OLT Control and management plane	0,00	incl in shelf	not considered
OLT Software	0,00	incl in shelf	not considered
OLT EDFA Booster	12,00	15,00	1 000 000
OLT Downlink line card Hybrid-PON (10 x 10G)	110,00	106,60	440000
OLT Diplexer card (16)	0,00	4,80	750 000
OLT Diplexer card (8)	0,00	2,40	1 500 000
OLT AWG (1:40)	0,00	12,00	4 000 000
OLT AWG (1:80)	0,00	24,00	4 000 000
OLT Splitter card (8x1:4)	0,00	8,00	1 312 500
OLT Splitter card (16x1:8)	0,00	28,80	562 500
OLT WSS (8x4:1) card	44	832,00	34 375
OLT WSS (16x8:1) card	96,00	2880,00	15 625
RN3 Outdoor cabinet (for max 8 RE)	40	150,00	1 500 000
RN3 EDFA based reach extender	100	40,00	1 000 000
RN2 Passive RN chassis (not incl AWG,..)	0,00	0,00	2 000 000
RN2 AWG (1:10)	0,00	3,00	4 000 000
RN2 AWG protection (2:10)	0,00	3,60	4 000 000
RN2 WSS option 1 (1:4 WSS, 1:10 AWG)	35,00	263,50	106 883
RN2 WSS option 1 protection (2:4 WSS, 1:10 AWG)	35,00	305,10	106 883
RN2 WSS option 2 (1:4 WSS, 1:5 AWG)	35,00	263,50	106 883
RN2 WSS option 2 protection (2:4 WSS, 1:5 AWG)	35,00	305,10	106 883
RN1 Passive RN chassis (not incl splitter)	0,00	0,00	2 000 000
RN1 Optical power splitter (1:32)	0,00	6,60	6 000 000
RN1 Optical power splitter (1:16)	0,00	3,40	7 500 000
Hybrid-PON ONT 10G tunable APD (hardware + software failures)	5,50	3,10	204 545
AON Ethernet with WDM-PtP backhaul			
OLT Active Shelf / Backplane (18 tributary slots)	90,00	100,00	1 500 000
OLT Power unit	0,00	incl in shelf	500 000
OLT Switch/Route processor (~800G)	800,00	80,00	370 000
OLT Control and management plane	0,00	incl in shelf	not considered
OLT Software	0,00	incl in shelf	not considered
OLT 4:1 AWG	0,00	1,20	4 000 000
OLT Downlink line card 4x40G channels (incl 4x40G TRx) (occupies 2 tributary slots)	114,00	36,80	235 294
RN1 Active Shelf / Backplane (18 tributary slots)	90,00	100,00	1 500 000
RN1 Power unit	0,00	incl in shelf	500 000
RN1 Switch/Route processor (~100G, 300Mb/s per client)	100,00	10,00	440 000
RN1 Switch/Route processor (~200G, 500Mb/s per client)	200,00	20,00	430 000
RN1 Control and management plane	0,00	incl in shelf	not considered
RN1 Software	0,00	incl in shelf	not considered
RN1 4:1 AWG	0,00	1,20	4 000 000
RN1 Uplink line card optical 4x40G (incl 4x40G TRx) (occupies 2 tributary slots)	114,00	36,80	235 294
RN1 Downlink line card optical 24 CompactSFP (equal to 48 x1G,not incl pluggables) (occupies 3 tributary slots)	34,00	12,00	800 000
RN1 Pluggable 2x1G (compact SFP)	1,00	0,72	3 000 000

P2P-ONT 1G (hardware + software failures)	3,50	0,96	310 345

- End of document -